UNIVERSIDADE FEDERAL DE PERNAMBUCO
CENTRO DE BIOCIÊNCIAS
PROGRAMA DE PÓS-GRADUAÇÃO EM CIÊNCIAS BIOLÓGICAS
DOUTORADO EM CIÊNCIAS BIOLÓGICAS

LYLYAN FRAGOSO PIMENTEL

TRIAGEM DE NOVAS VARIANTES E ESTUDO DE EXPRESSÃO DE GENES TRANSPORTADORES DE FOSFATO INORGÂNICO EM PACIENTES COM CALCIFICAÇÕES CEREBRAIS

Recife

2018

LYLYAN FRAGOSO PIMENTEL

TRIAGEM DE NOVAS VARIANTES E ESTUDO DE EXPRESSÃO DE GENES TRANSPORTADORES DE FOSFATO INORGÂNICO EM PACIENTES COM CALCIFICAÇÕES CEREBRAIS

Tese de doutorado apresentada ao Programa de Pós-Graduação em Ciências Biológicas da Universidade Federal de Pernambuco, como parte dos requisitos para obtenção do grau de Doutora em Ciências Biológicas.

Área de concentração: Biotecnologia

Orientador: Prof. Dr. João Ricardo Mendes de Oliveira

Recife

2018

Catalogação na fonte
Elaine C. Barroso (CRB4/1728)

Pimentel, Lylyan Fragoso

Triagem de novas variantes e estudo de expressão de genes transportadores de fosfato inorgânico em pacientes com calcificações cerebrais / Lylyan Fragoso Pimentel- 2018.

109 folhas: il., fig., tab.
Orientador: João Ricardo Mendes de Oliveira
Tese (doutorado) – Universidade Federal de Pernambuco. Centro de Biociências. Programa de Pós-Graduação em Ciências Biológicas. Recife, 2018.
Inclui referências, apêndices e anexos

1. Calcificações cerebrais 2. Sequenciamento genético 3. Expressão gênica I. Oliveira, João Ricardo Mendes de (orient.) II. Título

572.516 CDD (22.ed.) UFPE/CB-2018-417

LYLYAN FRAGOSO PIMENTEL

Triagem de Novas Variantes e Estudo de Expressão de Genes Transportadores de Fosfato Inorgânico em Pacientes com Calcificações Cerebrais

Tese de doutorado apresentada ao Programa de Pós-Graduação em Ciências Biológicas da Universidade Federal de Pernambuco, como parte dos requisitos para obtenção do grau de Doutora em Ciências Biológicas.

Aprovada em: 30 de julho de 2018

BANCA EXAMINADORA

_____

Prof. Dr. João Ricardo Mendes de Oliveira
Presidente (Orientador)
Departamento de Neuropsiquiatria – CCS/UFPE

_____

Prof. Dr. Michel Satya Naslavsky
1º Titular
Departamento de Genética e Biologia Evolutiva - IB/USP

_____

Prof. Dr. Rafael Lima Guimarães
2º Titular
Departamento de Genética – CB/UFPE

_____

Profª Drª. Luciana Patrizia Alves de Andrade Valença
3º Titular
Departamento de Neuropsiquiatria - CCS/UFPE

_____

Drª. Paula Sandrin Garcia
4º Titular
Departamento de Genética – CB/UFPE

_____

Profª. Drª. Danyelle Bruneska Gondim Martins
Suplente Interno
Departamento de Bioquímica - CB/UFPE

_____

Dr. Ronald Rodrigues de Moura
Suplente Externo
Laboratório de Imunopatologia Keizo Asami – UFPE

AGRADECIMENTOS

Encerramento de ciclos remetem ao sentimento de gratidão, qualquer que seja o contexto. Em uma análise retrospectiva e um tanto saudosista do que foi vivenciado, aprendido, resignificado, remontado e melhorado, agradeço a todos que me acompanharam durante essa jornada. Assim, agradeço a Deus, pelos momentos bons e, sobretudo, pelos difíceis que proporcionaram as maiores oportunidades de amadurecimento, e pelas pessoas à minha volta, com as quais este aprendizado se torna possível.

Aos meus pais, Pedro e Nadja, pelo amor e suporte incondicionais. Aos meus irmãos, Lívia e Lucas, por todo carinho e por estarem sempre ao meu lado, pois que irmã do meio nasci. Aos meus avós, referências familiares e os alicerces de quem eu sou. Aos incontáveis tios, tias, primos e primas pelas calorosas reuniões de família.

Ao meu grande amigo e parceiro, Juan Luiz, por sua dedicação, cumplicidade, paciência e pelo amor que, mesmo à distância, apertam os nós. Obrigada por partilhar a vida e pelos ensinamentos diários. Sigamos juntos, crescendo e aprendendo sempre, unidos.

Aos velhos e novos amigos que têm me acompanhado e me apoiado durante esta trajetória pelos ensinamentos e pelo aprendizado adquirido, Roberta Lemos, Eriton Cunha, Joana Braga, Regina Galdino, Matthew Keasey, Laura Durão, Denis Moura, Rayssa Medeiros e Eraldo Fonseca. Ao grupo de pesquisa do Dr. Hagg e a aos amigos conquistados em Johnson City, pelo acolhimento e carinho: a família Lovins (Chiharu, Deo e Madelin), Hannah Malone, Candice Broke, Makenzie e Howard Fulmer, Suman Dalal, Francine, Rebecca Jane, Dra. Jia.

Ao Professor João Ricardo, pela sua orientação e amizade desde o meu ingresso no mundo científico. Obrigado por ser um mestre, guia e modelo, pela confiança, por ter acreditado em mim.

Ao LIKA, por fornecer o espaço físico e as ferramentas necessárias para a realização da pesquisa. A Fundação de Amparo à Ciência e Tecnologia do Estado de Pernambuco (FACEPE) e a Coordenação de Aperfeiçoamento de Pessoal de Nível Superior (CAPES), pelo suporte financeiro durante a pós-graduação.

RESUMO

As Calcificações Cerebrais Familiais Primárias (CCFP) são uma condição neuropsiquiátrica rara caracterizada pela deposição mineral simétrica e bilateral nos núcleos da base e outras áreas do cérebro. Quatro genes com variações com padrão de herança autossômico dominante, foram identificados até o momento: *SLC20A2, XPR1, PDGFβ* e *PDGFRβ*. O presente trabalho teve como objetivos o sequenciamento dos genes supracitados, seguido do sequenciamento do exoma dos pacientes de uma família sem variação nesses alvos, e o estudo da expressão de genes transportadores de fosfato. Em 56 pacientes foram encontradas variantes classificadas como patogênicas ou provavelmente patogênicas (34 probandos) e com significado incerto (11 probandos). Os achados clínicos de 54 indivíduos foram analisados: 81,5% reportaram sintomas (parkinsonismo (54,5%), déficit cognitivo e distúrbios psiquiátricos (43,2%, cada)). Em dois pacientes brasileiros identificamos a variação *frameshift* p.(Pro397AlafsTer18) que causa um *stop* códon prematuro e foi predita como patogênica pela ferramenta *in silico* MutationTaster. Parkinsonismo, afasia e acidente vascular cerebral foram relatados. O sequenciamento do exoma de uma família brasileira sem variação nos genes conhecidos em associação às CCFP, revelou variantes raras e preditas deletérias por ferramentas *in silico,* em genes ligados ao metabolismo de cálcio. Análises posteriores excluíram esses candidatos e a busca por um novo gene causal das CCFP encontra-se em andamento. Nos pacientes com variações patogênicas no *SLC20A2*, o estudo de expressão revelou um decréscimo de 40% nos níveis de mRNA. Em contrapartida, não foram detectadas alterações nos indivíduos sem variação nesse gene ou nos outros três ligados à doença. Também não foi observada diferença significativa na expressão dos genes *SLC20A1* e *XPR1* entre os grupos estudados (pacientes com mutação e sem mutação, e grupo controle). Os achados sugerem que variações patogênicas no *SLC20A2* modulam a sua expressão e que as calcificações *per se*, não são capazes de afetar os perfis de expressão dos genes *SLC20A2, SLC20A1* e *XPR1*. Não encontramos evidências de um possível mecanismo de corregulação ou de compensação entre os genes transportadores de Pi à nível de mRNA.

Palavras-chave: Calcificações cerebrais. Sequenciamento genético. Exoma. Expressão gênica

ABSTRACT

Primary Familial Brain Calcifications (PFBC) are a rare neuropsychiatric condition characterized by a symmetric and bilateral deposition of minerals in the basal ganglia and other brain areas. It generally presents an autosomal-dominant inheritance and to date four causative genes have been identified: *SLC20A2*, *XPR1*, *PDGFβ* and *PDGFRβ*. The present study aimed to screen these genes followed by the exome sequencing of patients from a Brazilian family with no mutations and the phosphate transporters expression in these patients. 56 PFBC patients were carrying variants classified as: pathogenic or likely pathogenic (34 probands) and variant of uncertain significance (11 probands). Clinical summary was available in 54 variant-carrying patients: 81.5% were symptomatic (parkinsonism (54.5%), cognitive impairment and psychiatric disturbances (43.2% each)). Two Brazilian patients reported in the study carried a frameshift mutation p.(Pro397AlafsTer18) that causes a premature stop codon and was predicted as disease causing by *in silico* tool MutationTaster. Parkinsonism, aphasia and stroke were reported. Exome sequencing of the Brazilian family without mutation in the four causative genes, revealed rare variants that were predicted as deleterious and were found in genes related to calcium metabolism. These candidates were later excluded and the search for a new causative gene is in progress. In *SLC20A2* mutation-carriers, expression analyses showed a 40% decrease in mRNA levels of this gene. On the other hand, no changes were detected in patients without mutation neither in *SLC20A2* or in the other three genes linked to PFBC. Additionally, no significant changes were seen in *SLC20A1* and *XPR1* among the groups (patients with and without mutation, controls). Our findings suggest that pathogenic variations in *SLC20A2* can modulate its expression levels and that, calcifications *per se* are not capable to affect expression profiles of *SLC20A2*, *SLC20A1* and *XPR1*. We did not find evidences to support the existence of a possible corregulation or compensatory mechanism between the three phosphate transporters genes at mRNA level.

Keywords: Brain calcification. Gene sequencing. Exome. Gene expression

SUMÁRIO

1. INTRODUÇÃO

A estrutura do texto da tese foi elaborada com o intuito de abordar toda a produção científica gerada ao longo do doutorado com resultados publicados, alguns em fase de conclusão e outros que precisaram ser interrompidos. Ao longo do curso, diversos trabalhos foram desenvolvidos em parceria com pesquisadores do Brasil, Estados Unidos, Canadá e países da Europa, alguns em paralelo ao tema central da tese.

Nas seções Introdução, Objetivos e Revisão Bibliográfica são abordados os conteúdos indicados no título do trabalho, acerca de triagem de variantes genéticas e estudo de expressão gênica em pacientes com calcificações cerebrais. Dois trabalhos foram desenvolvidos paralelamente em torno desses temas. Como parte do projeto de triagem de novas variantes genéticas causadoras das Calcificações Cerebrais Familiais Primárias, congregamos os resultados gerados em nosso laboratório até o ano de 2016, com dados de grupos dos Estados Unidos, França e Itália. O artigo publicado na revista *European Journal Of Human Genetics* (fator de impacto: 4,35; Qualis CAPES: A2) (Capítulo I). O estudo de expressão intitulado *Phosphate Transporters Expression in Patients with Primary Familial Brain Calcifications*, foi publicado na revista *Journal of Molecular Neuroscience* (fator de impacto: 2,34; Qualis CAPES: B1) e está integralmente anexado no Capítulo II.

No início 2016, realizamos a captação de amostras dos indivíduos de uma grande família brasileira com casos de CCFP. O caso índex desse grupo já fazia parte do nosso banco de amostras desde o ano de 2013, e o mesmo havia sido triado quando a presença de variações nos quatro genes ligados à doença, resultando em dados negativos. Diante dos resultados negativos do caso índex e de seus familiares afetados, a família tornou-se elegível para o sequenciamento do exoma completo, na busca por novos genes ou variações não detectados com o método Sanger. Os dados parciais da triagem do exoma compõem o Capítulo III.

Em 2015, iniciamos a colaboração com o grupo liderado pelo Dr. Theodoor Hagg (https://www.etsu.edu/com/dbms/faculty/hagg.php) no laboratório do Departamento de Ciências Biomédicas da Universidade do Leste do Tennessee (EUA), O intercâmbio se repetiu nos meses de abril a outubro de 2017, com o doutorado sanduíche patrocinado pela Coordenação de Aperfeiçoamento de Pessoal de Nível Superior (CAPES). Na oportunidade,

foi finalizado o trabalho iniciado em 2015 que foi recentemente aceito para publicação no periódico *Journal of Cell Science* (fator de impacto: 4,706; Qualis CAPES: A2) (Anexo 1).

As Calcificações Cerebrais Familiais Primárias (CCFP) compõem uma condição neuropsiquiátrica rara que se distingue pelo depósito de hidroxiapatita no cérebro de indivíduos com níveis séricos normais de cálcio, fosfato, fosfatase alcalina e paratormônio. Como visualizado no exame de neuroimagem de pacientes afetados pelas CCFP, o processo de mineralização distribui-se em um padrão simétrico e bilateral ao longo dos núcleos basais, no tálamo e na região do núcleo dentado. Não obstante os relatos de casos assintomáticos, nos pacientes em que as CCFP manifestam-se clinicamente, os sintomas surgem por volta dos trinta ou quarenta anos e podem incluir distúrbios motores, sintomas neuropsiquiátricos, parkinsonismo, demência e enxaqueca crônica (Batla *et al.*, 2017; Manyam, 2005; Nicolas, Gael *et al.*, 2013; Taglia *et al.*, 2014).

Até o momento, foram identificados quatro genes com variações associadas às CCFP em casos familiares e esporádicos (*de novo*). Com um padrão de herança autossômico dominante, tais variações estão distribuídas em dois genes que codificam proteínas responsáveis pelo carreamento de fosfato inorgânico através da membrana celular (*SLC20A2* e *XPR1*) e em dois genes ligados à manutenção da integridade da barreira hematoencefálica (BHE) (*PDGFβ* e *PDGFRβ*) (Keller *et al.*, 2013; Legati, Giovannini, Nicolas, López-Sánchez, Quintáns, Oliveira, João R M, *et al.*, 2015; Nicolas, Gaël *et al.*, 2013; Wang, Li, Shi, Ren, Patti, Wang, Oliveira, de, *et al.*, 2012).

Animais *knockout* para o gene *SLC20A2*$^{(-/-)}$ e camundongos hipomórficos para o *PDGFβ* (*Pdgfb*$^{ret/ret}$) replicaram os achados patológicos encontrados nos pacientes, exibindo extensas calcificações nos núcleos da base, tálamo e em outras áreas do cérebro (Jensen *et al.*, 2013; Keller *et al.*, 2013). Modelos *in vitro* revelaram, ainda, que algumas variantes patogênicas identificadas no *SLC20A2* podem exercer uma função dominante-negativa na proteína selvagem e acarretar no comprometimento do influxo de fosfato, levando à deposição mineral no meio extracelular (Larsen *et al.*, 2017; Wang, Li, Shi, Ren, Patti, Wang, Oliveira, De, *et al.*, 2012). Estudos mostraram que os efeitos funcionais da depleção do gene *XPR1* se refletem na a exportação prejudicada de fosfato do citoplasma para o meio extracelular

enquanto a perda de função do *PDGFRβ* causa danos à BHE (Giovannini *et al.*, 2013; Nicolas, Gaël *et al.*, 2013).

Além das implicações na função proteica, variações genéticas também podem refletir-se na alteração dos níveis de expressão do gene que as contém ou em genes de vias adjacentes, a depender do tipo e da localização da mutação. Dessa forma, oscilações na expressão gênica podem fornecer indício a respeito da desregulação dos processos biológicos em que o gene está envolvido. A análise dos padrões de expressão de determinados genes é de grande utilidade clínica e vem sendo aplicada como teste de diagnóstico para condições como câncer e doenças coronárias (Bueno *et al.*, 2004; McPherson *et al.*, 2013; Rhees e Wingrove, 2015; Zanotti *et al.*, 2014; Zeller e Blankenberg, 2013). Estudos acerca do *SLC20A2* com amostras de sangue periférico de pessoas afetadas pelas CCFP, revelaram alterações no perfil de expressão do gene diante da presença de diferentes tipos de mutações patogênicas (Ferreira *et al.*, 2014; Zhang, Guo e Wu, 2013).

Juntamente com os achados minerais detectados na neuroimagem e a ausência de desordens metabólicas, infecções ou traumas, a confirmação do diagnóstico das CCFP pode ser realizada com testes genéticos capazes de identificar variações patogênicas em heterozigose (Ramos *et al.*, 2017). Dentre os testes genéticos disponíveis, está o sequenciamento do exoma completo (*WES – Whole Exome Sequencing*), capaz de triar aproximadamente 95% do exoma humano, composto por cerca de 180.000 sequências de DNA codificante. Apesar de o exoma humano corresponder a apenas 2% de todo o genoma, aproximadamente, nele está contida a maioria das variações raras associadas a doenças (Ramos *et al*., 2017).

Dessa forma, o sequenciamento do exoma vem sendo amplamente utilizado como ferramenta de diagnóstico clínico, uma vez que permite a identificação de novos genes ligados a condições genéticas que outros métodos não são capazes de detectar (Warr *et al.*, 2015). Nesse contexto, a descoberta dos genes relacionados às CCFP foi possível com o estudo do exoma completo de indivíduos diagnosticados com a doença (Keller *et al.*, 2013; Legati, Giovannini, Nicolas, López-Sánchez, Quintáns, Oliveira, João R.M., *et al.*, 2015; Nicolas, Gaël *et al.*, 2013; Wang, Li, Shi, Ren, Patti, Wang, Oliveira, De, *et al.*, 2012).

O trabalho reúne os resultados do sequenciamento genético pela plataforma Sanger de pacientes com CCFP na busca por novas variantes patogênicas além dos dados parciais da triagem do exoma em membros de uma nova família brasileira. Essa família possui indivíduos saudáveis e pacientes com CCFP sem variantes patogênicas na região codificante dos genes conhecidos em associação com a doença. A abordagem possibilitará a identificação de um novo gene causador das CCFP ou de novas variações não identificadas inicialmente devido à natureza do método de sequenciamento utilizado.

Adicionalmente, trazemos a análise do perfil de expressão gênica de transportadores de fosfato inorgânico (*XPR1*, *SLC20A2* e *SLC20A1*), em dois grupos de pacientes com calcificações cerebrais: 1) com mutações no gene *SLC20A2* e 2) sem variações nos quatro genes ligados à doença.

2 OBJETIVOS

2.1 OBJETIVO GERAL

Investigar pacientes com calcificações cerebrais quanto à presença de variantes genéticas ou um novo gene causador das Calcificações Cerebrais Familiais Primárias e avaliar o perfil de expressão de genes transportadores de fosfato inorgânico nesses indivíduos.

2.2 OBJETIVOS ESPECÍFICOS

- Avaliar a expressão dos genes *SLC20A1*, *SLC20A2* e *XPR1* por PCR Quantitativa em Tempo Real em amostras de sangue periférico de pacientes com calcificações cerebrais bilaterais;

- Sequenciar a região codificante dos genes associados às CCFP (*SLC20A2*, *PDGFRβ*, *PDGFβ* e *XPR1*), pelo método Sanger, em amostras de DNA genômico de pacientes com calcificações cerebrais para busca de variações patogênicas;

- Utilizar ferramentas de bioinformática para predição *in silico* dos efeitos biológicos das variações encontradas no sequenciamento;

- Sequenciar o exoma de membros de uma família brasileira com calcificações cerebrais e seus parentes saudáveis, para identificação de variações patogênicas em heterozigose ou de novos genes candidatos;

- Validar as variações candidatas com possíveis efeitos sob a função do gene e confirmação do perfil de segregação compatível com o padrão de herança autossômico dominante observado nas CCFP.

3 REFERENCIAL TEÓRICO

3.1 CALCIFICAÇÃO INTRACRANIANA

Calcificações intracranianas fisiológicas estão comumente associadas ao desbalanço de metais ou minerais e ocorrem em regiões perivasculares, glândulas e diversas áreas do cérebro. Na população geral, é um achado com incidência que varia de 1% a 50% (Daghighi *et al.*, 2007; Oliveira, Silva e Oliveira, 2013; Sedghizadeh, Nguyen e Enciso, 2012).

Além do zinco, ferro e magnésio, os depósitos calcificados no cérebro possuem a hidroxiapatita ($Ca_{10}[PO_4]_6[OH]_2$) como principal componente, também encontrada em cristais de fosfato de cálcio presentes nos ossos. Insolúvel em condições fisiológicas, a hidroxiapatita surge a partir de uma reação envolvendo alguns de seus precursores como o fosfato octacálcico (OCP) ($Ca_8H_2(PO_4)_6.5H_2O$), o fosfato de cálcio amorfo ($Ca_9(PO_4)_6$) e a bruxita, ou fosfato bicálcico diidratado ($CaHPO_4$) (Deng, Zheng e Jankovic, 2015; Villa-Bellosta e O'Neill, 2018).

Vários estudos populacionais relatam as calcificações cerebrais (CC) de causa inespecífica como um fenômeno idade-dependente que pode ocorrer em indivíduos saudáveis e são detectadas em exames imaginológicos de rotina. Em amostra representativa da população brasileira, verificou-se que o achado possui uma incidência de aproximadamente 17%, com maior prevalência em pessoas mais velhas (42% - 66% entre os 60 e 90 anos) (Oliveira, Silva e Oliveira, 2013).

Corroborando com tais constatações, estudos abrangendo coortes com centenas ou milhares de pessoas saudáveis entre 10 e 85 anos de idade, relataram o aumento progressivo da incidência de CC com o aumento da idade, especialmente em pessoas do sexo masculino (Daghighi *et al.*, 2007; Sedghizadeh, Nguyen e Enciso, 2012; Uduma, Pius e Mathieu, 2011; Yalcin *et al.*, 2016). Ademais, também notaram um tropismo das calcificações para áreas específicas do cérebro e que a frequência desse achado pode variar de acordo da faixa etária dos indivíduos. A maioria dos estudos reporta que a glândula pineal é a zona mais frequentemente afetada, cerca de 71-80% de prevalência, sendo mais comum em pessoas entre 15 e 54 anos de idade.

Na sequência, calcificações no plexo coroide apresentam uma prevalência que varia entre 66,2 a 70,2% na maioria dos estudos, e se mostra mais frequente a partir da quinta década, dos 55 aos 85 anos de idade. Também já foram relatadas calcificações na habênula (19,2 - 20,1%), na dura mater (12,5%), no tentório do cerebelo (7,3%), nos vasos (3,5 - 6,6%) e nos núcleos da base (0,8 - 1,3%) (Gráfico 1) (Daghighi *et al.*, 2007; Sedghizadeh, Nguyen e Enciso, 2012; Yalcin *et al.*, 2016).

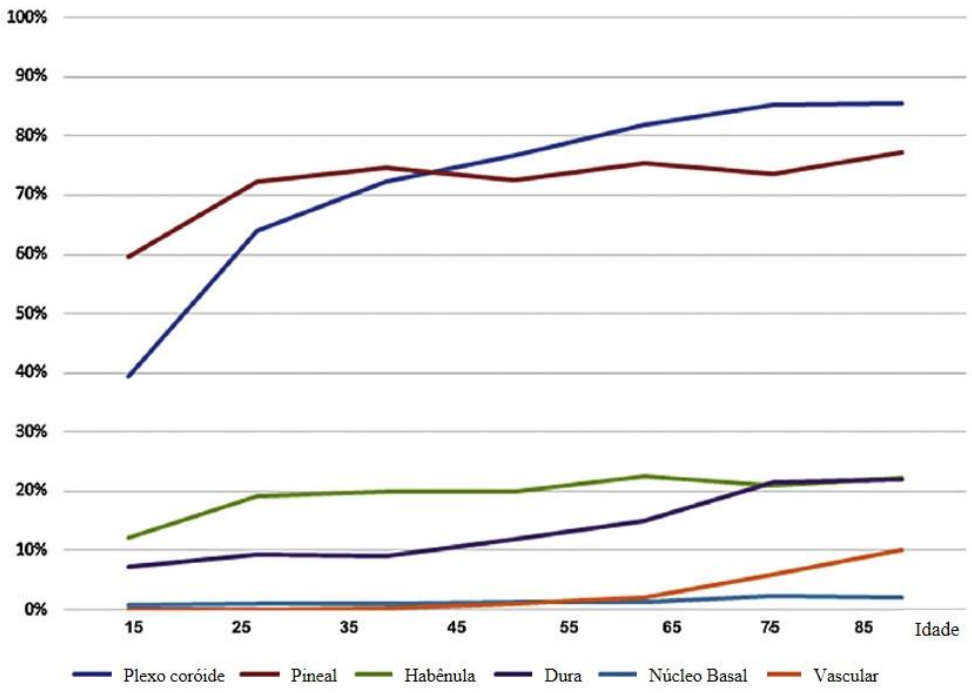

Gráfico 1. Distribuição da incidência de calcificações intracranianas fisiológicas em diferentes áreas do cérebro variando com a idade. Adaptado de Yalcin *et al*., 2016.

Em um contexto patológico, as CC estão presentes em inúmeras condições e podem representar uma importante variável no curso clínico da doença, quando esses estão presentes (Nash *et al.*, 2004; Oliveira, 2011). Dentre essas condições, estão distúrbios metabólicos como o hipoparatireoidismo, doenças neurológicas, mitocondriais, isquemia, doenças degenerativas, infecções, traumas e intoxicações (Bekiesinska-Figatowska, Mierzewska e Jurkiewicz, 2013; Oliveira, 2011).

Desde achados macroscópicos visíveis no exame de neuroimagem a acúmulos perivasculares microscópicos, no contexto patológico, pesquisas relatam que há uma grande vulnerabilidade seletiva dos núcleos basais à deposição dos cristais de hidroxiapatita (Bekiesinska-Figatowska, Mierzewska e Jurkiewicz, 2013; Deng, Zheng e Jankovic, 2015; Oliveira, 2011).

Assim, nota-se que as CC podem levar de meses a anos para se desenvolver e se apresentam em diferentes padrões de distribuição, podendo localizar-se pontualmente e dispersas ou concentradas de forma simétrica e bilateral em algumas regiões do cérebro (Bekiesinska-Figatowska, Mierzewska e Jurkiewicz, 2013; Brouwer *et al.*, 2018; Deng, Zheng e Jankovic, 2015; Nash *et al.*, 2004).

3.2 NÚCLEOS DA BASE

3.2.1 Anatomia e Função

Também conhecidos como gânglios da base por se formarem de corpos celulares neuronais, os núcleos da base (NB) do cérebro localizam-se no diencéfalo e no mesencéfalo e compreendem as seguintes regiões: estriato (núcleo caudado e putâmen), globo pálido (externo, GPe e interno, GPi), núcleo subtalâmico (*subthalamic nuclei* - STN) e substância nigra (reticulada, SNr e compacta, SNc, contendo neurônios GABAérgicos e dopaminérgicos, respectivamente) (Figura 1) (Oliveira, 2011; Smith e Wichmann, 2008). Dividido em duas porções, os NB estão associados com funções motoras e cognitivas na região dorsal do estriato, e funções motivacionais na porção ventral, composta por áreas próximas de estruturas do sistema límbico, como o núcleo accumbens (Kopell *et al.*, 2006).

Juntamente com o córtex e o tronco cerebral, essas estruturas quer formam os NB pertencem ao circuito conhecido como extrapiramidal, responsável, sobretudo, pelo controle de funções motoras e não motoras, cognitivas e emocionais (Bekiesinska-Figatowska, Mierzewska e Jurkiewicz, 2013; Tisch *et al.*, 2004).

O circuito ocorre de tal modo que informações ligadas à função motora adentram nos núcleos da base pelo estriato e do núcleo subtalâmico, enquanto o GPi e a SNr atuam como

zonas de saída dessa informação, enviando sinais inibitórios à áreas do córtex e do tronco cerebral (Smith e Wichmann, 2008; Tisch *et al.*, 2004; Wichmann e Delong, 2007).

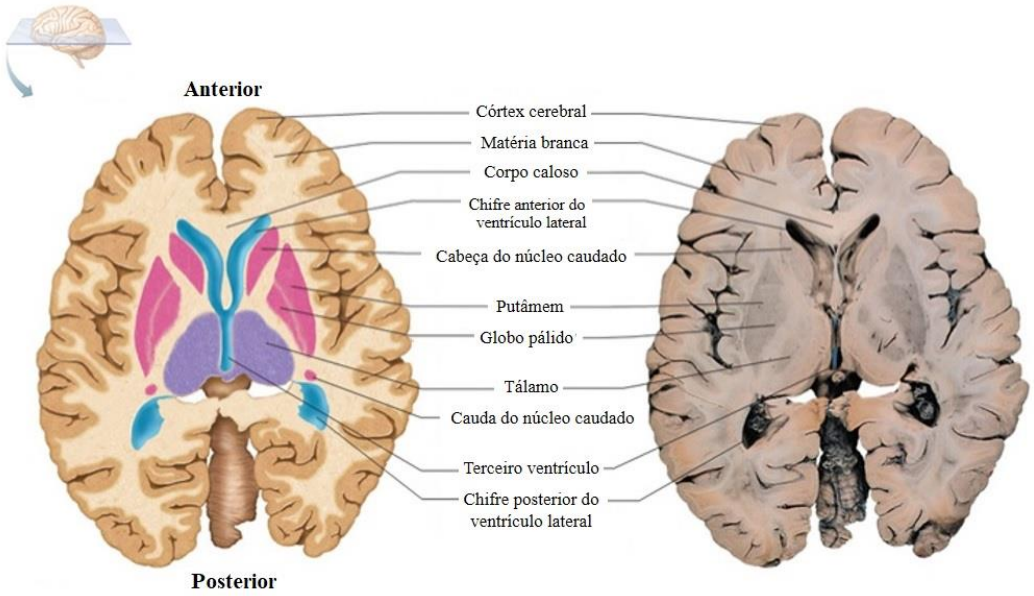

Figura 1. Corte horizontal do cérebro demonstrando a anatomia dos núcleos da base e áreas adjacentes. Adaptado de www.antranik.org

3.2.2 Desordens Associadas à Calcificações nos Núcleos Basais

Os primeiros relatos de calcificação nos NB datam do século 19 quando, em 1850, Delacour descreveu o caso de um paciente com calcificações observadas na autopsia. Tratava-se de um homem de 56 anos que apresentava fraqueza e rigidez nas extremidades inferiores e cujo exame patológico revelou processos de mineralização vascular bilaterais no estriato. (Manyam, 2005).

Achado bastante comum em exames de neuroimagem, as calcificações bilaterais nos gânglios basais já foram relatadas em cerca de 21,5 a 75% de casos de hipoparatireoidismo idiopático. Iniciando, geralmente, na infância e na adolescência, a condição acarreta na diminuição da concentração sérica do paratormônio (PTH), levando ao quadro de hipocalcemia e hiperfosfatemia. Formas genéticas já foram descritas em associação a anormalidades nos cromossomos 21 e 22, e em genes específicos (*PTH*, *GCM2*, *SOX3*, *CASR*

e *GNA11*) (Ramos, 2017). Além dos NB, as calcificações observadas nos casos de hipoparatireoidismo também se mostram simétricas no tálamo, cerebelo e na substância branca subcortical e podem manifestar sintomas como convulsões e distúrbios psiquiátricos (Figura 2A) (Abate e Clarke, 2017; Lu, 2014; Mendes *et al.*, 2018).

Episódios de calcificações bilaterais nos NB também foram descritos em doenças mitocondriais, a exemplo da Síndrome de Leigh e da Encefalomiopatia Mitocondrial com acidose láctica e episódios semelhantes a acidente vascular cerebral (*Mitochondrial encephalomyopathy, actic acidosis, and stroke-like episodes* - MELAS). A primeira, uma encefalomielopatia necrosante subaguda, é transmitida de forma autossômica dominante e afeta bebês e crianças. Pacientes acometidos pela doença mitocondrial hereditária mais comum, a MELAS, apresentam comprometimento no sistema nervoso, nos músculos e atrofia cerebral. Nesses dois exemplos, adicionalmente aos NB, também pode ocorrer mineralização no tronco cerebral, no STN e no putâmen (Figura 2B) (Aron *et al.*, 2010; Bekiesinska-Figatowska, Mierzewska e Jurkiewicz, 2013; Farina *et al.*, 2002; Khandwala, Ahmed e Sheikh, 2018).

Outro exemplo de patologia ligada às calcificações no NB são as Calcificações Cerebrais Familiais Primárias (CCFP) que, em sua origem, foram nomeadas como Doença de Fahr (DF) ou Calcificações Idiopáticas nos Gânglios da Base (IBGC) (Figura 2C). Desde então, inúmeras entidades patológicas vêm sendo, equivocadamente, classificadas como DF, a despeito de possuírem etiologias distintas (Oliveira, 2011). Essa questão será novamente abordada e aprofundada no item 3.3.

Infecções por citomegalovírus, as síndromes DiGeorge e Aicardi-Goutieres, além de outras condições em que calcificações nos NB são frequentemente encontradas, estão listadas na Tabela 1 (Bekiesinska-Figatowska, Mierzewska e Jurkiewicz, 2013; Deng, Zheng e Jankovic, 2015; Oliveira, 2011; Quintáns, Oliveira e Sobrido, 2018).

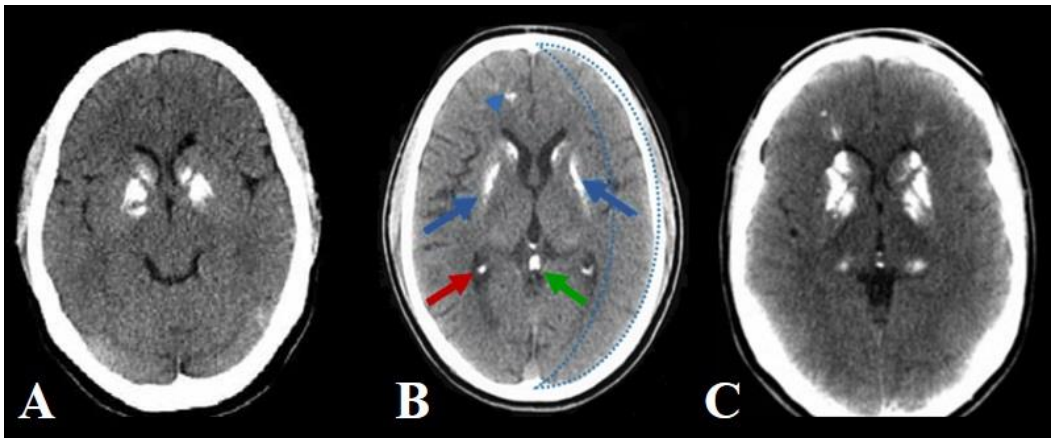

Figura 2. Plano horizontal do cérebro em imagem de tomografia computadorizada. Sinais hiperdensos (brilhoso) representam tecidos densos (ossificados). Nota-se a semelhança de intensidade do sinal da calota craniana com as calcificações simétricas e bilaterais nos núcleos da base (seta azul), no plexo coróide (seta vermelha) e na pineal (seta verde). **(A)** Cérebro de paciente com hipoparatireoidismo (Lu, 2014), **(B)** cérebro de paciente com a MELAS (Hatamian, Bakhshayesh e Rahman-a, 2015) e **(C)** cérebro de paciente com CCFP (Oliveira e Oliveira, 2016).

Tabela 1. Doenças que podem causar calcificações intracranianas. Adaptado de Quintáns, Oliveira e Sobrido, 2018.

Genéticas	Genes
Hipoparatireoidismo primário	PTH, CASR, GNA11, GCM2
Pseudohipoparatireoidismo, Pseudohipoparatireoidismo	GNAS
Hipofosfatemih Hereditária	FGF23, FAM20C
Síndrome DiGeorge	TBX1
Síndrome Sanjad–Sakati	TBCE
Síndrome Kenny–Caffey	TBCE, FAM111A
Neurofibromatose	NF1, NF2
Esclerose Tuberosa	TSC1, TSC2
Calcificação em bandas com giração simplificada e polimicrogiria	OCLN
Síndrome Aicardi–Goutières	TREX1, SAMHD1, ADAR, IFIH1, RNASEH2C, RNASEH2A
Destruição hemorrágica do cérebro, calcificação subependimal e catarata congênita	JAM3
Vasculopatia proliferativa com hidranencefalia-hidrocefalia	FLVCR2
Displasia oculodentodigital	GJA1
Síndrome de Cockayne	ERCC6, ERCC8

Tabela 1. Continuação

Doença de Krabbe	GALC
Ataxia spinocerebelar	duplicação do 11q
Atrofia dentatorubro-palidolusiana	ATN1
Leucodistrofia metacromática	ARSA
Adenoleucodistrofia ligada ao cromossomo X	ABCD1
Doença de Wilson	ATP7B
Neurodegeneração com acúmulo de ferro (NBIA)	PANK2, WDR45, PLA2G6, FTL, C19ORF12, COASY
Aceruloplasminemia CP	CP
Deficiência de biotinidase	BTD
Má absorção hereditária de folato	SLC46A1
Diabetes insipidus central	AVP, WFS
Diabetes insipidus nefrogênica	AVPR2, AQP2
Síndrome de Gitelman	SLC12A3
Fenilcetonúria	PAH
Deficiência de diidropiridina redutase	QDPR
Microangiopatia cerebroretinal com calcificações e cistos	CTC1
Autoinflamação, lipodistrofia e síndrome de dermatose	PSMB8
Imunodeficiência com calcificação nos gânglios basais	ISG15
Osteodisplasia lipomembranosa policística com leucoencefalopatia esclerosante (Doença de Nasu–Hakola)	TREM2, TYROBP
Citopatia mitocondrial	POLG, MTTS1, MTTS2, MTTL1, MTTF, MTTQ, MTTH, MTTC, MTTK, MTND1, MTND5, MTND6
Não genéticas	Causas
Metabólicas	Hipervitaminose D, hipoparatireoidismo secundário, hiperparatireoidismo, hipotireoidismo
Tóxicas	CO, chumbo, cobre, radioterapia
Infecciosas	CMV, HIV, VZV, toxoplasmose, tuberculose, cisticercose
Autoimune	SLE, doença Behçet, doença celíaca
Cerebrovascular	Acidente vascular cerebral, má formações vasculares

CMV, citomegalovírus; CO, monóxido de carbono; HIV, vírus da imunodeficiência humana; SLE, lúpus eritematoso sistêmico; VZV, vírus varicelazoster.

3.2.3 Técnicas de Neuroimagem na Detecção das Calcificações Cerebrais

Desde a sua descoberta em 1895 pelo físico alemão Wilhem Röentgen, os raios-X têm sido amplamente utilizados para visualização de estruturas ósseas e vem sendo aplicado como o princípio de diversos exames na rotina da clínica médica (Mondschein, 2018). Outrora, a constatação de regiões mineralizadas no cérebro era realizada com exames de radiografia que permitiam a observação de grandes lesões sob a forma de manchas nebulosas. Entretanto, para fins de diagnóstico das CC, esse exame se mostra impreciso e inapropriado (Oliveira, 2011).

Dessa forma, técnicas de captura de imagem mais sensíveis vem se desenvolvendo, visando a correta identificação de enfermidades que acometem o cérebro bem como a definição de subgrupos neurobiológicos. Elas contribuem para a elucidação de doenças complexas, como observado nos estudos das Desordens do Espectro Autista e, particularmente, a respeito das CC, facilitam sua visualização nas mais variadas desordens (Daghighi *et al.*, 2007; Martino *et al.*, 2017; Yalcin *et al.*, 2016).

Embora muitas das tecnologias disponíveis possam servir como ferramenta para detecção das CC, a tomografia computadorizada (TC) se mostra mais apropriada na avaliação dessas lesões. Técnica amplamente disponível e de alta resolução, ela possui alta sensibilidade para áreas ricas em cálcio, dimensionando a extensão e a localização das calcificações intracranianas (Ramos *et al*., 2017). Portanto, a fim de estabelecer um diagnóstico mais preciso das CC, a TC fornece informações cruciais na determinação do volume dos depósitos minerais e se mostra relevante para o prognóstico da doença (Sedghizadeh, Nguyen e Enciso, 2012). Um aprimoramento dessa tecnologia se reflete nos modelos tridimensionais construídos a partir de cortes 2-D de TC. A técnica possibilitou, inclusive, a reconstrução computacional do cérebro de figuras ilustres da história da filosofia, da música e da ciência. Recentemente, uma modelagem tridimensional do cérebro do filósofo francês René Descartes foi desenvolvida a partir do seu crânio, que encontra-se conservado no Museu de História Natural (França/Paris) (Philippe *et al.*, 2017).

Na imagem de TC, diferentes tipos de materiais são detectados dentro de um espectro de intensidade de sinal, conhecido como a escala de Hounsfield. Tecidos densos (calcificados) emitem sinais hiperdensos (brilhantes), igualmente ao osso do crânio (Kamaruddin *et al.*, 2016). Enquanto que, tecidos macios e ricos em gordura, como o encéfalo, são vistos como áreas escuras, ou hipodensas (Figura 3A) (Filloux, Marotte e Miossec, 2003; Kalita *et al.*, 2010; Nicolas *et al.*, 2014)

Outro exame imaginológico comumente utilizado como ferramenta de diagnóstico é a ressonância magnética (RM). Ela possui algumas modalidades e seu aspecto visual traz vantagens à TC no tocante a uma melhor distinção entre a substância branca e a cinzenta (Ferguson *et al.*, 2018). Variações da RM como a imagem ponderada por difusão (*Diffusion-weighted imaging* - DWI) e a imagem ponderada por suscetibilidade (*susceptibility-weighted imaging* - SWI) representam aprimoramento da técnica e proporcionam uma maior sensibilidade em comparação à RM convencional (Adams *et al.*, 2017; Drake-Pérez *et al.*, 2018).

Formações contendo cálcio podem gerar diferentes padrões de alteração no sinal em imagens de RM, a depender da sequência utilizada. Essas diferenças de intensidades de sinal nas áreas calcificadas podem ser observadas nas imagens sem contraste capturadas em SWI com filtro de fase, T1 e FLAIR (*Fluid attenuation inversion recovery*) (Figura 3B-D), mostrando-se com hiperintensidade (brilhante), semelhante à TC. Enquanto que, nas sequências SWI com magnitude de imagem e em T2, as calcificações se mostram com sinais hipointensos (escuro), o que dificulta sua diferenciação de focos de hemorrágicos (Figura 3E e 3F) (Adams *et al.*, 2017; Filloux, Marotte e Miossec, 2003; Iglesia *et al.*, 2006; Nicolas, Gaël *et al.*, 2013; Wu *et al.*, 2009). Por outro lado, há casos em que a calcificação pode mostrar-se heterogênea e, por essa razão, exibir perfis semelhantes em T1 e T2, com sinal hiperintenso (Avrahami *et al.*, 1994).

Como mencionado anteriormente, devido à alta sensibilidade e melhor resolução da imagem na detecção e caracterização de calcificações intracranianas, a TC tem sido mais adotada nesses casos. Entretanto, dentro das suas particularidades, ambas as abordagens (TC e RM) possuem vantagens e desvantagens por isso, ainda há casos em que se faz necessária a complementação do diagnóstico com imagens de RM (Kalita *et al.*, 2010).

Com o avanço das técnicas imaginológicas, estudos mostraram que as calcificações nos NB possuem um caráter ubíquo, uma vez que acometem o cérebro em diferentes contextos patológicos e, por vezes, se assemelham em distribuição e tamanho. Dessa forma, elas se mostram um marcador não específico, demonstrando a necessidade de exames complementares a fim de determinar um diagnóstico preciso (Batla *et al.*, 2017; Oliveira, 2011).

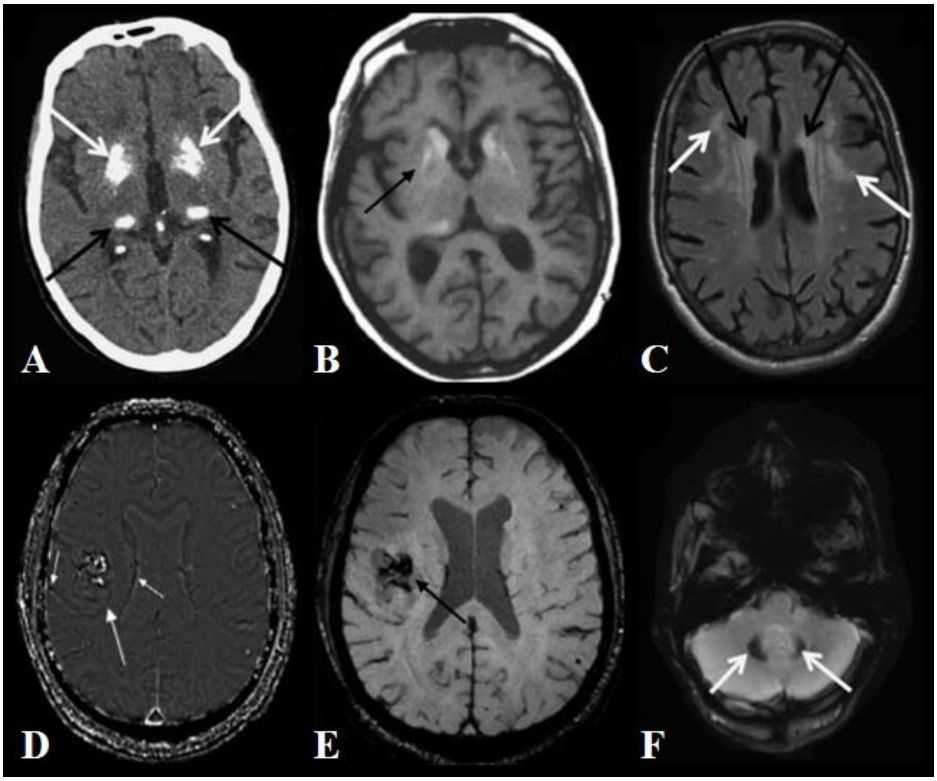

Figura 3. Plano horizontal do cérebro em diferentes técnicas de neuroimagem. (A-D) As setas indicam depósitos calcificados no cérebro com sinais hiperdensos ou hiperintensos (brilhantes). (A) Tomografia Computadorizada (Nicolas *et al.*, 2013), (B) RM na sequência T1 (Filloux, Marotte e Miossec, 2003), (C) RM na sequência FLAIR (Nicolas *et al.*, 2013), (D) RM na sequência SWI com filtro de fase (Wu *et al.*, 2009). (E-F) As setas mostras regiões escuras (hipointensas) indicando a presença de calcificações nessas áreas. (E) RM na sequência SWI com magnitude (Wu *et al.*, 2009), (F) RM na sequência T2 (Nicolas *et al.*, 2013).

3.3 CALCIFICAÇÃO CEREBRAL FAMILIAL PRIMÁRIA

3.3.1 Histórico e Nomenclatura

Após os relatos de Delacour em 1850, muitos outros casos se sucederam descrevendo de novos pacientes com os mesmos achados, neuropatológicos e clínicos. Ainda na mesma década, Virchow e Bamberger, descreveram de forma independente a presença de calcificações vasculares na análise histopatológica do cérebro de uma mulher com retardo mental e convulsões. No século seguinte, Pick atribuiu às calcificações a causa de isquemia nas áreas lesionadas. Geyelin e Penfield, em 1929, associaram a condição a um quadro inflamatório que ocorria na túnica interna das artérias e posteriormente, constataram que as calcificações afetam os vasos de camadas corticais profundas e a matéria branca adjacente (Casanova e Araque, 2003).

As calcificações cerebrais idiopáticas nos NB tornaram-se mais conhecidas em 1930 após Karl Theodor Fahr (1877-1945) reportar um novo caso de mineralizações vasculares cerebrais. Na ocasião, Fahr relatou que o paciente apresentava amplo quadro clínico composto por histórico de demência, imobilidade sem paralisia, febre alta, visão dupla, úlceras de decúbito e tosse. O exame do cérebro do paciente revelou calcificações microscópicas no córtex, nos ventrículos laterais e no estriato (Batla *et al.*, 2017; Casanova e Araque, 2003; Manyam, 2005; Tadic *et al.*, 2015).

Desde então, epônimos passaram a ser adotados para referir-se a vários tipos de calcificação bilateral nos NB e em outras áreas do cérebro. Não raro observam-se relatos de casos e artigos com as expressões “doença de Fahr” ou “síndrome de Fahr”, essa última mais aplicada para descrever o conjunto de sintomas neuropsiquiátricos. Entretanto, os autores anteriores haviam relatado casos semelhantes e com maior profundidade e riqueza de detalhes. (Batla *et al.*, 2017; Tadic *et al.*, 2015).

Dessa forma, a inconsistência na terminologia de doenças envolvendo mineralização nos NB levou ou surgimento de dezenas de termos, vastamente utilizados no passado, resultando em equívocos no diagnóstico de muitos casos (Tabela 2) (Manyam, 2005; Oliveira, 2011).

Tabela 2. Lista com diferentes termos utilizados para nomear formas idiopáticas e não idiopáticas de calcificações nos núcleos da base do cérebro (Oliveira, 2011).

Bilateral striopallidodentate calcinosis	Ferrocalcinosis
Bilateral-symmetrical calcification of basal ganglia	Hirnsteine (stone-hard)
Bochnick‘s neurogel	Idiopathic basal ganglia calcification
Brain calcification	Idiopathic calcification of the basal ganglia
Brain calcinosis	Idiopathic cerebral calcifications
Brain stones	Idiopathic familial brain calcifications
Basal ganglia calcification	Idiopathic familial cerebrovascular ferrocalcinosis
Calcification of the basal ganglia of the brain	Idiopathic nonarteriosclerotic cerebral calcification
Calcification of the striopallidodentate system	Morbus Fahr
Cerebral calcinosis	Mulberry bodies
Corticostriopallidodentate calcifications	Pallido-dentate calcifications
Fahr‘s disease	Physiological calcifications
Fahr‘s syndrome	Pseudo calcareous foci
Familial basal ganglia calcification	Psammoma bodies
Familial bilateral vascular calcification in the central nervous system	Senescent calcifications
Familial calcific dentato-striatal degeneration	Spatz‘s pseudocalcium
Familial calcification of the basal ganglia	Striopallidodentate calcifications
Familial calcification of the basal ganglions	Striopallidodentate calcinosis
Familial idiopathic basal ganglia calcification	Symmetric cerebral calcification
Familial idiopathic cerebral calcifications	Symmetrical basal ganglia sclerosis
Familial idiopathic striopallidodentate calcifications	Symmetrical calcification of brainstem ganglia
Familial striopallidodentate calcification	Symmetrical intracranial advanced pseudocalcium

O termo “calcificação cerebral idiopática familiar” foi sugerido inicialmente por Boller em 1977, quando descreveu o caso de nove indivíduos de três gerações de uma família. Analisando as imagens de radiografia, Boller constatou a presença de calcificação bilateral nos gânglios da base do cérebro. Os testes bioquímicos detectaram níveis normais de cálcio e fósforo (Boller, Boller e Gilbert, 1977).

A identificação dos primeiros genes associados à doença proporcionou um avanço na busca pelas bases moleculares das calcificações cerebrais hereditárias. Dessa forma, o termo "idiopático", usado para doenças de causa desconhecida, passou a ser substituído pelo termo "primário". Esse último, se refere aos casos em que há uma origem genética, em oposição às calcificações secundárias, causadas por infecções, inflamações, problemas metabólicos, traumas, etc. (Batla *et al.*, 2017). O termo "Calcificações Cerebrais Familiais Primárias" (CCFP) foi, então, proposto a fim de uniformizar a nomenclatura das calcificações simétricas bilaterais de causa genética. Assim, o uso do termo "Fahr", ambiguamente utilizado como referência às calcificações hereditárias ou idiopáticas nos NB, vem sendo fortemente combatido e evitado (Ramos *et al*., 2017).

3.3.2 Sintomas, Diagnóstico e Tratamento

A maioria dos indivíduos afetados pelas CCFP são saudáveis durante a infância e na fase adulta. O surgimento dos sintomas ocorre, em média, aos 31 anos, mas pode variar dos 6 aos 77 (Nicolas *et al.*, 2015). Entretanto, há casos em que a doença não exerce impacto clínico, permanecendo assintomática durante toda a vida do paciente. Nos relatos de indivíduos sintomáticos, problemas psiquiátricos são mais prevalentes, seguidos de distúrbios motores e comprometimento cognitivo (Nicolas, Gael *et al.*, 2013; Tadic *et al.*, 2015).

Diferentemente dos achados de neuroimagem (100%), nota-se uma penetrância incompleta do fenótipo clínico das CCFP, estimado em 61% (Tadic *et al.*, 2015). Quadros convulsivos, transtorno de personalidade, parkinsonismo, distonia, dificuldade na memória, depressão, ansiedade e enxaqueca podem ser observados. Estimada em 24,6% em estudo envolvendo pacientes com CCFP confirmada geneticamente, a enxaqueca nem sempre está segregando com a doença. Contrapondo-se a 14,7% na população geral, ela é um sintoma que necessita de mais estudos sistemáticos a fim de se determinar sua relação na clínica as CCFP (Nicolas *et al.*, 2015; Nicolas, Gael *et al.*, 2013; Vos *et al.*, 2012).

A proporção entre pacientes sintomáticos e assintomáticos pode variar amplamente, a depender dos critérios de inclusão adotados em cada estudo. Frequentemente, isso se deve ao fato de que pacientes com indicação clínica têm mais chances de serem encaminhados à

triagens posteriores, como exames de neuroimagem e testes genéticos (Nicolas *et al.*, 2015; Oliveira, 2011; Tadic *et al.*, 2015).

Devido ao amplo espectro fenotípico das CCFP e mesmo à falta desse, estimar a prevalência da doença se torna um desafio. A grande sobreposição clínica com outras entidades patológicas e até mesmo a semelhança no padrão de calcificação, causa erros de diagnóstico e a perda de informações relevantes sobre número de afetados. Estudo recente buscou avaliar essa questão com base em dados genômicos, constatando que, diferentemente do que se acreditava, elas são subestimadas e subdiagnosticadas, pois que são relativamente comuns. (Nicolas *et al.*, 2017).

Por esse motivo, o diagnóstico diferencial das CCFP exige a análise de critérios específicos com base no que segue: 1) exame de neuroimagem (idealmente TC) apontando a presença de calcificações bilaterais e simétricas predominantemente nos NB, 2) ausência de anormalidades nos testes bioquímicos e de características somáticas a fim de 3) excluir quadros sugestivos de doenças mitocondriais, desordens metabólicas ou infecções, 4) presença, apesar de não mandatória, de disfunções neurológicas progressivas, incluindo desordens psiquiátricas e do movimento. Há casos em que se atenta para o histórico familiar, frequentemente compatível com o padrão de herança autossômico dominante (Ramos *et al*., 2017; Batla *et al.*, 2017; Nicolas *et al.*, 2015; Tadic *et al.*, 2015).

Em trabalho publicado em 2013, Nicolas e colaboradores encontraram uma correlação entre a gravidade dos sintomas, a extensão das calcificações e o gene portador de mutação. De forma sistemática, os pesquisadores desenvolveram um sistema padronizado de pontuação das calcificações com base na análise visual do exame de neuroimagem em um estudo duplo-cego: 0 = ausência de calcificação, 1 = pontual; 2 = fraca; 3 = moderada; 4 = severa; 5 = severa e confluente (Figura 4).

Atribuída a pontuação do nível de calcificação das áreas examinadas e determinado o status genético dos pacientes, eles observaram uma maior severidade das calcificações nos pacientes sintomáticos, porém sem relação clara com a severidade clínica. Constataram, também, maior uma pontuação na classificação das calcificações dos pacientes portadores de mutações no gene *SLC20A2*, em comparação aos que têm variação no *PDGFRB* (Nicolas, Gael *et al.*, 2013).

Até o momento, não há um tratamento específico para as CCFP. A grande heterogeneidade clínica da doença mostra que os sintomas, apesar de semelhantes, são também bastante variáveis e por isso não podem ser tratados com um único agente (Lemos *et al.*, 2013). Atualmente, o tratamento pode ser baseado nos principais sintomas e há relatos de casos de pacientes tratados com várias medicações como anticonvulsivantes, estabilizadores de humor, antipsicóticos, antiparkinsonismo, analgésicos, antidepressivos e benzodiazepinos. O prognóstico também é variável com alguns casos em que os sintomas são transitórios após o tratamento (Ramos *et al*., 2017). Estudo pioneiro avaliou pacientes com CCFP quanto aos efeitos do uso de bifosfonatos, uma classe de medicamento vastamente utilizada no tratamento de doenças vasculares e do metabolismo ósseo. Os resultados revelaram que os pacientes tiveram ótima resposta à administração do Alendronato, sem efeitos colaterais, relataram atenuação dos sintomas e o exame de neuroimagem não detectou expansão das calcificações ao longo dos anos (Oliveira e Oliveira, 2016).

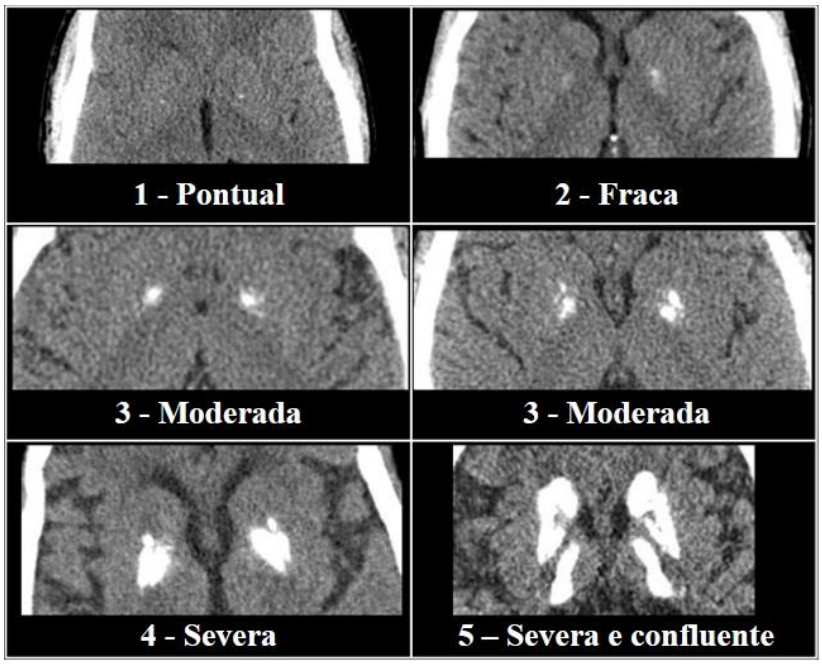

Figura 4. Exemplos da escala de pontuação das calcificações bilaterais nos núcleos basais. Os valores de Hounsfield foram usados a fim de garantir que os sinais hiperdensos realmente indicavam calcificações (Nicolas, Gael *et al.*, 2013).

3.3.3 Genética

Na maioria dos relatos de CCFP hereditárias, observa-se um padrão de segregação autossômico dominante. No entanto, existem casos raros reportados com modelo recessivo, apesar de não serem bem definidos, analisados com base na presença de cruzamentos consanguíneos (Elsaid *et al.*, 2010; Yao *et al.*, 2018).

A caracterização clínica adequada e, sobretudo, a análise da neuroimagem assumem grande importância na definição do modo de herança das CCFP. Muitos são os casos em que a segregação da doença é interpretada como recessiva quando, na verdade, trata-se de um modelo dominante que está sendo mascarado pela ausência de sintomas e pela falta de exames de neuroimagem de pessoas de gerações mais antigas, levando à detecção de falsos negativos (indivíduos saudáveis) (Oliveira, 2011).

A fim de auxiliar nessa questão, a investigação das causas da CCFP assume papel de grande importância, sendo realizada à nível molecular com testes genéticos que têm como objetivo a identificação de variantes patogênicas no DNA. Eles podem incluir desde triagens seriais de genes específicos de forma pontual, painéis que cobrem vários genes simultaneamente a testes genômicos em larga escala (Ramos *et al*., 2017).

3.3.3.1 Mapeamento Genético

A descoberta da estrutura do DNA representou um marco histórico nas pesquisas genéticas e promoveu grandes avanços do desenvolvimento de técnicas de sequenciamento. Os primeiros métodos que permitiram o mapeamento das marcas deixadas pela seleção natural no DNA, envolviam o uso de material radioativo, oferecendo alto risco e com alto nível de complexidade (Tipu e Shabbir, 2015). Grande progresso dessa metodologia foi alcançado quando Frederick Sanger implementou uma forma automatizada com base no uso de terminações fluorescentes acrescentadas às fitas de DNA com posterior análise em sistema de eletroforese capilar (Sanger, Nicklen e Coulson, 1977).

Conhecido como tecnologia de sequenciamento primeira geração, o método Sanger ainda é vastamente utilizado para investigações pontuais e de pequena escala, oferecendo resultados de alta qualidade (Marziali e Akeson, 2001). A plataforma vem sendo aplicada há

décadas e, desde o seu surgimento, vem se aprimorando significativamente culminando em grandes melhorias durante o famoso Projeto do Genoma Humano, iniciado em 1990.

A iniciativa que contou com uma ampla rede internacional, ficou conhecida como o maior projeto colaborativo do mundo e sequenciou o primeiro genoma humano completo, revelando as causas genéticas de centenas de doenças (Consortium, 2004; Metzker, 2009).

No entanto, apesar das vantagens que oferece e dos aperfeiçoamentos alcançados, o sequenciamento capilar automático desenvolvido por Sanger apresenta limitações, o que demonstrava a necessidade de novos métodos (Metzker, 2009).

O próximo passo no avanço das pesquisas do DNA foi dado com o desenvolvimento de tecnologias mais eficiente e de alto rendimento para sequenciamentos em larga escala, conhecidos como sequenciamento de nova geração (*Next-Generation Sequencing - NGS*). Plataformas de NGS, como o sequenciamento do genoma completo (*whole genome sequencing - WGS*) e o sequenciamento do exoma completo (*whole exome sequencing - WES*), têm se tornado cada vez mais acessíveis e usuais com amplo leque de aplicações que vão desde a rotina de laboratórios de diagnóstico à biologia de conservação. Com capacidade de mapeamento de centenas à milhões de sequências com alta precisão e eficiência, um dos avanços proporcionados pelo NGS se reflete na identificação de variações naturais e mutações patogênicas do genoma humano, relevante para o desenvolvimento de terapias personalizadas para portadores de condições genéticas (Besser *et al.*, 2018; Dijk *et al.*, 2018; Fuentes-pardo e Ruzzante, 2017; Fujiki *et al.*, 2018; Lazaridis *et al.*, 2016; Mardis, 2008; Mcginn e Gut, 2013; Tipu e Shabbir, 2015; Warr *et al.*, 2015).

O exoma humano corresponde a cerca de 2% do conteúdo do genoma e é composto por aproximadamente 180.000 sequências de DNA codificante que são transcritas em fitas de RNA, e contêm a maioria das variações genéticas de efeito patogênico. Por meio do WES, é possível mapear quase 95% da totalidade do exoma (Lek *et al.*, 2016; Ramos *et al*., 2017).

As análises e a posterior validação dos resultados de NGS demandam o trabalho de uma equipe multidisciplinar capaz de interpretar o impacto clínico e molecular das variações candidatas. A triagem e refinamento dos dados envolve várias etapas que vão desde de o uso de ferramentas de bioinformática a estudos funcionais que confirmem os efeitos biológicos das variantes (Richards *et al.*, 2015; Warr *et al.*, 2015).

Com esse propósito, os pesquisadores seguem as diretrizes estabelecidas pelo Colégio Americano e Genética Médica e Genômica (*American College of Medical Genetics and Genomics* – ACMG) juntamente com a Associação de Patologia Molecular (*Association for Molecular Pathology* - AMP), que traz os critérios para classificação de variantes observadas em doenças Mendelianas (Tabelas 3 e 4) (Richards *et al.*, 2015).

Paralelamente ao desenvolvimento das técnicas sequenciamento, surge a necessidade de acesso a informações genômicas da população geral que possam ser usadas como parâmetro na classificação de alterações no DNA. Assim, grandes bancos de dados foram fundados (populacionais, de doenças e de sequências genéticas) com a finalidade de agregar informações de centenas de milhares de pessoas, saudáveis e portadoras de doenças, revelando as variações presentes nesses indivíduos e em que frequência elas se apresentam. Do mesmo modo, surgiram inúmeras ferramentas computacionais (*in silico*) que, com base em algoritmos de predição, buscam inferir a patogenicidade das variações genéticas (Richards *et al.*, 2015).

3.3.3.2 Genes Relacionados

As CCFP são geneticamente heterogêneas e o primeiro locus gênico associado à patologia, conhecido como IBGC1 (IBGC - *idiopathic basal ganglia calcification*), foi encontrado em uma extensa família estadunidense que segregava a doença de forma autossômica dominante. Entretanto, os estudos acerca da correlação desse locus com as CCFP se mostraram divergentes e variáveis (Oliveira, 2011).

A região IBGC1 foi identificada durante o estudo de ligação que mapeou o braço longo do cromossomo 14. Geschwind e colaboradores identificaram um haplótipo em comum entre os afetados dessa família, em uma região entre os marcadores D14S70 e D14S66 (Geschwind, Loginov e Stern, 1999). Logo em seguida, o locus IBGC1 foi excluído como candidato à causa das CCFP em cinco famílias, de um total de seis, mapeadas para os mesmos marcadores utilizados por Geschwind em 1999 (Oliveira *et al.*, 2004). Em seu trabalho subsequente, Oliveira e colaboradores decidiram estreitar a busca e sequenciaram 26 genes candidatos dentre o locus IBGC1, descobrindo um polimorfismo não-sinônimo de nucleotídeo único no gene MGEA6/c-TAGE (Oliveira *et al.*, 2007). No entanto,

corroborando com os resultados de Oliveira e colaboradores em 2004, estudos posteriores não confirmaram a segregação do IBGC1 com as CCFP, excluindo esse locus como causal (Brodaty *et al.*, 2002; Volpato *et al.*, 2008).

Posteriormente, duas novas regiões foram identificadas em outros estudos de ligação: IBGC2 (2q37), localizada no cromossomo 2 em extensa família italiana, porém sem gene específico identificado; IBGC3 (8p21.1-q11.23), no cromossomo 8, encontrada em uma família chinesa (Dai *et al.*, 2010; Volpato *et al.*, 2009).

Em decorrência dos avanços nos métodos de mapeamento genético, maiores esclarecimentos acerca das bases moleculares das CCFP foram alcançados. A utilização do WES permitiu a identificação dos quatro genes com variações patogênicas em heterozigose causadoras dessa condição, *SCL20A2*, *PDGFRB*, *PDGFB* e *XPR1*, proporcionando grande avanço no entendimento das bases moleculares da doença (Keller *et al.*, 2013; Legati *et al.*, 2015; Nicolas *et al.*, 2013; Wang *et al.*, 2012).

Em 2012 foi identificada a primeira mutação associada com a CCFP no gene responsável pela codificação do tipo III de um transportador de fosfato inorgânico sódio-dependente (PiT2), o *SLC20A2* (8p11.21) (Wang, Li, Shi, Ren, Patti, Wang, Oliveira, De, *et al.*, 2012). Ele concentra a maioria das variações encontradas nos casos genéticos das CCFP e é reportado como o principal elemento do mecanismo patológico da doença, visto que, sua perda funcional acarreta o acúmulo de fosfato inorgânico (Pi) na matriz extracelular, causando a deposição de fosfato de cálcio (Bøttger and Pedersen, 2011; Wang *et al*., 2012; Yamada *et al*., 2014; Lemos *et al*., 2015; Legati *et al*., 2015b; Ramos *et al*., 2017).

Além de alterações pontuais, variações no número de cópia como duplicações e grandes deleções cromossômicas envolvendo todo o gene *SLC20A2* ou parte dele, também foram relatadas em famílias com membros afetados pelas CCFP (Barker *et al.*, 2014; David *et al.*, 2016; Grütz *et al.*, 2016; Pasanen *et al.*, 2016).

Modelos animais *knock-out* demonstraram que o silenciamento do *SLC20A2* foi capaz de replicar os achados patológicos observados nos pacientes, revelando extensas áreas de calcificações nos gânglios basais, no tálamo, cerebelo e córtex (Jensen, Schrøder e Hejbøl, 2013; Wallingford *et al.*, 2017). Ademais, também foi relatado o impacto da deficiência do *SLC20A2* acarretando no aumento dos níveis de Pi no líquido cefalorraquidiano (CSF –

cerebrospinal fluid), apoiando a ideia de que a PiT2 atuaria no transporte do fosfato presente no CSF para o sangue (Jensen, Autzen e Pedersen, 2016).

Tabela 3. Critérios para classificação de variantes patogênicas (Richards *et al.*, 2015).

Evidence of pathogenicity	Category
Very strong	PVS1 null variant (nonsense, frameshift, canonical ±1 or 2 splice sites, initiation codon, single or multiexon deletion) in a gene where LOF is a known mechanism of disease
	Caveats: • Beware of genes where LOF is not a known disease mechanism (e.g., *GFAP*, *MYH7*) • Use caution interpreting LOF variants at the extreme 3′ end of a gene • Use caution with splice variants that are predicted to lead to exon skipping but leave the remainder of the protein intact • Use caution in the presence of multiple transcripts
Strong	PS1 Same amino acid change as a previously established pathogenic variant regardless of nucleotide change
	Example: Val→Leu caused by either G>C or G>T in the same codon
	Caveat: Beware of changes that impact splicing rather than at the amino acid/protein level
	PS2 De novo (both maternity and paternity confirmed) in a patient with the disease and no family history
	Note: Confirmation of paternity only is insufficient. Egg donation, surrogate motherhood, errors in embryo transfer, and so on, can contribute to nonmaternity.
	PS3 Well-established in vitro or in vivo functional studies supportive of a damaging effect on the gene or gene product
	Note: Functional studies that have been validated and shown to be reproducible and robust in a clinical diagnostic laboratory setting are considered the most well established.
	PS4 The prevalence of the variant in affected individuals is significantly increased compared with the prevalence in controls
	Note 1: Relative risk or OR, as obtained from case–control studies, is >5.0, and the confidence interval around the estimate of relative risk or OR does not include 1.0. See the article for detailed guidance.
	Note 2: In instances of very rare variants where case–control studies may not reach statistical significance, the prior observation of the variant in multiple unrelated patients with the same phenotype, and its absence in controls, may be used as moderate level of evidence.
Moderate	PM1 Located in a mutational hot spot and/or critical and well-established functional domain (e.g., active site of an enzyme) without benign variation
	PM2 Absent from controls (or at extremely low frequency if recessive) (**Table 6**) in Exome Sequencing Project, 1000 Genomes Project, or Exome Aggregation Consortium
	Caveat: Population data for insertions/deletions may be poorly called by next-generation sequencing.
	PM3 For recessive disorders, detected in *trans* with a pathogenic variant
	Note: This requires testing of parents (or offspring) to determine phase.
	PM4 Protein length changes as a result of in-frame deletions/insertions in a nonrepeat region or stop-loss variants
	PM5 Novel missense change at an amino acid residue where a different missense change determined to be pathogenic has been seen before
	Example: Arg156His is pathogenic; now you observe Arg156Cys
	Caveat: Beware of changes that impact splicing rather than at the amino acid/protein level.
	PM6 Assumed de novo, but without confirmation of paternity and maternity
Supporting	PP1 Cosegregation with disease in multiple affected family members in a gene definitively known to cause the disease
	Note: May be used as stronger evidence with increasing segregation data
	PP2 Missense variant in a gene that has a low rate of benign missense variation and in which missense variants are a common mechanism of disease
	PP3 Multiple lines of computational evidence support a deleterious effect on the gene or gene product (conservation, evolutionary, splicing impact, etc.)
	Caveat: Because many in silico algorithms use the same or very similar input for their predictions, each algorithm should not be counted as an independent criterion. PP3 can be used only once in any evaluation of a variant.
	PP4 Patient's phenotype or family history is highly specific for a disease with a single genetic etiology
	PP5 Reputable source recently reports variant as pathogenic, but the evidence is not available to the laboratory to perform an independent evaluation

LOF, loss of function; OR, odds ratio.

Tabela 4. Critérios para classificação de variantes benignas (Richards *et al.*, 2015).

Evidence of benign impact	Category
Stand-alone	BA1 Allele frequency is >5% in Exome Sequencing Project, 1000 Genomes Project, or Exome Aggregation Consortium
Strong	BS1 Allele frequency is greater than expected for disorder (see **Table 6**)
	BS2 Observed in a healthy adult individual for a recessive (homozygous), dominant (heterozygous), or X-linked (hemizygous) disorder, with full penetrance expected at an early age
	BS3 Well-established in vitro or in vivo functional studies show no damaging effect on protein function or splicing
	BS4 Lack of segregation in affected members of a family
	Caveat: The presence of phenocopies for common phenotypes (i.e., cancer, epilepsy) can mimic lack of segregation among affected individuals. Also, families may have more than one pathogenic variant contributing to an autosomal dominant disorder, further confounding an apparent lack of segregation.
Supporting	BP1 Missense variant in a gene for which primarily truncating variants are known to cause disease
	BP2 Observed in *trans* with a pathogenic variant for a fully penetrant dominant gene/disorder or observed in *cis* with a pathogenic variant in any inheritance pattern
	BP3 In-frame deletions/insertions in a repetitive region without a known function
	BP4 Multiple lines of computational evidence suggest no impact on gene or gene product (conservation, evolutionary, splicing impact, etc.)
	Caveat: Because many in silico algorithms use the same or very similar input for their predictions, each algorithm cannot be counted as an independent criterion. BP4 can be used only once in any evaluation of a variant.
	BP5 Variant found in a case with an alternate molecular basis for disease
	BP6 Reputable source recently reports variant as benign, but the evidence is not available to the laboratory to perform an independent evaluation
	BP7 A synonymous (silent) variant for which splicing prediction algorithms predict no impact to the splice consensus sequence nor the creation of a new splice site AND the nucleotide is not highly conserved

Posteriormente à identificação do gene *SLC20A2*, variantes patogênicas foram encontradas no gene responsável pela codificação do receptor de um membro da família do fator de crescimento derivado de plaqueta, o *PDGFRβ* (*platelet-derived growth fator receptor beta*), e em seu principal ligante, o *PDGFβ* (Keller *et al.*, 2013; Nicolas, Gaël *et al.*, 2013).

O gene *PDGFRβ* (5q32) codifica uma proteína receptora de tirosina quinase presente na membrana celular e é expresso em células neuronais, células vasculares da musculatura lisa, pericitos, plexo coroide, núcleo dentado e gânglios da base do cérebro humano. A via celular envolvendo os genes *PDGFβ* (22q13.1) e seu receptor desempenha função importante no processo de angiogênese, recrutamentos de pericitos e na manutenção da integridade da barreira hematoencefálica (*BBB - blood brain barrier*). Mutações de perda de função nesses dois genes comprometem a permeabilidade da BBB e podem ocasionar, potencialmente, calcificações vasculares e na região perivascular do cérebro. Camundongos hipomórficos para o gene *PDGFβ* também reproduziram os fenômenos observados em pacientes, desenvolvendo progressivos processos de calcinose devido à deficiência de pericitos na

proteção da BBB (Betsholtz e Keller, 2014; Daneman R, Zhou L, Kebede AA, 2010; Keller *et al.*, 2013; Nakamura, Arimura e Nishimura, 2016; Vanlandewijck *et al.*, 2015).

O gene *XPR1* (1q25.3) (*xenotropic and polytropic retrovirus receptor 1*) codifica uma proteína transmembrana identificada em células de mamíferos como o receptor retroviral de vírus xenotrópico e politrópico de murinos. A função da proteína codificada pelo *XPR1* é bastante conservada evolutivamente e envolve a homeostase de fosfato celular, mediando sua exportação do citoplasma para o meio extracelular (Giovannini *et al.*, 2013).

Mutações ligadas às CCFP relatadas nesse gene são herdadas sob um caráter autossômico dominante e localizam-se no domínio regulatório da proteína, inibindo a exportação do Pi e alterando a expressão proteica na superfície celular (Anheim *et al.*, 2016; Legati *et al.*, 2015).

A descoberta dos genes relacionados a fisiopatologia das CCFP, sugere que diferentes vias celulares podem acarretar em fenótipos semelhantes (Figura 5) (Batla *et al.*, 2017).

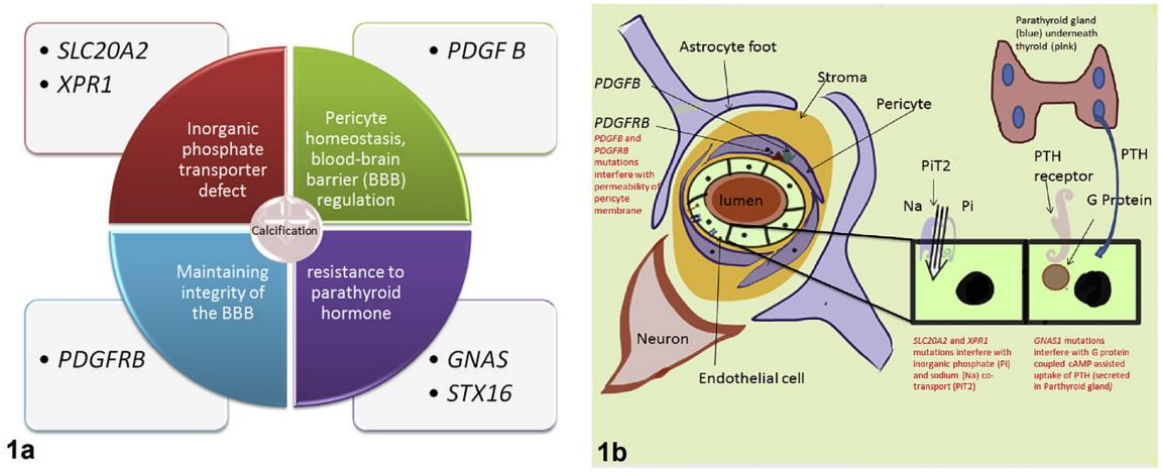

Figura 5. a. Gráfico representativo contendo os principais mecanismos responsáveis por calcificações cerebrais e os genes envolvidos. **b.** Representação esquemática dos mecanismos de causa genética envolvidos com deposição microvascular de cálcio no cérebro. A figura mostra um corte transversal de um vaso sanguíneo do cérebro demonstrando a localização dos pericitos e de células do sistema nervoso (astrócito e neurônio). A perda de função dos genes *PDGFβ* e *PDGFβ*, localizados nos pericitos, pode causar alterações nessas células de forma gradativa, provocando a formação de calcificação microvascular. O fluxo de fosfato inorgânico é prejudicado por mutações patogênicas nos genes *SLC20A2* e *XPR1*. A captação do paratormônio é facilitada pela atividade do AMP cíclico acoplado à proteína G. esse mecanismo pode ser interrompido quando há mutações no gene GNAS1. Adaptado de Batla et al., 2017.

3.3.3.3 Expressão Gênica

Além de prejuízos funcionais à nível proteico, variações genéticas são capazes de produzir efeitos biológicos que se refletem na alteração dos níveis de expressão do gene afetado ou de genes da mesma via celular. Estudar a associação entre variações no DNA e os genes que as carregam representa um desafio, uma vez que os mecanismos celulares de regulação da expressão gênica ocorrem em múltiplos níveis e de diversas formas. A interpretação biológica de como uma mutação afeta os níveis de um gene, depende também do tipo de variação (Jia e Zhao, 2017).

Por exemplo, fitas de mRNA que contenham uma mutação que introduza um *stop* códon prematuramente em sua sequência, serão tipicamente degradadas pelo mecanismo chamado *nonsense-mediated decay* (NMD), o que levará a diminuição da concentração desse transcrito e do seu produto proteico (Ferreira *et al.*, 2014).

Assim, mudanças no padrão de expressão de determinados genes podem ser um indicativo da desregulação dos processos biológicos em que o gene está envolvido. Desse modo, testes baseados na análise dos padrões de expressão de determinados genes são de grande utilidade clínica e vem sendo aplicados como ferramentas no diagnóstico de condições como câncer e doenças coronárias (Bueno *et al.*, 2004; McPherson *et al.*, 2013; Rhees e Wingrove, 2015; Zanotti *et al.*, 2014; Zeller e Blankenberg, 2013).

Alguns estudos demonstraram a capacidade de aferir alterações no perfil de expressão do gene *SLC20A2* diante da presença de diferentes tipos de mutações patogênicas, utilizando amostras de sangue periférico de pessoas afetadas pelas CCFP (Ferreira *et al.*, 2014; Zhang, Guo e Wu, 2013). Em contrapartida, análises com amostras de fibroblastos de pacientes não detectaram diferenças na expressão do *SLC20A2* em comparação aos indivíduos saudáveis, mas detectaram diminuição na internalização do Pi e diferenças na localização sub celular da proteína PiT2 (Taglia *et al.*, 2018).

4 MÉTODO

4.1 PACIENTES E AMOSTRAS

Os pacientes incluídos no trabalho foram triados quanto à 1) presença de calcificações bilaterais e simétricas nos gânglios basais observados em exame de neuroimagem e 2) ausência de doenças metabólicas investigadas no exame de sangue demonstrando níveis séricos normais de fosfato, cálcio e hormônios da tireoide. Foram coletadas amostras de sangue periférico de 21 membros de uma família brasileira agrupados em quatro categorias: 1) afetados (pacientes com calcificações bilaterais observadas no exame de TC); 2) não afetados (pessoas com resultado negativo na TC para calcificações); 3) *status* desconhecido (indivíduos assintomáticos e sem exame de neuroimagem disponível); 4) portadores obrigatórios (de acordo com o padrão de herança autossômico dominante das CCFP, indivíduos assintomáticos sem exame de neuroimagem disponível porém, com filhos afetados) (Tabela 1). Todos os participantes do estudo assinaram termo de consentimento. O projeto foi aprovado pelo comitê de ética da Universidade Federal de Pernambuco (CAAE-0296.0.172.000-08 e CAAE - 09475912.8.0000.5208).

4.2 EXTRAÇÃO DE DNA

O DNA genômico foi extraído com o kit Wizard® Genomic DNA Purification Kit (Promega), segundo instruções do fabricante. A concentração e o grau de pureza das amostras foram obtidos por meio da absorbância a 260nm com o espectrofotômetro NanoDrop® (Thermo Scientific).

Tabela 1. Achados clínicos dos indivíduos da família brasileira (ND = não sisponível).

STATUS	ID	PEDIGREE	IDADE	NEUROIMAGEM	SINTOMAS	OBSERVAÇÕES
Afetado	1G01BR	III.6	44	TC	Assintomático	
	1G02BR15	II.14	55	TC	Disfonia, disfagia, paralisia das pregas vocais (revertida), vertigem, tremores, dor de cabeça, paralisia facial, desequilíbrio, indisposição, paresia em musculatura proximal de membro superior esquerdo	Tratamento com Alendronato iniciado em 2016
	1G08BR16	II.4	70	TC	Perda de memória moderada, ansiedade, dor de cabeça e vertigem	Realizou histerectomia
	1G14BR16	III.7	41	TC	Depressão, ansiedade, insônia, perda de memória leve, dor de cabeça desde a infância	Tratamento com Rivotril e Paroxetina
	1G17BR16	III.10	37	TC	Enxaqueca frequente, vertigem	
Portador obrigatório	1G05BR16	II.9	65	RM (laudo)	Assintomático	Realizou cirurgia para hidrocefalia em 2014
	1G07BR16	II.7	68	ND	Ansiedade e dor de cabeça	Tratamento com ansiolítico
Não afetado	1G03BR16	II.12	62	TC/RM (laudo)	Dor de cabeça, depressão	Tratamento contra depressão com Efexor-XR75; Calcificação na pineal e no plexo coroide
	1G09BR16	II.3	71	TC	AVC, artrite reumatóide	Apresenta afasia em decorrência do AVC; faz uso de Alendronato, vitamina D, anticonvulsivantes e medicamentos para tratamento da artrite
	1G19BR16	III.12	40	TC	Síndrome do pânico, depressão, ansiedade, dor de cabeça	Calcificação na pineal e no plexo coroide
	1G20BR16	III.14	35	TC	Epilepsia desde a infância, depressão, ansiedade, dor de cabeça rara, vertigem, perda de memória recorrente.	Tratamento para epilepsia cessou as crises nos últimos 7 anos
Status desconhecido	1G04BR16	II.11	63	ND	Dor de cabeça (sinusite)	Fez tireoidectomia aos 17 anos
	1G06BR16	II.8	67	ND	Dor de cabeça (sinusite)	
	1G10BR16	II.2	72	ND	Ansiedade	Tratamento para ansiedade com Somalium
	1G11BR16	III.1	48	ND	Tremor essencial	
	1G12BR16	III.4	41	ND	Dor de cabeça	
	1G13BR16	III.5	48	ND	Nefrolitiase, ansiedade, insônia, dor de cabeça	Fez tireoidectomia; diminuição das dores de cabeça após a cirurgia; tratamento com suplementação hormonal
	1G15BR16	III.8	36	ND	Assintomático	
	1G16BR16	III.9	36	ND	TDAH	
	1G18BR16	III.11	36	ND	Assintomático	
	1G21BR16	IV.1	24	ND	Dor de cabeça	

4.3 SEQUENCIAMENTO SANGER

A triagem de variantes genéticas foi iniciada com a amplificação do DNA genômico pela técnica de PCR (*polymerase chain reaction*) seguida do sequenciamento na plataforma Sanger da região codificante dos quatro genes associados às CCFP na seguinte ordem: *SLC20A2*, *PDGFRβ*, *PDGFβ* e *XPR1*.

O caso *índex*, ou probando (primeiro indivíduo afetado a ser estudado, antes da captação das amostras dos seus familiares), também fora triado por outra estudante em 2013 (dados não publicados) para genes candidatos pertencentes à família PDGF (*PDGFA*, *PDGFRA*, *PDGFC* e *PDGFD*). Os primers utilizados foram extraídos de estudos previamente publicados na literatura e cada par amplifica um produto correspondente a uma região codificante do gene (Keller *et al.*, 2013; Legati, Giovannini, Nicolas, López-Sánchez, Quintáns, Oliveira, João R.M., *et al.*, 2015; Nicolas, Gaël *et al.*, 2013; Wang, Li, Shi, Ren, Patti, Wang, Oliveira, De, *et al.*, 2012).

Os resultados do sequenciamento Sanger foram analisados no *software* CLC Main Workbench (Qiagen, EUA) e as variações encontradas foram anotadas no banco de variações do nosso grupo e pesquisadas em bancos de dados online: dbSNP (http://www.ncbi.nlm.nih.gov/projects/SNP/), *Exome Variant Server* (http://evs.gs.washington.edu/EVS/), e *Ensembl* (http://grch37.ensembl.org/Homo_sapiens/Info/Index). Variantes com frequência alélica (MAF – *minor allele frequency*) menores que 1% foram classificadas como candidatas, em seguida, analisadas em *softwares* de predição da patogenicidade, a fim de testar seus possíveis efeitos. Para isso, foram utilizadas ferramentas como o MutationTaster2 (http://www.mutationtaster.org/), PolyPhen2 (http://genetics.bwh.harvard.edu/pph2/index.shtml) e SIFT (http://sift.jcvi.org/).

4.4 SEQUENCIAMENTO DO EXOMA COMPLETO

A região do exoma de quatro membros da família brasileira (três afetados e um não afetado) foi isolada pelo kit SeqCap EZ Human Exome Kit v3.0 (Roche NimbleGen, Madison, WI) e sequenciada na plataforma Illumina HiSeq2500 no Centro de Genômica e Neurociência da Universidade da Califórnia (www.semel.ucla.edu/ungc).

As sequências lidas no exoma foram mapeadas no genoma de referência GRCh37/hg19 a as variantes analisadas simultaneamente em todas as amostras com a ferramenta GATK Haplotype Caller segundo recomendações do *GATK Best Practices* (Mckenna *et al.*, 2010). Ingenuity Variant Analysis (QIAGEN, Redwood City, CA) e Ensembl Variant Effect Predictor (http://grch37.ensembl.org/Homo_sapiens/Tools/VEP) foram usados para anotação e filtragem das variantes.

A região exônica dos quatro genes conhecidos causadores das CCFP foram triados prioritariamente para investigar a presença de novas variações ou já conhecidas. Os transcritos usados como referência (RefSeq ID) para estes genes, foram: NM_006749 (*SLC20A2*), NM_002608 (*PDGFB*), NM_002609 (*PDGFRB*), e NM_004736 (*XPR1*). Às variantes candidatas foram aplicados os seguintes filtros: 1) foram excluídas variantes com MAF maior que 1% anotadas nos bancos de dados *1000 Genomes* (1000G: http://browser.1000genomes.org/), *Exome Variant Server* (EVS: http://evs.gs.washington.edu/EVS/) e *Exome Aggregation Consortium* (ExAC: http://exac.broadinstitute.org/); 2) em seguida, foram agrupadas variantes missense, indels, start/stop códon, de alteração de sítios de splice e, por fim 3) aquelas que estivessem co-segregando com a doença sob um modelo dominante (indivíduos afetados são heterozigotos enquanto não afetados são portadores do alelo de referência).

Para validação das variantes candidatas e identificação de possíveis falsos positivos gerados por erros no sequenciamento, amplificação do DNA genômico por PCR seguida por sequenciamento Sanger foi realizado nas regiões flanqueadoras dessas variações.

5 RESULTADOS

Os exames de tomografia computadorizada revelaram calcificações simétricas e bilaterais nos afetados da família brasileira, na região do núcleo caudado, tálamo e putâmen (Figura 1).

O sequenciamento do exoma completo gerou 101.889 leituras com uma média de cobertura de 79x dentro de uma região de 64Mb (89,9% com no mínimo 20x de cobertura) (Tabela 1). Ao todo, observamos cinco variações na região codificante de alguns dos genes

SLC20A2, *PDGFRβ*, *PDGFβ* e *XPR1*, porém não foram identificadas variantes patogênicas (Tabela 2).

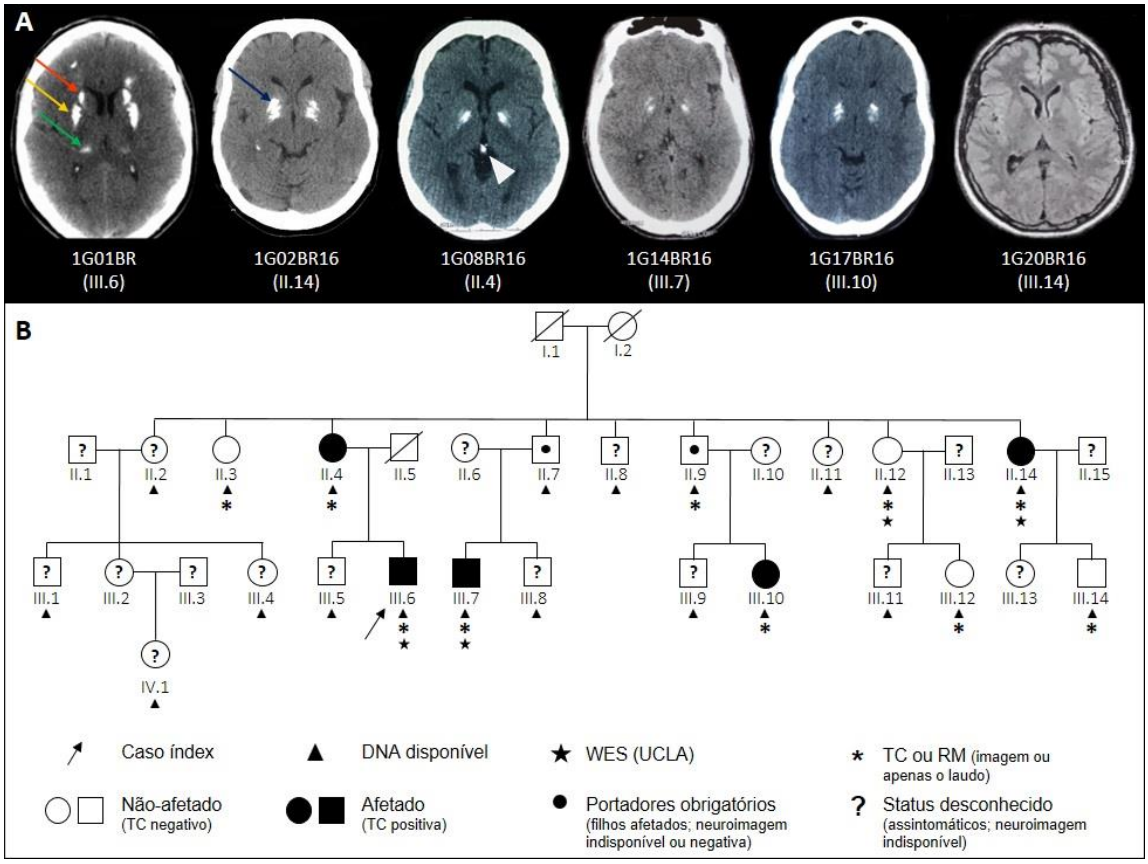

Fig. 1 (A) TC e RM (FLAIR - 1G20BR16) do cérebro de seis membros da família brasileira: 1G01BR (III.6), 1G02BR15 (II.14), 1G08BR16 (II.4), 1G14BR16 (III.7) e 1G17BR16 (III.10) são pacientes com CCFP e não têm variações patogênicas na região codificante dos genes *SLC20A2*, *PDGFB*, *PDGFRB* e *XPR1*; o indivíduo 1G20BR16 (III.14) não apresenta calcificações no exame de RM (FLAIR). As calcificações aparecem como áreas de hiperdensidade (brilhantes) na TC: núcleo caudado (seta vermelha); putâmem (seta amarela); tálamo (seta verde); globo pálido (seta azul), pineal (cabeça de seta). **(B)** Heredograma da nova família candidata para as CCFP.

Tabela 2. Número total de leituras e cobertura de cada amostra.

ID da amostra	Número total de leituras (milhões)	Média da profundidade de cobertura	Região alvo com cobertura mínima de 20x
1G01BR	108	84x	91,3%
1G02BR	111	78x	80,4%
1G14BR	108	76x	89,7%
1G03BR	108	77x	89,1%

Ao longo dos quatro exomas sequenciados, identificamos 101.899 variantes no total. Após a aplicação dos filtros e exclusão das variações comuns na população geral (MAF>1%) e das que não segregavam com a doença, restaram 493. Dessas, apenas 49 foram preditas como causadoras de danos à nível proteico, incluindo: 2 in-frame, 2 splice-aceptor, 2 *stop gained* e 43 variações missenses. Dentre essas variações, algumas foram preditas como potenciais artefatos, isto é, aquelas com frequência alélica menor que 20 % (proporção de números de leituras com o alelo alternativo em determinada posição em relação ao número total de leituras naquela mesma posição). Outros potenciais artefatos também são das inserções e deleções em regiões repetidas em tandem associadas a doenças conhecidas.

A fim de reduzir substancialmente o número de variações candidatas, seguimos as recomendações do *American College of Medical Genetics and Genomics* (ACMG) que orientam a investigação por evidências de patogenicidade (Richards *et al.*, 2015). A observação da presença de algumas variações em homozigose em controles, também é indício de inconsistência da sua patogenicidade.

Tabela 3. Variantes encontradas na região codificante dos genes ligados à CCFP (* indica portadores homozigotos para aquela variante).

ID da amostra	Posição	Alelos		Símbolo do gene	Transcrito Canônico			Predição da Função		dbSNP ID	MAF (%)		
		Ref	Alt		Variante Codificante	Variante Proteica	Impacto na translação	SIFT	Polyphen		1000 G	EVS	ExAC
1G01BR	8:42323380	C	T	*SLC20A2*	c.345G>A	p.T115T	sinônima	-	-	rs34124953	0.5	0.5	0.7’
1G01BR 1G02BR15* 1G03BR16* 1G14BR16	5:149495395	T	C	*PDGFRβ*	c.3252A>G	p.P1084P	sinônima	-	-	rs246388	28.5	39.9	34.7
1G03BR16	5:149497228	G	A	*PDGFRβ*	c.3090C>T	p.P1030P	sinônima	-	-	rs2228440	6.2	10.0	7.6
1G01BR 1G02BR15* 1G03BR16 1G14BR16	5:149499672	T	C	*PDGFRβ*	c.2601A>G	p.L867L	sinônima	-	-	rs246395	23.6	28.1	28.7
1G02BR15	5:149509446	C	T	*PDGFRβ*	c.1453G>A	p.E485K	sinônima	Tolerada	Benigna	rs41287110	1.1	1.9	1.9

Foram identificados de 1 a 83 homozigotos para 15 variantes dentre as 60.706 sequências de indivíduos depositados no ExAC. Ao passo que é importante não supervalorizar dados de ferramentas *in silico*, é importante ressaltar que 29 variações foram preditas como não exercendo impacto na função do gene ou na proteína, por múltiplos algoritmos computacionais (classificadas como não deletérias por pelo menos dois das ferramentas usadas: SIFT, Polyphen, CADD e Condel).

Dentre as variantes candidatas mais promissoras, identificamos algumas presentes em genes associados com o transporte de cálcio. Assim, decidimos seguir com a investigação, agora por Sanger, priorizando a análise das variações raras (sem homozigotos reportados no ExAC) preditas deletérias *in silico* ligadas ao metabolismo de cálcio: *PLCB2*, *RYR1*, *MKNK2* e *RYR3*.

Identificamos uma variante em um sítio de splice do gene *PLCB2*, que codifica a Fosfolipase C Beta 2, c.2432-1G>A (reportada no ExAC em apenas um indivíduo de ancestralidade Africana). Funções ligadas a esse gene incluem ativação plaquetária, via de dor neuropática em neurônios dorsais da medula, ligação de íons de cálcio e atividade da diester fosfórico hidrolase (Gene Cards: http://www.genecards.org/cgi-bin/carddisp.pl?gene=PLCB2). O sequenciamento Sanger confirmou a presença dessa variação apenas nos três indivíduos afetados estando ausente na amostra controle, corroborando com o achado no exoma. Entretanto, a análise revelou que a variação c.2432-1G>A também estava segregando nos outros três indivíduos (dois afetados e um controle), mostrando que ela não atende aos critérios de patogenicidade uma vez que está presente em indivíduo saudável.

Outra variante em um sítio de splice (c.420-2A>C) foi encontrada no gene *MKNK2*, responsável por codificar um membro da família de proteínas kinases dependentes do complexo cálcio/calmodulina (CAMK) Ser/Thr (GeneCards: http://www.genecards.org/cgi-bin/carddisp.pl?gene=MKNK2). No entanto, como sugerido pelo baixo valor da frequência alélica dessa variação, somado à baixa cobertura de leitura, o sequenciamento Sanger revelou que se tratava de um artefato, pois que nenhuma das amostras portava essa variante.

Variações missense em outros dois genes ligados a via de transporte de cálcio, receptores de rianodina (*RYR1* e *RYR3*) foram classificadas como deletérias. *RYR1* dá origem a uma proteína receptora de rianodina encontrado nos músculos esqueléticos e que funciona como um canal de liberação de cálcio do retículo sarcoplasmático para o citoplasma e, assim, exerce papel importante na contração muscular (GeneCards: http://www.genecards.org/cgi-bin/carddisp.pl?gene=RYR1&keywords=RYR1). Ficou confirmada, pelo sequenciamento Sanger, a presença da variação missense c.1474C>G:p.Arg492Gly em quatro dos cinco

indivíduos afetados triados no laboratório da UCLA. Desse modo, por não estar presente em todos os pacientes, essa variação foi excluída da análise. Similarmente, ao *RYR1*, o gene *RYR3* também codifica um receptor de rianodina que atua na exportação de cálcio do retículo sarcoplasmático para o meio citosólico.

Diferentemente do seu homólogo, o *RYR3* é vastamente expresso, com níveis mais altos nos gânglios basais, amigdala e córtex (GTEx data: http://www.gtexportal.org/home/), e assim, também media a liberação de cálcio do retículo endoplasmático em células não musculares (GeneCards: http://www.genecards.org/cgi-bin/carddisp.pl?gene=RYR1&keywords=RYR3). A variação missense c.2486G>A:p.Arg829His no *RYR3* foi confirmada pelo método Sanger, segregando nas amostras de todos os afetados enviados para análise, e ausente nos indivíduos controle. Os resultados eram indicativos de que o gene *RYR3* seria um forte candidato a novo gene causal das CCFP, uma vez que a variação encontrada preenchia os critérios de seleção e, sobretudo, o gene está diretamente ligado a uma via celular relevante na fisiopatologia das calcificações cerebrais.

Em seguida, expandimos a análise a todos os outros membros da família de que dispomos amostras em nosso banco, a fim de confirmar o padrão de segregação autossômico dominante da variação c.2486G>A:p.Arg829His identificada no *RYR3*. Surpreendentemente, a variante também está segregando 1) nos dois indivíduos classificados como portadores obrigatórios, corroborando com a possibilidade de serem, na verdade, afetados, 2) em dois indivíduos categorizados como status desconhecido e 3) em um não afetado.

Então, voltamos aos dados inicias do exoma e realizamos nova análise da lista com 49 variações candidatas, aplicando outros critérios de exclusão, e agrupamos variações em seis novos genes (Figura 2). Após triagem com o sequenciamento Sanger, constatamos que as novas variantes também não atendiam aos requisitos para serem classificadas como causais, pois elas segregavam 1) em ambos afetados e não afetados ou 2) estavam ausentes nos afetados.

STATUS	SAMPLE ID	PEDIGREE	AGE	RYR3	ZNF233	REV3L	ZNF546	KIR2DL3		KIR3DL3
				c.2486G>A	c.1356T>G	c.731A>C	c.1991C>A	c.662C>T	c.110C>G	c.961A>T
Affected	1G01BR	III.6	44							
	1G02BR	II.14	55							
	1G08BR	II.4	70							
	1G14BR	III.7	41							
	1G17BR	III.10	37							
Obligate carrier	1G05BR	II.9	65							
	1G07BR	II.7	68							
Non-affected	1G03BR	II.12	62							
	1G09BR	II.3	71							
	1G19BR	III.12	40							
	1G20BR	III.14	35							
Unknown status	1G04BR	II.11	63							
	1G06BR	II.8	67							
	1G10BR	II.2	72							
	1G11BR	III.1	48							
	1G12BR	III.4	41							
	1G13BR	III.5	48							
	1G15BR	III.8	36							
	1G16BR	III.9	36							
	1G18BR	III.11	36							
	1G21BR	IV.1	24							

Fig. 2. Status dos indivíduos investigados para as variações candidatas identificadas no sequenciamento do exoma. Verde: portador da variação; vermelho: não portador; branco: amostra não sequenciada.

5.1 PERSPECTIVAS

Seguindo as recomendações de investigação e diagnóstico das CCFP, após o contato com os membros da família brasileira e investigação clínica dos membros afetados e saudáveis, foi realizada a triagem da região codificante de cada um dos quatro genes ligados a doença. Com base na frequência relativa de variantes patogênicas, priorizamos o sequenciamento do gene *SLC20A2* e, na ausência de mutações patogênicas, seguimos com as análises para os genes *PDGFβ*, *PDGFRβ* e *XPR1*, nessa ordem.

A ausência de variações nos quatro genes conhecidos, tornou a família elegível para a investigação do exoma, na busca por novos genes ou variações não observadas no método Sanger.

Os resultados acerca da variação no gene *RYR3* ainda se mostram bastante promissores. Entretanto, devido aos resultados negativos obtidos até o momento, faz-se necessária uma maior investigação clínica de alguns indivíduos dos quais temos poucas informações ou não possuímos exames de neuroimagem. O primeiro passo será confirmar o status dos indivíduos categorizados como portadores obrigatórios, status desconhecido e não afetados. Novos exames de neuroimagem como tomografia computadorizada permitirão esclarecer essa questão.

Outro ponto a ser refletido é que resultados de sequenciamento do exoma podem apresentar limitações devido ao seu design e não revelam, diretamente, a presença de grandes duplicações ou deleções, sejam parciais ou totais.

Em parceria com o grupo liderado pelos Dr. Hannequin e Dr. Nicolas, em 2015 encaminhamos ao seu laboratório em Rouen (França) algumas amostras do nosso banco de pacientes (casos índex de 29 famílias), a fim de investiga-los quanto à presença de variações do número de cópia (CNV – *copy number variation*) (David *et al.*, 2016; Nicolas *et al.*, 2014).

No momento, possuíamos em nosso laboratório, apenas a amostra do caso índex (1G01BR) dessa família, que foi mapeado para o gene *SLC20A2* em ensaio capaz de identificar CNVs completos e parciais (envolvendo apenas um éxon). Os resultados foram negativos e então, seguiu-se com a análise dos *PDGFβ* e *PDGFRβ*, apenas para dois éxons de cada gene, devido à falta de primers para mapeá-los em tua totalidade. Também não foi identificada a presença de CNVs nesse ensaio. Na época, ainda não se conhecia a relação causal do gene XPR1 e as CCFP, portanto, ele não foi incluído nas análises.

A falta de resultados conclusivos do primeiro exoma e das posteriores triagens por Sanger, nos levaram a enviar as amostras de afetados e alguns controles da família brasileira para um novo WES, que será realizado em Rouen. O exoma será mapeado com outro kit de captura (Agilent Sureselect All Exons Human V5 Kit - Agilent technologies, Santa Clara, CA, USA) e os resultados serão submetidos à uma investigação mais abrangente para a presença de CNVs porém, com a ferramenta *in silico* desenvolvida pelos pesquisadores do grupo francês, o CANOES (David *et al.*, 2016).

6 CONCLUSÕES

- ✓ As CCFP são uma condição neuropsiquiátrica clinicamente heterogênea que pode manifestar-se já durante a infância, em casos mais raros, ou entre a quinta e a sexta década de vida.

- ✓ A popularização de exames não invasivos para a detecção das calcificações cerebrais, bem como os avanços nas técnicas de neuroimagem, permitirão o diagnóstico precoce da doença em casos hereditários da doença.

- ✓ Os resultados do presente trabalho, realizado em parceria com grandes centros internacionais, reforçam o papel dos genes já conhecidos associados às bases moleculares das CCFP.

- ✓ As novas variantes reportadas ajudarão a esclarecer casos futuros CCFP hereditários e auxiliarão na interpretação do impacto de novas variações genéticas. Além disso, fornecem uma lista de candidatos para ensaios funcionais.

- ✓ São necessários estudos prospectivos que acompanham a progressão de pacientes portadores de variações genéticas patogênicas nos genes ligados às CCFP, a fim de expandir nosso conhecimento acerca do curso da doença, dos fatores genéticos e ambientais que podem influenciar na progressão e na penetrância da patologia.

- ✓ Devido às limitações técnicas e metodológicas de ambas as plataformas de sequenciamento, capilar (Sanger) e NGS (exoma), não identificamos variações candidatas nos pacientes da família brasileira reportada no estudo.

- ✓ Também não foram encontradas CNVs nos gene *SLC20A2*, *PDGFβ* e *PDGFRβ*, parciais nem totais. Um ensaio para o gene *XPR1* ainda se faz necessário.

- ✓ Uma nova triagem do exoma da família brasileira por meio de novo kit de captura e método de triagem dos dados, poderá auxiliar a responder os casos negativos pendentes em nosso banco de amostras, bem como nos bancos dos grupos colaboradores.

- ✓ Devido ao fato de os genes *SLC20A1*, *SLC20A2* e *XPR1* estarem ligados ao transporte de fosfato inorgânico através da membrana celular, ainda que em direções opostas (*SLC20A1* e *SLC20A2*, importação; *XPR1*, exportação), é comum a suspeita de um mecanismo de coregulação entre eles.

- ✓ Os estudos de expressão demonstraram que mutações de diferentes naturezas no *SLC20A2* diminuiu seus níveis de mRNA porém, os genes *SLC20A1* e *XPR1* não sofreram efeitos colaterais explícitos desse mecanismo.

- ✓ Tais resultados sugerem que não há uma compensação da haploinsuficiência do *SLC20A2* por parte dos outros dois genes transportadores de fosfato.

REFERÊNCIAS

ABATE, E. G.; CLARKE, B. L. Review of hypoparathyroidism. **Frontiers in Endocrinology**, v. 7, n. JAN, p. 1–7, 2017.

ADAMS, L. C.; BRESSEM, K.; BÖKER, S. M.; BENDER, Y.-N. Y.; NÖRENBERG, D.; HAMM, B.; MAKOWSKI, M. R. Diagnostic performance of susceptibility-weighted magnetic resonance imaging for the detection of calcifications: A systematic review and meta-analysis. **Scientific Reports**, v. 7, n. 1, p. 15506, 2017.

ANHEIM, M. *et al.* XPR1 mutations are a rare cause of primary familial brain calcification. **Journal of Neurology**, v. 263, n. 8, p. 1559–1564, 2016.

ARON, S.; ANUPRIYA, A.; SUNITHI, M.; MATHEW, V.; MAYA, T.; GOYAL, M. K.; ALENXANDER, M. MELAS: Recurrent reversible hemianopia. **Neurology India**, v. 58, n. 5, p. 791–793, 2010.

AVRAHAMI, E.; COHN, D. F.; FEIBEL, M.; TADMOR, R. MRI Demonstration and CT Correlation of the Brain in Patients with Idiopathic Intracerebral Calcification. **J Neurol**, v. 241, n. 6, p. 381–384, 1994.

BARKER, M. *et al.* SLC20A2 and THAP1 deletion in familial basal ganglia calcification with dystonia. **Neurogenetics**, v. 15, n. 1, p. 23–30, 2014.

BATLA, A.; TAI, X. Y.; SCHOTTLAENDER, L.; ERRO, R.; BALINT, B.; BHATIA, K. P. Deconstructing Fahr's disease/syndrome of brain calcification in the era of new genes. **Parkinsonism and Related Disorders**, v. 37, p. 1–10, 2017.

BEKIESINSKA-FIGATOWSKA, M.; MIERZEWSKA, H.; JURKIEWICZ, E. Basal ganglia lesions in children and adults. **European Journal of Radiology**, v. 82, n. 5, p. 837–849, 2013.

BESSER, J.; CARLETON, H. A.; LINDSEY, R. L.; TREES, E. Next-generation sequencing technologies and their application to the study and control of bacterial infections. **Clinical Microbiology and Infection**, v. 24, n. 4, p. 335–341, 2018.

BETSHOLTZ, C.; KELLER, A. PDGF, pericytes and the pathogenesis of idiopathic basal ganglia calcification (IBGC). **Brain Pathology**, v. 24, n. 4, p. 387–395, 2014.

BOLLER, F.; BOLLER, M.; GILBERT, J. Familial idiopathic cerebral calcifications. **Journal of neurology, neurosurgery, and psychiatry**, v. 40, p. 280–285, 1977.

BØTTGER, P.; PEDERSEN, L. Mapping of the minimal inorganic phosphate transporting unit of human PiT2 suggests a structure universal to PiT-related proteins from all kingdoms of life. **BMC biochemistry**, v. 12, n. 1, p. 21, jan. 2011.

BRODATY, H.; MITCHELL, P.; LUSCOMBE, G.; KWOK, J. B. J.; BADENHOP, R. F.; MCKENZIE, R.; SCHOFIELD, P. R. Familial idiopathic basal ganglia calcification (Fahr ' s disease) without neurological , cognitive and psychiatric symptoms is not linked to the IBGC1 locus on chromosome 14q. **Human Genetics**, v. 110, p. 8–14, 2002.

BROUWER, E. J. M. DE; KOCKELKOREN, R.; CLAUS, J. J.; WILLEM, P. Hippocampal Calcifications : Risk Factors and Association with Cognitive Function. 2018.

BUENO, R.; LOUGHLIN, K. R.; POWELL, M. H.; GORDON, G. J. A diagnostic test for prostate cancer from gene expression profiling data. **The Journal of urology**, v. 171, n. 2 Pt 1, p. 903–6, 2004.

CASANOVA, M. F.; ARAQUE, J. M. Mineralization of the basal ganglia: implications for neuropsychiatry, pathology and neuroimaging. **Psychiatry research**, v. 121, p. 59–87, 2003.
CONSORTIUM, I. H. G. S. Finishing the euchromatic sequence of the human genome. **Nature**, v. 21, p. 931–945, 2004.

DAGHIGHI, M. H.; REZAEI, V.; ZARRINTAN, S.; POURFATHI, H. Intracranial physiological calcifications in adults on computed tomography in Tabriz, Iran. **Folia Morphologica**, v. 66, n. 2, p. 115–119, 2007.

DAI, X.; GAO, Y.; XU, Z.; CUI, X.; LIU, J.; LI, Y.; XU, H.; LIU, M.; WANG, Q. K.; LIU, J. Y. Identification of a Novel Genetic Locus on Chromosome 8p21.1–q11.23 for Idiopathic Basal Ganglia Calcification. **American Journal of Medical Genetics - Part B Neuropsychiatric Genetics**, n. June, p. 1305–1310, 2010.

DANEMAN R, ZHOU L, KEBEDE AA, B. B. Pericytes are required for blood–brain barrier integrity during embryogenesis. **Nature**, v. 468, n. 7323, p. 562–566, 2010.

DAVID, S.; FERREIRA, J.; QUENEZ, O.; ROVELET-LECRUX, A.; RICHARD, A.; VÉRIN, M.; JURICI, S.; BER, I. LE; BOLAND, A.; DELEUZE, J.-F.; FREBOURG, T. Identification of partial SLC20A2 deletions in primary brain calcification using whole-exome sequencing. **European journal of human genetics : EJHG**, n. April, p. 1–5, 2016.

DENG, H.; ZHENG, W.; JANKOVIC, J. Genetics and molecular biology of brain calcification. **Ageing Research Reviews**, v. 22, p. 20–38, 2015.

DIJK, E. L. VAN; JASZCZYSZYN, Y.; NAQUIN, D.; THERMES, C. The Third Revolution in Sequencing Technology. **Trends in Genetics**, v. xx, 2018.

DRAKE-PÉREZ, M.; BOTO, J.; FITSIORI, A.; LOVBLAD, K.; VARGAS, M. I. Clinical applications of diffusion weighted imaging in neuroradiology. **Insights Into Imaging**, v. May 30, 2018.

ELSAID, M. F.; CROW, Y. J.; LIVINGSTON, J. H.; BEN-OMRAN, T. New Subtype of Familial Intracranial Calcification in a Mother and Two Children. **American Journal of Medical Genetics - Part A**, n. March, p. 943–946, 2010.

FARINA, L.; CHIAPPARINI, L.; UZIEL, G.; BUGIANI, M.; ZEVIANI, M.; SAVOIARDO, M. MR findings in Leigh syndrome with COX deficiency and SURF-1 mutations. **American Journal of Neuroradiology**, v. 23, n. 7, p. 1095–1100, 2002.

FERGUSON, K. J.; CVORO, V.; MACLULLICH, A. M. J.; SHENKIN, S. D.; SANDERCOCK, P. A. G.; SAKKA, E.; WARDLAW, J. M. Visual Rating Scales of White Matter Hyperintensities and Atrophy: Comparison of Computed Tomography and Magnetic Resonance Imaging. **Journal of Stroke and Cerebrovascular Diseases**, v. 27, n. 7, p. 1815–1821, 2018.

FERREIRA, J. B. *et al.* First Report of a De Novo Mutation at SLC20A2 in a Patient with Brain Calcification. **Journal of molecular neuroscience : MN**, 27 jun. 2014.

FILLOUX, V.; MAROTTE, H.; MIOSSEC, P. Cerebral calcifications in an elderly lupus patient. **Annals of the rheumatic diseases**, v. 62, n. 3, p. 283–284, 2003.

FUENTES-PARDO, A. P.; RUZZANTE, D. E. Whole-genome sequencing approaches for conservation biology: Advantages, limitations and practical recommendations. **Molecular Ecology**, v. 26, n. April, p. 5369–5406, 2017.

FUJIKI, R. *et al.* Assessing the accuracy of variant detection in cost-effective gene panel testing by next-generation sequencing. **The Journal of Molecular Diagnostics**, 2018.

GESCHWIND, D. H.; LOGINOV, M.; STERN, J. M. Identification of a locus on chromosome 14q for idiopathic basal ganglia calcification (Fahr disease). **American journal of human genetics**, v. 65, n. 3, p. 764–72, set. 1999.

GIOVANNINI, D.; TOUHAMI, J.; CHARNET, P.; SITBON, M.; BATTINI, J. Inorganic Phosphate Export by the Retrovirus Receptor XPR1 in Metazoans. **Cell Reports**, v. 3, n. 6, p. 1866–1873, 2013.

GRÜTZ, K. *et al.* Primary familial brain calcification in the “IBGC2” kindred: All linkage roads lead to SLC20A2. **Movement Disorders**, v. 31, n. 12, p. 1901–1904, 2016.

HATAMIAN, H. R.; BAKHSHAYESH, B.; RAHMAN-A, N. Unilateral cortical thickening and hyper-intensity due to mitochondrial encephalopathy, lactic acidosis, and stroke like episodes (MELAS). **International Clinical Neuroscience Journal**, v. 1, n. 2, p. 69–72, 2015.

IGLESIA, M. I. M. S. DE LA; CORTÉS, G. L.; CORTÉS, I. L.; ZUFIRIA, L. O.; FONTAN, M. I.; ICARAN, D. G. Calcificaciones intracraneales. Imagen por RM Intracranial calcifications on MRI. **Radiología**, v. 48, n. 1, p. 19–26, 2006.

JENSEN, N.; AUTZEN, J. K.; PEDERSEN, L. Slc20a2 is critical for maintaining a physiologic inorganic phosphate level in cerebrospinal fluid. p. 125–130, 2016.

JENSEN, N.; SCHRØDER, H. D.; HEJBØL, E. K. Loss of Function of Slc20a2 Associated with Familial Idiopathic Basal Ganglia Calcification in Humans Causes Brain Calcifications in Mice. p. 994–999, 2013.

JENSEN, N.; SCHRØDER, H. D.; HEJBØL, E. K.; FÜCHTBAUER, E.-M.; OLIVEIRA, J. R. M. DE; PEDERSEN, L. Loss of function of SLC20A2 associated with familial idiopathic Basal Ganglia calcification in humans causes brain calcifications in mice. **Journal of molecular neuroscience : MN**, v. 51, n. 3, p. 994–9, nov. 2013.

JIA, P.; ZHAO, Z. Impacts of somatic mutations on gene expression: An association perspective. **Briefings in Bioinformatics**, v. 18, n. 3, p. 413–425, 2017.

KALITA, J.; KUMAR, N.; MAURYA, P. K.; MISRA, U. K. A study of computed tomography scan and magnetic resonance imaging findings in pseudohypoparathyroidism. **Annals of Indian Academy of Neurology**, v. 13, n. 3, p. 13–16, 2010.

KAMARUDDIN, N.; RAJION, Z. A.; YUSOF, A.; AZIZ, M. E. Relationship between Hounsfield unit in CT scan and gray scale in CBCT. **AIP Conference Proceedings**, v. 1791, 2016.

KELLER, A. *et al.* Mutations in the gene encoding PDGF-B cause brain calcifications in humans and mice. **Nature genetics**, v. 45, n. 9, p. 1077–82, set. 2013.

KHANDWALA, K.; AHMED, A.; SHEIKH, T. MELAS : A Complex and Challenging Diagnosis. **Journal of College of Physicians and Surgeons Pakistan**, v. 28, p. 46–48, 2018.

KOPELL, B. H.; REZAI, A. R.; CHANG, J. W.; VITEK, J. L. Anatomy and Physiology of the Basal Ganglia: Implications for Deep Brain Stimulation for Parkinson's Disease. **Movement Disorders**, v. 21, n. 14, p. 238–246, 2006.

LARSEN, F. T.; JENSEN, N.; AUTZEN, J. K.; KONGSFELT, I. B.; PEDERSEN, L. Primary Brain Calcification Causal PiT2 Transport-Knockout Variants can Exert Dominant Negative Effects on Wild-Type PiT2 Transport Function in Mammalian Cells. **Journal of Molecular Neuroscience**, v. 61, n. 2, p. 215–220, 2017.

LAZARIDIS, K. N. *et al.* Outcome of Whole Exome Sequencing for Diagnostic Odyssey Cases of an Individualized Medicine Clinic: The Mayo Clinic Experience. **Mayo Clinic proceedings**, v. 91, p. 297–307, 2016.

LEGATI, A.; GIOVANNINI, D.; NICOLAS, G.; LÓPEZ-SÁNCHEZ, U.; QUINTÁNS, B.; OLIVEIRA, J. R. M.; *et al.* Mutations in XPR1 cause primary familial brain calcification associated with altered phosphate export. **Nature Genetics**, v. 47, n. 6, p. 579–581, 2015.

LEGATI, A.; GIOVANNINI, D.; NICOLAS, G.; LÓPEZ-SÁNCHEZ, U.; QUINTÁNS, B.; OLIVEIRA, J. R. M.; *et al.* Mutations in XPR1 cause primary familial brain calcification associated with altered phosphate export. **Nature genetics**, v. 47, n. 6, p. 579–81, jun. 2015.

LEK, M. *et al.* Analysis of protein-coding genetic variation in 60,706 humans. **Nature Publishing Group**, v. 536, n. 7616, p. 285–291, 2016.

LEMOS, R. R.; FERREIRA, J. B. M. M.; KEASEY, M. P.; OLIVEIRA, J. R. M. **An update on primary familial brain calcification.** 1. ed. [s.l.] Elsevier Inc., 2013. v. 110

LEMOS, R. R.; RAMOS, E. M.; LEGATI, A.; NICOLAS, G.; JENKINSON, E. M.; LIVINGSTON, J. H.; CROW, Y. J.; CAMPION, D.; COPPOLA, G.; OLIVEIRA, J. R. M. Update and mutational analysis of SLC20A2: A major cause of primary familial brain

calcification. **Human Mutation**, v. 36, n. 5, p. 489–495, 2015.

LU, H. Idiopathic Hypoparathyroidism (IHP) Presenting as “Schizophrenia:” A Case Report. **Noro Psikiyatri Arsivi**, v. 51, n. 4, p. 401–402, 2014.

MANYAM, B. V. What is and what is not “Fahr”s disease’. **Parkinsonism & related disorders**, v. 11, n. 2, p. 73–80, mar. 2005.

MARDIS, E. R. Next-Generation DNA Sequencing Methods. **Annu. Rev. Genomics Hum. Genet**, v. 9, p. 387–402, 2008.

MARTINO, A. DI *et al.* Enhancing studies of the connectome in autism using the autism brain imaging data exchange II. **Nature Scientific Data**, v. 4, p. 1–15, 2017.

MARZIALI, A.; AKESON, M. New DNA Sequencing Methods. **Annu. Rev. Biomed.**, v. 3, n. 1, p. 195–223, 2001.

MCGINN, S.; GUT, I. G. DNA sequencing – spanning the generations. **New BIOTECHNOLOGY**, v. 30, n. 4, p. 366–372, 2013.

MCKENNA, A.; HANNA, M.; BANKS, E.; SIVACHENKO, A.; CIBULSKIS, K.; KERNYTSKY, A.; GARIMELLA, K.; ALTSHULER, D.; GABRIEL, S.; DALY, M.; DEPRISTO, M. A. The Genome Analysis Toolkit : A MapReduce framework for analyzing next-generation DNA sequencing data. **Genome Research**, v. 20, n. 9, p. 1297–1303, 2010.

MCPHERSON, J. A; DAVIS, K.; YAU, M.; BEINEKE, P.; ROSENBERG, S.; MONANE, M.; FREDI, J. L. The clinical utility of gene expression testing on the diagnostic evaluation of patients presenting to the cardiologist with symptoms of suspected obstructive coronary artery disease: results from the IMPACT (Investigation of a Molecular Personalized Coro. **Critical pathways in cardiology**, v. 12, n. 2, p. 37–42, 2013.

MENDES, E. M.; MEIRELES-BRANDÃO, L.; MEIRA, C.; MORAIS, N.; RIBEIRO, C.; GUERRA, D. Primary hypoparathyroidism presenting as basal ganglia calcification secondary to extreme hypocalcemia. **Clinics and Practice**, v. 8, n. 5, p. 8–10, 2018.

METZKER, M. L. Sequencing technologies - the next generation. **Nature Reviews Genetics**, v. 11, p. 31, 8 dez. 2009.

MONDSCHEIN, J. I. Perspectives from Human Interventional Radiology. **Veterinary Clinics of North America - Small Animal Practice**, p. 1–7, 2018.

NAKAMURA, K.; ARIMURA, K.; NISHIMURA, A. Possible involvement of basic FGF in the upregulation of PDGFR β in pericytes after ischemic stroke. **Brain Research**, v. 1630, p. 98–108, 2016.

NASH, T. E. *et al.* Calcific neurocysticercosis and epileptogenesis. **Neurology**, v. 62, n. 11, p. 1934–1938, 2004.

NICOLAS, G. *et al.* Phenotypic spectrum of probable and genetically-confirmed idiopathic basal ganglia calcification. **Brain**, v. 136, n. 11, p. 3395–3407, 2013.

NICOLAS, G. *et al.* Mutation of the PDGFRB gene as a cause of idiopathic basal ganglia calcification. **Neurology**, v. 80, n. 2, p. 181–187, 2013.

NICOLAS, G. *et al.* PDGFB partial deletion: A new, rare mechanism causing brain calcification with leukoencephalopathy. **Journal of Molecular Neuroscience**, v. 53, n. 2, p. 171–175, 2014.

NICOLAS, G. *et al.* Brain calcification process and phenotypes according to age and sex: Lessons from SLC20A2, PDGFB, and PDGFRB mutation carriers. **American Journal of Medical Genetics, Part B: Neuropsychiatric Genetics**, v. 168, n. 7, p. 586–594, 2015.

NICOLAS, G.; CHARBONNIER, C.; CAMPION, D.; VELTMAN, J. A. Estimation of minimal disease prevalence from population genomic data : Application to primary familial brain calcification. **American Journal of Medical Genetics**, n. August, p. 1–7, 2017.

OLIVEIRA, J. R. M. *et al.* Genetic heterogeneity in familial idiopathic basal ganglia calcification (Fahr disease). **Neurology**, v. 63, n. 11, p. 2165–2167, 2004.

OLIVEIRA, J. R. M. **Managing Idiopathic Basal Ganglis Calcification ("Fahr's Disease")**. New York: Nova Science Publishers, 2011.

OLIVEIRA, J. R. M.; OLIVEIRA, M. F. Primary brain calcification in patients undergoing treatment with the biphosphanate alendronate. **Scientific reports**, v. 6, n. August 2015, p. 22961, 2016.

OLIVEIRA, J. R. M.; SOBRIDO, M. J.; SPITERI, E.; HOPFER, S.; MERONI, G.; PETEK, E.; BAQUERO, M.; GESCHWIND, D. H. Analysis of candidate genes at the IBGC1 locus associated with idiopathic basal ganglia calcification ("Fahr's disease"). **Journal of Molecular Neuroscience**, v. 33, n. 2, p. 151–154, 2007.

OLIVEIRA, M. F. DE; SILVA, E. B. E; OLIVEIRA, J. R. M. DE. Prevalence of brain calcifications in a Brazilian cohort. **Dementia & Neuropsychologia**, v. 7, n. 2, p. 210–215, 2013.

PASANEN, P.; MÄKINEN, J.; MYLLYKANGAS, L.; GUERREIRO, R.; BRAS, J.; VALORI, M.; VIITANEN, M.; BAUMANN, P.; TIENARI, P. J.; PÖYHÖNEN, M.; BAUMANN, P. Primary familial brain calcification linked to deletion of 5 ' noncoding region of SLC20A2. **Acta Neurologica Scandinavica**, v. 0, p. 1–5, 2016.

PHILIPPE, C.; ISABELLE, H. C.; PHILIPPE, F.; RUSSELL, S.; NADIA, B.; ALAIN, F.; DOMINIQUE, G. H.; SAUDAMINI, D.; ANAÏS, A.; LOU, A.; ANTOINE, B. The brain of René Descartes (1650): A neuro-anatomical analysis. **Journal of the Neurological Sciences**, v. 378, p. 12–18, 2017.

QUINTÁNS, B.; OLIVEIRA, J.; SOBRIDO, M. J. **Primary familial brain calcifications**. 1. ed. [s.l.] Elsevier B.V., 2018. v. 147

RHEES, B.; WINGROVE, J. A. Developing Peripheral Blood Gene Expression-Based Diagnostic Tests for Coronary Artery Disease: a Review. **Journal of Cardiovascular Translational Research**, v. 8, n. 6, p. 372–380, 2015.

RICHARDS, S. *et al.* Standards and guidelines for the interpretation of sequence variants: A joint consensus recommendation of the American College of Medical Genetics and Genomics and the Association for Molecular Pathology. **Genetics in Medicine**, v. 17, n. 5, p. 405–424, 2015.

SANGER, F.; NICKLEN, S.; COULSON, A. R. DNA sequencing with chain-terminating inhibitors. **Proceedings of the National Academy of Sciences of the United States of America**, v. 74, n. 12, p. 5463–5467, 1977.

SEDGHIZADEH, P. P.; NGUYEN, M.; ENCISO, R. Intracranial physiological calcifications evaluated with cone beam CT. **Dentomaxillofacial Radiology**, v. 41, n. 8, p. 675–678, 2012.

SMITH, Y.; WICHMANN, T. Functional Anatomy and Physiology of the Basal Ganglia: Motor Functions. *In*: TARSY, D.; VITEK, J. L.; STARR, P. A.; OKUN, M. S. (Eds.). . **Deep Brain Stimulation in Neurological and Psychiatric Disorders**. Totowa, New Jersey: Humana Press, 2008. p. 3–32.

TADIC, V.; WESTENBERGER, A.; DOMINGO, A.; ALVAREZ-FISCHER, D.; KLEIN, C.; KASTEN, M. Primary Familial Brain Calcification With Known Gene Mutations. A Systematic Review and Challenges of Phenotypic Characterization. **JAMA Neurology**, v. 72, n. 4, p. 460, 2015.

TAGLIA, I.; FORMICHI, P.; BATTISTI, C.; PEPPOLONI, G.; BARGHIGIANI, M.; TESSA, A.; FEDERICO, A. Primary familial brain calcification with a novel SLC20A2 mutation: Analysis of PiT-2 expression and localization. **Journal of Cellular Physiology**, v. 233, n. 3, p. 2324–2331, 2018.

TAGLIA, I.; MIGNARRI, A.; OLGIATI, S.; MENCI, E.; PETROCELLI, P. L.; BREEDVELD, G. J.; SCAGLIONE, C.; MARTINELLI, P.; FEDERICO, A.; BONIFATI, V.; DOTTI, M. T. Primary familial brain calcification: Genetic analysis and clinical spectrum. **Movement disorders : official journal of the Movement Disorder Society**, v. 0, n. 0, p. 1–5, 4 out. 2014.

TIPU, H. N.; SHABBIR, A. Evolution of DNA Sequencing. **Journal of the College of Physicians and Surgeons Pakistan**, v. 25, n. March, p. 210–215, 2015.

TISCH, S.; SILBERSTEIN, P.; LIMOUSIN-DOWSEY, P.; JAHANSHAHI, M. The basal ganglia: Anatomy, physiology, and pharmacology. **Psychiatric Clinics of North America**, v. 27, n. 4, p. 757–799, 2004.

UDUMA, F. U.; PIUS, F.; MATHIEU, M. Computed Tomographic Pattern of Physiological Intracranial Calcifications in a City in Central Africa. **Global Journal of Health Science**, v. 4, n. 1, p. 184–191, 2011.

VANLANDEWIJCK, M. *et al.* Functional Characterization of Germline Mutations in PDGFB and PDGFRB in Primary Familial Brain Calcification. **PloS one**, v. 10, n. 11, p. e0143407, 2015.

VILLA-BELLOSTA, R.; O'NEILL, W. C. Pyrophosphate deficiency in vascular calcification. **Kidney International**, v. 93, n. 6, p. 1293–1297, 2018.

VOLPATO, C. B.; GRANDI, A. DE; BUFFONE, E.; FACHERIS, M.; PRAMSTALLER, P. P. 2q37 as a Susceptibility Locus for Idiopathic Basal Ganglia Calcification (IBGC) in a Large South Tyrolean Family. **Journal of Molecular Neuroscience**, v. 39, p. 346–353, 2009.

VOLPATO, C. B.; GRANDI, A. DE; BUFFONE, E.; PICHLER, I.; GEBERT, U.; SCHIFFERLE, G.; SCHÖNHUBER, R.; PRAMSTALLER, P. P. Brief Research Communication Exclusion of Linkage to Chromosome 14q in a Large South Tyrolean Family With Idiopathic Basal Ganglia Calcification (IBGC). **American Journal of Medical Genetics Part B (Neuropsychiatric Genetics)**, v. 147B, n. March, p. 1319–1322, 2008.

VOS, T. *et al.* Years lived with disability (YLDs) for 1160 sequelae of 289 diseases and injuries 1990-2010: A systematic analysis for the Global Burden of Disease Study 2010. **The Lancet**, v. 380, n. 9859, p. 2163–2196, 2012.

WALLINGFORD, M. C.; CHIA, J. J.; LEAF, E. M.; BORGEIA, S.; CHAVKIN, N. W.; SAWANGMAKE, C.; MARRO, K.; COX, T. C.; SPEER, M. Y.; GIACHELLI, C. M. SLC20A2 Deficiency in Mice Leads to Elevated Phosphate Levels in Cerbrospinal Fluid and Glymphatic Pathway- Associated Arteriolar Calcification , and Recapitulates Human Idiopathic Basal Ganglia Calcification. **Brain Pathology**, v. 3, n. 28, p. 64–76, 2017.

WANG, C.; LI, Y.; SHI, L.; REN, J.; PATTI, M.; WANG, T.; OLIVEIRA, J. R. M. DE; *et al.* Mutations in SLC20A2 link familial idiopathic basal ganglia calcification with phosphate homeostasis. **Nature Genetics**, v. 44, n. 3, p. 254–256, 2012.

WANG, C.; LI, Y.; SHI, L.; REN, J.; PATTI, M.; WANG, T.; OLIVEIRA, J. R. M. DE; *et al.* Mutations in SLC20A2 link familial idiopathic basal ganglia calcification with phosphate homeostasis. **Nature genetics**, v. 44, n. 3, p. 254–6, mar. 2012.

WARR, A.; ROBERT, C.; HUME, D.; ARCHIBALD, A.; DEEB, N.; WATSON, M. Exome Sequencing: Current and Future Perspectives. **G3: Genes|Genomes|Genetics**, v. 5, n. 8, p. 1543–1550, 2015.

WICHMANN, T.; DELONG, M. R. Anatomy and physiology of the basal ganglia: relevance to Parkinson's disease and related disorders. *In*: W.C. KOLLER, E. M. (Ed.). . **Handbook of Clinical Neurology**. 3rd series ed. Atlanta: Elsevier B.V., 2007. p. 1–17.

WU, Z.; MITTAL, S.; KISH, K.; YU, Y.; HU, J.; HAACKE, E. M. Identification of calcification with MRI using susceptibility-weighted imaging: A case study. **Journal of Magnetic Resonance Imaging**, v. 29, n. 1, p. 177–182, 2009.

YALCIN, A.; CEYLAN, M.; BAYRAKTUTAN, O. F.; SONKAYA, A. R.; YUCE, I. Age and gender related prevalence of intracranial calcifications in CT imaging; data from 12,000 healthy subjects. **Journal of Chemical Neuroanatomy**, v. 78, p. 20–24, 2016.

YAMADA, M. *et al.* Evaluation of SLC20A2 mutations that cause idiopathic basal ganglia calcification in Japan. **Neurology**, v. 82, n. 8, p. 705–12, 25 fev. 2014.

YAO, X. P. *et al.* Biallelic Mutations in MYORG Cause Autosomal Recessive Primary Familial Brain Calcification. **Neuron**, v. 98, p. 1–8, 2018.

ZANOTTI, L.; BOTTINI, A.; ROSSI, C.; GENERALI, D.; CAPPELLETTI, M. R. Diagnostic tests based on gene expression profile in breast cancer: from background to clinical use. **Tumor Biology**, v. 35, n. 9, p. 8461–8470, 2014.

ZELLER, T.; BLANKENBERG, S. Blood-Based Gene Expression Tests. **Circulation: Cardiovascular Genetics**, v. 6, p. 139–140, 2013.

ZHANG, Y.; GUO, X.; WU, A. Association between a novel mutation in SLC20A2 and familial idiopathic basal ganglia calcification. **PloS one**, v. 8, n. 2, p. e57060, jan. 2013.

APÊNDICE A – Artigo publicado no periódico *European Journal Of Human Genetics*

Eliana Marisa Ramos, PhD, Miryam Carecchio, MD, Roberta Lemos, PhD, Joana Ferreira, PhD, et al. (2017) Primary brain calcification: an international study reporting novel mutations and phenotypes

Fator de impacto 2016: 4,35

Classificação Qualis na área Ciências Biológicas I (2016): A2

European Journal of Human Genetics
https://doi.org/10.1038/s41431-018-0185-4

ESHG

ARTICLE

Primary brain calcification: an international study reporting novel variants and associated phenotypes

Eliana Marisa Ramos[1] · Miryam Carecchio[2,3,4] · Roberta Lemos[5] · Joana Ferreira[5] · Andrea Legati[1] · Renee Louise Sears[1] · Sandy Chan Hsu[1] · Celeste Panteghini[2] · Luca Magistrelli[6] · Ettore Salsano[7] · Silvia Esposito[3] · Franco Taroni[8] · Anne-Claire Richard[9] · Christine Tranchant[10,11] · Mathieu Anheim[10,11] · Xavier Ayrignac[12] · Cyril Goizet[13,14] · Marie Vidailhet[15] · David Maltete[16] · David Wallon[17] · Thierry Frebourg[9] · Lylyan Pimentel[5] · Daniel H. Geschwind[1] · Olivier Vanakker[18] · Douglas Galasko[19] · Brent L. Fogel[20] · A Micheil Innes[21] · Alison Ross[22] · William B. Dobyns[23] · Diana Alcantara[24] · Mark O'Driscoll[24] · Didier Hannequin[25] · Dominique Campion[9,26] · João R. Oliveira[5] · Barbara Garavaglia[2] · Giovanni Coppola[1] · Gaël Nicolas[9] · The French PFBC study group

Received: 19 December 2017 / Revised: 21 March 2018 / Accepted: 8 May 2018

Abstract

Primary familial brain calcification (PFBC) is a rare cerebral microvascular calcifying disorder with a wide spectrum of motor, cognitive, and neuropsychiatric symptoms. It is typically inherited as an autosomal-dominant trait with four causative genes identified so far: *SLC20A2, PDGFRB, PDGFB*, and *XPR1*. Our study aimed at screening the coding regions of these genes in a series of 177 unrelated probands that fulfilled the diagnostic criteria for primary brain calcification regardless of their family history. Sequence variants were classified as pathogenic, likely pathogenic, or of uncertain significance (VUS), based on the ACMG-AMP recommendations. We identified 45 probands (25.4%) carrying either pathogenic or likely pathogenic variants ($n = 34$, 19.2%) or VUS ($n = 11$, 6.2%). *SLC20A2* provided the highest contribution (16.9%), followed by *XPR1* and *PDGFB* (3.4% each), and *PDGFRB* (1.7%). A total of 81.5% of carriers were symptomatic and the most recurrent symptoms were parkinsonism (54.5% of symptomatic patients), cognitive impairment, and psychiatric disturbances (43.2% each), with a wide range of age at onset (from childhood to 81 years). While the pathogenic and likely pathogenic variants identified in this study can be used for genetic counseling, the VUS will require additional evidence, such as recurrence in unrelated patients, in order to be classified as pathogenic.

Introduction

Primary familial brain calcification (PFBC) is a rare neuropsychiatric disorder characterized by abnormal calcium–phosphate deposits in the microvessels of the basal ganglia and other brain regions. Clinical manifestations can start at any age (median 31 years, range 6–77 years) [1], and include a wide spectrum of movement disorders (dystonia, parkinsonism, tremor, and chorea), neuropsychiatric symptoms (behavioral disturbances, psychosis, mood disorder, and cognitive impairment), cerebellar signs, and other symptoms [2], while up to 42% of the patients remain asymptomatic [1]. Even though the clinical presentation is variable, the neuroradiological picture (evidence of bilateral calcification affecting at least the basal ganglia) is thought to be invariably present by the age of 50. Hence, the diagnosis relies on a computerized tomography (CT) scan, in the absence of other known causes of brain calcification [2]. PFBC is typically inherited as an autosomal-dominant trait, and to date four causative genes have been identified.

These authors contributed equally: Eliana Marisa Ramos, Miryam Carecchio.

Electronic supplementary material The online version of this article (https://doi.org/10.1038/s41431-018-0185-4) contains supplementary material, which is available to authorized users.

✉ Giovanni Coppola
gcoppola@ucla.edu

✉ Gaël Nicolas
gaelnicolas@hotmail.com

Extended author information available on the last page of the article.

SLC20A2 (solute carrier family 20, member 2) was the first gene to be linked to PFBC [3]. Since its discovery, many protein-truncating and deleterious missense variants have been identified, accounting for up to 40% of the familial cases [4]. *SLC20A2* encodes the transmembrane sodium-inorganic phosphate cotransporter PiT2, suggested to have a role in phosphate clearance from the cerebrospinal fluid by recent in vitro and knockout mice studies [5].

Variants in the *PDGFRB* gene [6–8], encoding the platelet-derived growth factor receptor β (PDGF-Rβ), and in the *PDGFB* gene (PDGF-Rβ's main ligand) [9–12], have been reported in more than 20 unrelated probands so far. PDGFB–PDGF-Rβ signaling mediates survival, differentiation, and migration of mesenchymal cells, including the vascular smooth muscle cells affected by calcifications in PFBC [13]. While increased signaling is associated with cancers, overgrowth, and progeria syndromes [14–18], in PFBC patients, protein-truncating *PDGFB* and missense *PDGFB* and *PDGFRB* variants lead to decreased PDGFB–PDGF-Rβ signaling [8, 19, 20]. Although PDGFB–PDGF-Rβ signaling is implicated in the regulation of inorganic phosphate transport [21], the mechanisms leading to microvascular calcification remain unknown [19].

More recently, missense variants in another phosphate transporter, encoded by the *XPR1* gene, were identified in several PFBC families [22]. Subsequent functional studies showed that XPR1 mutant proteins had severely reduced membrane localization and/or impaired phosphate efflux activity [22, 23].

The interpretation of sequence variants identified in genetic screens for rare diseases remains challenging. The American College of Medical Genetics and Genomics and the Association for Molecular Pathology (ACMG-AMP) recently established a set of guidelines to classify genetic variants into five categories from benign (1) to pathogenic (5) [24]. While large sequence variant databases, such as gnomAD [25], are helpful in estimating allele frequencies in control populations, for rare diseases with incomplete penetrance (such as PFBC), variant recurrence in unrelated patients and family segregation data remain critical for interpretation.

In an international effort, four centers from France, USA, Italy, and Brazil gathered and analyzed sequence data from the four genes known to cause autosomal-dominant PFBC.

Materials and methods

Patients

We included patients with brain calcification who were referred to four centers of expertise: University of California, Los Angeles, USA; IRCCS Neurological Institute C. Besta, Milan, Italy; Inserm U1245, Rouen, France; and Universidade Federal de Pernambuco, Recife, Brazil. All patients presented calcifications affecting at least both lenticular nuclei, beyond the age-specific severity threshold [7], a normal phospho-calcic assessment (including at least calcium, phosphate, and PTH) in blood, and no other known etiology. Probands and, if available, family members underwent clinical examination and blood sampling. Details on clinical and family history were obtained by direct interview and/or by reviewing medical records. All individuals included in this study had a brain CT scan; for some, however, details about the extent and localization of brain calcifications were not available. Detailed inclusion criteria are reported in Supplementary Methods. All participants signed written informed consent for genetic analyses.

Genetic screening

Genomic DNA was extracted from peripheral blood by standard methods. For samples from the French, US, and Brazilian series, PCR amplification and subsequent Sanger sequencing of all protein-coding exons and exon–intron boundaries of *SLC20A2*, *PDGFB*, *PDGFRB*, and *XPR1* genes was performed as previously described [3, 6, 9, 22]. All 49 patients from the Italian series were screened with a customized gene panel (Nextera Rapid Capture Custom Enrichment), which included the *PFBC* genes and 55 additional genes responsible for diseases characterized by cerebral calcification (Supplementary Methods). The following genomic and transcript references were used for variant nomenclature and exon numbering: NG_032161.1 and NM_006749.4 for *SLC20A2*, NG_012111.1 and NM_002608.2 for *PDGFB*, NG_023367.1 and NM_002609.3 for *PDGFRB*, and NG_050964.1 and NM_004736.3 for *XPR1*.

Copy-number variation

Quantitative multiplex PCR of short fluorescent fragments (QMPSF) was used to assess the presence of copy-number variations (CNVs) encompassing *SLC20A2* and *PDGFB*, in the French and Brazilian series, as previously described [12, 26]. For the US series, CNVs were genotyped using TaqMan copy-number assays, following the manufacturer's instructions. Commercially available assays for the *SLC20A2* (Hs00279506_cn, Hs00383415_cn), *PDGFB* (Hs00902096_cn and Hs01735391_cn), and *PDGFRB* (Hs01615581_cn, Hs02279533_cn, and Hs02258542_cn) genes were used. For the Italian series, the cn.MOPS tool was applied to next-generation sequencing data for CNV detection [27].

Table 1 Details on *SLC20A2* variants and phenotype of variant carriers

Family number	Case ID	Study	Novel variant or ref.	ACMG class	Variant type	cDNA	Protein	Domain (missense) or predicted protein consequences	gnomAD	Mutation Taster	Polyphen2	SIFT	Ethnicity	Sex	Clinical summary	AAO	Family history	CT scan
1	EXT 1291 001	France	Novel	5	Nonsense	c.149T>G	p.(Leu50Ter)	Premature stop codon	Absent	NA	NA	NA	Caucasian	F	Psychosis and extrapyramidal syndrome	63	Negative	Pa, Pu, WM, and D
2	IT-PFBC-7	Italy	32	4	Missense	c.212G>A	p.(Arg71His)	Phosphate transporter	Absent	DC (0.9)	PD (1)	D (0)	Caucasian	F	Asymptomatic	NA	Negative	Pa, Pu, Ca, and T
3	EXT 878 001	France	Novel	3	Predicted splicing	c.289+5G>A	p.?	Predicted loss of 5' splicing donor site	Absent	NA	NA	NA	Caucasian	F	Pain, akinetic–rigid syndrome with tremor, gait disorder, and hypophonia	72	Negative	Pa, Pu, Ca, D, T, Co, WM, and Ver
4	IT-PFBC-1	Italy	Novel	3	Predicted splicing	c.290-8A>G	p.?	Predicted loss of 3' splicing acceptor site	Absent	NA	NA	NA	Caucasian	F	Akinetic–rigid parkinsonism, LD responsive	65	Negative	Pa, Pu, and D
5	EXT 1132 001	France	Novel	3	Missense/ splicing?	c.290G>A	p.(Gly97Asp)	First base of exon 3; however, splicing tools predict a minor effect on splicing (MaxEntScan score change:-7%)	Absent	DC (1)	PD (1)	D (0.02)	Polynesian	M	Anxiety, depression, apathy, somatoform signs, and attention deficit	18	Positive	Pa, Pu, Ca, T, WM, and Co
6	Proband	USA	28,29	5	Nonsense	c.338C>G	p.(Ser113Ter)	Premature stop codon	Absent	DC (1)	NA	NA	NA	F	NA	NA	Positive	NA
7	IT-PFBC-6	Italy	28 [same patient]	5	Nonsense	c.338C>G	p.(Ser113Ter)	Premature stop codon	Absent	DC (1)	NA	NA	Caucasian	M	Focal unilateral chorea (hand)	53	Negative	Pa, Pu, Ca, T, and D
8	EXT 945 001	France	Novel	5	Frameshift	c.382del	p.(Val128SerfsTer43)	Premature stop codon	Absent	NA	NA	NA	Caucasian	M	Cerebellar ataxia, dysarthria, memory impairment with dysexecutive signs, and depression	76	Negative	Pa, Pu, Ca, T, D, WM, Co, and Ver
9	Proband	USA	Novel	4	Missense	c.541C>T	p.(Arg181Trp)	Phosphate transporter domain	4.084e−6 (4.512e−5, NFE)	DC (0.99)	PD (0.995)	T (0.06)	Caucasian	M	Progressive involuntary movements, neuropathic pain, and chronic headache	60	Positive	Pa, Pu, and Ca
	Father													M	Asymptomatic	NA		Pa, Pu, and Ca
10	ROU 375 004 (mother)	France	6	5	Missense	c.551C>T	p.(Pro184Leu)	Cytoplasmic	Absent	DC (1)	?PD (0.98)	D (0.05)	Caucasian	F	Restless leg syndrome	55	Positive	Pa, Pu, Ca, T, and D
	ROU 375 003 (sister)													F	Asymptomatic (migraine)	NA		Pa, Pu,

Table 1 (continued)

Family number	Case ID	Study	Novel variant or ref.	ACMG class	Variant type	cDNA	Protein	Domain (missense) or predicted protein consequences	gnomAD	Mutation Taster	Polyphen2	SIFT	Ethnicity	Sex	Clinical summary	AAO	Family history	CT scan
	ROU 375 002 (sister)													F	Pyramidal signs	26		Ca, and T Pa, Pu, Ca, T, and WM
	ROU 375 001 (proband)													F	Asymptomatic (migraine)	NA		Pa, Pu, Ca, and T
I1	EXT 1146 001	France	7	4	Missense	c.581A>G	p.(Asn194Ser)	Transmembrane	01.446e −5 (1.556e −4, NFE)	DC (0.99)	B (0.155)	T	NA	M	Akinetic–rigid syndrome, tremor, cerebellar ataxia, dysexecutive signs, and memory impairment	68	Positive	Pa, Pu, Ca, D, T, Co, WM, and Ver
I2	EXT 1180 001	France	Novel	5	Splicing	c.730+1G>T	p.?	Predicted skipping of exon 6 (in-frame) or use of alternative splice site	Absent	NA	NA	NA	Caucasian	F	Bradykinesia, tremor, and dysexecutive signs	40	Negative	Pa, Pu, T, D, and Co
I3	IT-PFBC-5b (first cousin)	Italy	Novel	5	Nonsense	c.739C>T	p.(Gln247Ter)	Premature stop codon	Absent	DC (1)	NA	NA	Caucasian	F	Asymptomatic	NA	Positive	Pa, Pu, Ca, T, and D
	IT-PFBC-5a (proband)													M	Chorea, orofacial dyskinesia, depression, and cognitive decline	65		Pa, Pu, Ca, T, D, Co, and WM
I4	ROU 5028 001	France	30	5	Nonsense	c.1158C>A	p.(Tyr386Ter)	Premature stop codon with evidence of nonsense-mediated decay	Absent	DC (1)	NA	NA	Caucasian	F	Asymptomatic (migraine)	NA	Positive	Pa, Pu, D, and Co
I5	EXT 1118 001	France	30	5	Nonsense	c.1158C>A	p.(Tyr386Ter)	Premature stop codon with evidence of nonsense-mediated decay	Absent	DC (1)	NA	NA	Caucasian	M	Akinetic–rigid syndrome, orofacial dyskinesia and dystonia (induced by L-dopa), pyramidal signs, gait disorder, and hallucinations (induced by L-dopa)	51	Negative	Pa, Pu, Ca, D, T, Co, WM, and Ver
I6	1B02BR	Brazil	Novel	5	Frameshift	c.1187dup	p.(Pro397AlafsTer18)	Premature stop codon	Absent	DC (1)	NA	NA	NA	F	Parkinsonism	NA	Positive	NA
	1B01BR													M	Stroke, aphasia, and parkinsonism	NA		NA
I7	EXT 1083 001	France	Novel	5	Nonsense	c.1207C>T	p.(Arg403Ter)	Premature stop codon	Absent	DC (1)	NA	NA	Caucasian	M	Akinetic–rigid syndrome	65	Negative	Pa, Pu, Ca, D, T, Co,

Table 1 (continued)

Family number	Case ID	Study	Novel variant or ref.	ACMG class	Variant type	cDNA	Protein	Domain (missense) or predicted protein consequences	gnomAD	Mutation Taster	Polyphen2	SIFT	Ethnicity	Sex	Clinical summary	AAO	Family history	CT scan
																		WM, and Ver
18	IT-PFBC-2	Italy	31	4	Missense	c.1301C>G	p.(Ser434Trp)	Phosphate transporter domain	3.228e−5 (6.663e−5, NFE)	DC (0.99)	PD (0.997)	D (0.00)	Caucasian	F	Parkinsonism and postural/kinetic tremor. Comorbid Down syndrome	3	Negative	Pa, Pu, and D
19	EXT 1063 001	France	Novel	5	Nonsense	c.1426G>T	p.(Glu476Ter)	Premature stop codon	Absent	DC (1)	NA	NA	Caucasian	M	Akinetic–rigid syndrome, bipolar disorder. Mild cerebellar ataxia	44	Positive	Pa, Pu, Ca, D, T, Co, WM, and Ver
20	IT-PFBC-3	Italy	Novel	3	Missense	c.1463A>G	p.(His488Arg)	Phosphate transporter	Absent	DC (0.99)	B (0.005)	T (0.83)	Caucasian	F	Subjective memory impairment, normal psychometry	59	Negative	Pa, Pu
21	Proband	USA	3	5	Missense	c.1492G>A	p.(Gly498Arg)	Phosphate transporter	Absent	DC (0.99)	PD (0.994)	D (0.00)	Caucasian	M	L-dopa-responsive parkinsonism also increased muscle tone and pain	NA	Negative	Pa, Pu, Ca, and T
22	IT-PFBC-8a (proband)	Italy	3	5	Missense	c.1492G>A	p.(Gly498Arg)	Phosphate transporter	Absent	DC (0.9)	PD (1)	D (0)	Caucasian	M	Akinetic–rigid parkinsonism, dysarthria	68	Positive	Pa, Pu, Ca, T, D, Co, and WM
	IT-PFBC-8b (daughter)													F	Asymptomatic	NA		Pa, Pu
23	EXT 1136 001	France	Novel	5	Splicing	c.1524-2A>G	p.?	Predicted skipping of exon 9 (in-frame) or use of alternative splice site	Absent	NA	NA	NA	Caucasian	F	Dysarthria, gait disorder, akinetic–rigid syndrome, memory impairment, and dysexecutive signs	71	Negative	Pa, Pu, Ca, T, D, Ve, and Co
24	EXT 1318 001	France	Novel	3	Missense /splicing	c.1523G>A	p.(Ser508Asn)	Last base of exon 8; splicing tools predict a major effect on splicing (MaxEntScan score change:-59.5%)	Absent	DC	PD	D	Caribbean	F	Right upper-limb dystonia, intention tremor, and bradykinesia, mood disorder, and migraine	33	Positive for psychiatric signs	Pa
25	Proband	USA	Novel	5	Frameshift	c.1637_1638delCA	p.(Thr546ArgfsTer52)	Premature stop codon	Absent		NA	NA	Caucasian	F	Migraine, vestibular signs	NA	Positive	Pa, Pu, Ca, and T
26	EXT 1235 001	France	4	4	Missense	c.1753G>A	p.(Ala585Thr)	Phosphate transporter	Absent	DC	PD	T	African	F	Dementia and parkinsonism	NA	Negative	Pa, Pu, T, Ca, D, and Co
27	EXT 1138 001	France	4	5	Frameshift	c.1755_1768del	p.(Asn587SerfsTer7)	Premature stop codon	Absent	NA	NA	NA	Caucasian	M	Mild-to- moderate intellectual disability, bipolar disorder, mild	3	Positive	Pa, Pu, Ca, T, D, T,

Table 1 (continued)

Family number	Case ID	Study	Novel variant or ref.	ACMG class	Variant type	cDNA	Protein	Domain (missense) or predicted protein consequences	gnomAD	Mutation Taster	Polyphen2	SIFT	Ethnicity	Sex	Clinical summary	AAO	Family history	CT scan
															akinetic–rigid syndrome signs, ataxia, and mild postural and intention tremor			and Co
28	IT-PFBC-4	Italy	Novel	3	Missense	c.1765G>A	p.Gly589Arg	Phosphate transporter	Absent	DC (0.99)	PD (0.99)	D (0.01)	Caucasian	F	Dementia	81	Positive	Pa, D
29	Proband	USA	Novel	4	In-frame deletion (27 bp)	c.1822_1848del	p.(Ile608_Trp616del)	Phosphate transporter	Absent	NA	NA	NA	Caucasian	M	ADHD	NA	Positive	Pa, Pu, Ca, T, and Co
	Father													M	Anxiety, dystonia	NA		Pa
30	EXT 1020 001	France	Novel	3	Missense	c.1871T>A	p.(Val624Glu)	Phosphate transporter	Absent	DC (1)	PossD (0.503)	T (0.15)	Caucasian	M	Tremor of the four limbs, memory impairment with dysexecutive signs. NB: tremor, beginning from age 7, is also present in two sibpairs in the absence of brain calcification	7	Negative	Pa, Pu, D, and WM

ACMG class: 5—pathogenic, 4—likely pathogenic, and 3—variant of unknown significance. Novel variant refers to variants that have not been previously reported in PFBC patients. gnomAD frequency, in parentheses is the maximal subpopulation frequency for non-Finnish Europeans (NFE). Family history was considered positive if at least one first-degree relative exhibited at least one neuropsychiatric symptom by interview

Variants were submitted to the https://coppolalab.ucla.edu/lovd_pfbc/genes/SLC20A2 database. Reference sequences: NG_032161.1 and NM_006749.4

~~Associated references: [3, 4, 6, 7,28–32]~~

AAO age at onset, *Pa* pallidum, *Pu* putamen, *Ca* caudate nuclei, *T* thalamus, *D* dentate nuclei, *Co* cerebral cortex, *WM* subcortical white matter, *Ver* vermis, *NA* not available, *DC* disease causing, *PossD* possibly damaging, *PD* probably damaging, *T* tolerated, *D* deleterious.

Table 2 Details on *PDGFB* variants and phenotype of variant carriers

Family number	Case ID	Study	Novel variant or ref.	ACMG class	Variant type	cDNA	Protein	Domain (missense) or predicted protein consequences	gnomAD	Mutation Taster	Polyphen2	SIFT	Ethnicity	Sex	Clinical summary	AAO	Family History	CT scan
31	EXT 929 001	France	Novel	4	Missense	c.394G>C	p.(Gly132Arg)	PDGF domain	Absent	DC (1)	PD (1)	D (0)	Caucasian	F	Asymptomatic	NA	Negative	Pa, Pu, D
32	ROU 1184 001	France	Novel	3	Missense	c.425G>A	p.(Arg142His)	PDGF domain	Absent	DC (0.97)	PD (1)	T (0.33)	Caucasian	F	Personality disorder, depressive episodes with memory impairment. Progressive cognitive decline. Akinetic–rigid syndrome, pyramidal signs, gait disorder, frontal behavioral disorder	68	Negative	Pa, Pu, D
33	EXT 1196 001	France	9	5	Nonsense	c.445C>T	p.(Arg149Ter)	Premature stop codon	Absent	DC (1)	NA	NA	Caucasian	M	Dysexecutive syndrome with memory impairment, anxiety, depression, akinetic–rigid syndrome, tremor	44	Positive	Pa, Pu, Ca, D, T (MR)
34	Proband	USA	Novel	5	Splicing	c.456+1G>A	p.?	Predicted skipping of exon 4 introducing a frameshift	Absent	NA	NA	NA	NA	F	Severe migraine, history of depression	20	Positive	Pa, Pu, Ca, WM, D, Co
	Mother													F	Migraine, history of depression	26		Pa, Pu, Ca, T, D, WM
35	EXT 1251 001	France	Novel	5	Stop loss	c.724T>C	p.(Ter242GlnExtTer89)	Extended protein, loss of function	Absent	NA	NA	NA	Caucasian	F	Seizures, migraine, depression, cognitive impairment (memory, executive dysfunction)	25	Negative	Pa, Pu, Ca, D (MRI)
36	ROU 5019 001	France	9	5	Stop loss	c.726G>C	p.(Ter242TyrExtTer89)	Extended protein, loss of function	Absent	NA	NA	NA	Caucasian	M	Orofacial dyskinesia, oral tics, pyramidal	NA	Positive	Pa, Pu, Ca, D, T,

Table 2 (continued)

Family number	Case ID	Study	Novel variant or ref.	ACMG class	Variant type	cDNA	Protein	Domain (missense) or predicted protein consequences	gnomAD	Mutation Taster	Polyphen2	SIFT	Ethnicity	Sex	Clinical summary	AAO	Family History	CT scan
															signs, alcohol abuse, comorbid aneurysm of the right medial cerebral artery			Co, WM

ACMG class: 5—pathogenic, 4—likely pathogenic, 3—variant of unknown significance. Novel variant refers to variants that have not been previously reported in PFBC patients. Family history was considered positive if at least one first-degree relative exhibited at least one neuropsychiatric symptom by interview

The variants were submitted to the following database; https://coppolalab.ucla.edu/lovd_pfbc/genes/PDGFB. Reference sequences: NG_012111.1 and NM_002608.2

~~Associated reference: [9]~~

AAO age at onset, *Pa* pallidum, *Pu* putamen, *Ca* caudate nuclei, *T* thalamus, *D* dentate nuclei, *Co* cerebral cortex, *WM* subcortical white matter, *NA* not available, *DC* disease causing, *PossD* possibly damaging, *PD* probably damaging, *T* tolerated, *D* deleterious.

Variant assessment

Variant classification was conducted following ACMG-AMP recommendations [24]. Briefly, these criteria included prior identification as a PFBC-causing variant (reported in the literature, HGMD, Clinvar, and/or the PFBC variant database https://coppolalab.ucla.edu/lovd/genes), allele frequency in population databases (gnomAD [25], http://gnomad.broadinstitute.org/), computational and predictive data (Polyphen2, SIFT, MutationTaster, and splicing predictions provided by the Alamut visual software (Interactive Biosoftware, Rouen, France)), functional studies (reported in the literature), and segregation data. Each variant was first classified into one of the five ACMG-AMP classes by an investigator from the group where it was identified and then reviewed by the entire study group. All variants reported in this study were added to the PFBC database https://coppolalab.ucla.edu/lovd/genes.

Affected relatives

Clinical and imaging data from affected relatives were collected, and genetic testing was performed on available DNA samples to ascertain variant cosegregation.

Results

Genetic screening in four series

By screening the four known PFBC-causative genes in 177 unrelated probands from four independent international series, we identified 34 probands (19.2%) carrying a variant classified as pathogenic (class 5) or likely pathogenic (class 4), while 11 carried a variant of uncertain significance (VUS) (class 3, 6.2%). In contrast, CNV analysis did not reveal any clear large deletion or duplication in the *PFBC* genes screened. The overall variant detection rate was therefore 25.4% (45/177) (Supplementary Table 1). Only 2 out of the 177 unrelated probands were previously reported [23, 28]. After including 11 variant-carrying affected relative members, 56 individuals are described herein.

SLC20A2 variants

We identified 27 distinct *SLC20A2* variants in 30 unrelated probands (16.9%, Table 1). Nine of these variants had previously been reported in other PFBC patients [3, 4, 6, 7, 29–32], including six missense variants for which pathogenicity was uncertain and that can now be classified as pathogenic: p.(Pro184Leu) and p.(Gly498Arg), or likely pathogenic: p.(Arg71His), p.(Asn194Ser), p.(Ser434Trp), and p.(Ala585Thr). These variants were seen in 12 of our

unrelated probands, including one case already reported in the literature [28]. The remaining 18 *SLC20A2* variants were novel, of which nine were protein-truncating variants (PTV) and were therefore classified as pathogenic.

Two novel likely pathogenic variants were also identified. First, an in-frame deletion of 27 nucleotides (c.1822_1848del) in exon 11 of *SLC20A2* was identified in a proband and his affected father. This variant is predicted to cause a deletion of nine amino acids, p.(Ile608_Trp616del), at the C-terminal domain of Pit-2, in a transmembrane region. Second, a predicted-damaging missense variant, c.541C>T, p.(Arg181Trp) in exon 5 was identified in a patient and his affected father. This variant was found in one individual from the gnomAD database (MAF = 4.1e−06). Other missense pathogenic variants in nearby residues have been reported in PFBC patients [4], supporting evidence for pathogenicity.

Among the additional seven novel VUS identified, two were intronic (c.289+5G>A, c.290–8A>G), absent from gnomAD, and with strong in silico predictions of a splicing defect at the closest canonical site (MaxtEntScan score change of –80.7% and –54.4%, respectively, with the c.290–8A>G predicted to create a new acceptor site at position c.290–7). Two other novel missense VUS were located at exon boundaries. The c.290G>A, p.(Gly97Asp) variant, affecting the first base of exon 3, was predicted as damaging by in silico tools and to cause a slight effect in splicing (MaxEntScan score change: –7%). The c.1523G>A variant, p.(Ser508Asn), affecting the last base of exon 8, was also predicted to be damaging, in addition to a strong effect on splicing (MaxEntScan score change: –59.5%). RNA from these patients was not available to confirm the hypothesis of a protein-truncating effect through altered splicing, precluding their classification as (likely) pathogenic. The other novel VUS, p.(His488Arg), p.(Gly589Arg), and p.(Val624Glu), were not detected in gnomAD and are predicted to be damaging by in silico analysis. Even though other missense pathogenic variants in nearby residues have been reported, there was not sufficient evidence to classify these specific variants as (likely) pathogenic.

PDGFB variants

We identified six distinct *PDGFB* variants in 6 unrelated probands (3.4%, Table 2). Two of these variants had already been reported in other PFBC patients: nonsense p.(Arg149Ter) and, stop loss c.726G>C, p.(Ter242TyrExtTer89) that adds 89 residues to the protein [9]. We identified a novel stop loss variant, c.724T>C, p.(Ter242GlnExtTer89), which is also predicted to cause an elongation of the reading frame by 89 amino acids. Functional studies have shown that proteins with variants causing a C-terminal extension, namely p.(Ter242TyrExtTer89), failed to induce any detectable PDGF-Rβ autophosphorylation [19]. A novel canonical splice site variant, c.456+1G>A (Table 2), predicted to affect splicing of exon 4 in *PDGFB*, was identified in a proband and the affected mother. Both of these novel variants were absent from gnomAD. Therefore, there was enough evidence to support these variants as pathogenic for PFBC.

We also identified two novel missense variants, both absent from gnomAD and predicted damaging by in silico analysis: p.(Gly132Arg) and p.(Arg142His) (Table 2). Variant p.(Gly132Arg) was identified in an additional unrelated French patient with brain calcifications (enrolled after the data freeze, hence not included in this series) and was therefore classified as likely pathogenic.

PDGFRB variants

Three distinct *PDGFRB* variants were found in three unrelated probands (1.7%, Table 3): p.(Arg226Cys), p.(Pro596Leu), and p.(Asp844Gly), all novel missense variants, predicted damaging. Of these, only the p.(Pro596Leu) variant was present in two individuals in gnomAD (MAF = 8.1e−06). Segregation data was only available for the family carrying the p.(Asp884Gly) variant and we showed that this variant resulted in a loss of PDGFRβ autophosphorylation (Supplementary Figure 1). Based on this evidence, this variant was classified as pathogenic, while the other two were classified as VUS.

XPR1 variants

Five distinct *XPR1* variants were found in six unrelated probands (3.4%, Table 4). Two of these variants had already been associated with PFBC. One of our unrelated French patients carried the same p.(Leu145Pro) variant reported in the original *XPR1* paper [22]. The other variant, p.(Leu87Pro), was found in a case already reported [23]. These two variants were not found in gnomAD and can be classified as pathogenic based on published functional evidence [22, 23]. Three additional predicted-damaging missense variants were found (Table 4). While p.(Thr233Ser) was found in two unrelated PFBC individuals, it was also found in two individuals within the gnomAD database (MAF = 8.1e−06). On the other hand, both p.(Arg459Cys) and p.(Asn619Asp) were not found in gnomAD. Furthermore, for p.(Arg459Cys), the unaffected proband's mother did not carry this variant and had a normal brain CT scan. Both p.(Thr233Ser) and p.(Arg459Cys) variants were therefore classified as likely pathogenic, while there was not sufficient evidences for p.(Asn619Asp), hence classified here as VUS.

Table 3 Details on *PDGFRB* variants and phenotype of variant carriers

Family number	Case ID	Study	Novel variant or ref.	ACMG class	Variant type	cDNA	Protein	Domain (missense) or predicted protein consequences	gnomAD	Mutation Taster	Polyphen2	SIFT	Ethnicity	Sex	Clinical summary	AAO	Family History	CT scan
37	IT-PFBC-9[a]	Italy	Novel	3	Missense	c.676C>T	p.(Arg226Cys)	Extracellular, Ig-like C2-type 3	Absent	DC (0.99)	PD (1)	D (0.01)	Caucasian	M	Paroxysmal kinesigenic dyskinesia[a], CBZ responsive	11	Negative	Pa, Pu, Ca, T, D
38	IT-PFBC-10	Italy	Novel	3	Missense	c.1787C>T	p.(Pro596Leu)	Outside of Protein Kinase domain, Cytoplasmic	8.147e−6 (3.254e−5, South Asian; 8.988e−6, NFE)	DC	PD (1)	D (0)	Caucasian	F	Asymptomatic (migraine)	NA	Negative	Pa, Pu
39	Proband	USA	Novel	5	Missense	c.2531A>G	p.(Asp844Gly)	Cytoplasmic, protein kinase	Absent	DC (0.99)	PD (0.998)	D (0.01)	Caucasian	F	Sleepwalking	Childhood	Positive	Pa, Pu, WM, D
	Paternal aunt													F	NA	NA		NA

ACMG class: 5—pathogenic, 4—likely pathogenic, 3—variant of unknown significance. Novel variant refers to variants that have not been previously reported in PFBC patients. gnomAD frequency, in parentheses is the maximal subpopulation frequency for South Asians andNon-Finnish Europeans (NFE). Family history was considered positive if at least one first-degree relative exhibited at least one neuropsychiatric symptom by interview

Variants were submitted to the following database; https://coppolalab.ucla.edu/lovd_pfbc/genes/PDGFRB database. Reference sequence: NM_002609.3

AAO age at onset, *Pa* pallidum, *Pu* putamen, *Ca* caudate nuclei, *T* thalamus, *D* dentate nuclei, *Co* cerebral cortex, *WM* subcortical white matter, *CBZ* carbamazepine, *NA* not available, *DC* disease causing, *PossD* possibly damaging, *PD* probably damaging, *T* tolerated, *D* deleterious.

[a]The *PRRT2* and *PNKD* genes were sequenced in this patient and no change was detected

Table 4 Details on *XPR1* variants and phenotype of variant carriers

Family number	Case ID	Study	Novel variant or ref.	ACMG class	Variant type	cDNA	Protein	Domain (missense) or predicted protein consequences	gnomAD	Mutation Taster	Polyphen2	SIFT	Ethnicity	Sex	Clinical summary	AAO	Family History	CT scan
40	EXT 1003 001	France	23 [same patient]	5	Missense	c.260T>C	p.(Leu87Pro)	SPX domain	Absent	DC (1)	PD (1)	D (0)	Caucasian	M	Dysarthria with parkinsonian and cerebellar features, concentration deficit, mild executive dysfunction, micrography, parkinsonism, anxiety	37	Positive	Pa, Pu, Ca, T, D, Ve, WM, Co
41	EXT 1187 001	France	22	5	Missense	c.434T>C	p.(Leu145Pro)	SPX domain	Absent	DC (1)	PD (1)	D (0.01)	Caucasian	M	Extrapyramidal syndrome, cognitive impairment, dysarthria, behavioral disturbances	29	Positive	Pa, Pu, Ca, T, D, Co (MRI)
	EXT 1187 002													F	Bradykinesia, psychomotor slowing	38		Pa, Pu, Ca, T, D, Co
42	IT-PFBC-11	Italy	Novel	4	Missense	c.697A>T	p.(Thr233Ser)	Outside from SPX domain	8.133e −6 (1.795e −5, NFE)	DC (0.99)	PossD (0.885)	D (0.03)	Caucasian	F	Mild Cognitive Impairment	81	Negative	Pu, Pa
43	IT-PFBC-12	Italy	Novel	4	Missense	c.697A>T	p.(Thr233Ser)	Outside from SPX domain	8.133e −6 (1.795e −5, NFE)	DC (0.99)	PossD (0.885)	D (0.03)	Caucasian	F	Vertigo	50	Negative	Pa, Pu
44	ROU 5059 001	France	Novel	4	Missense	c.1375C>T	p.(Arg459Cys)	Outside from SPX domain	Absent	DC (1)	PD (1)	D (0)	Caucasian	M	L-Dopa-responsive extrapyramidal syndrome, mild intellectual disability	55	Negative	Pa, Pu, Ca, D
45	EXT 1219 001	France	Novel	3	Missense	c.1855A>G	p.(Asn619Asp)	Outside from SPX domain	Absent	DC (1)	PD (1)	D (0)	Caucasian	M	Sudden deafness, mild cerebellar syndrome	69	Positive	Pa, Pu, Ca, D, T

ACMG class: 5—pathogenic, 4—likely pathogenic, 3—variant of unknown significance. Novel variant refers to variants that have not been previously reported in PFBC patients. gnomAD frequency, in parentheses is the maximal subpopulation frequency for Non-Finnish Europeans (NFE). Family history was considered positive if at least one first-degree relative exhibited at least one neuropsychiatric symptom by interview

Variants were submitted to the following database; https://coppolalab.ucla.edu/lovd_pfbc/genes/XPR1 database. Reference sequence: NM_004736.3

Associated references: [22, 23]

AAO age at onset, *Pa* pallidum, *Pu* putamen, *Ca* caudate nuclei, *T* thalamus, *D* dentate nuclei, *Co* cerebral cortex, *WM* subcortical white matter, *NA* not available, *DC* disease causing, *PossD* possibly damaging, *PD* probably damaging, *T* tolerated, *D* deleterious

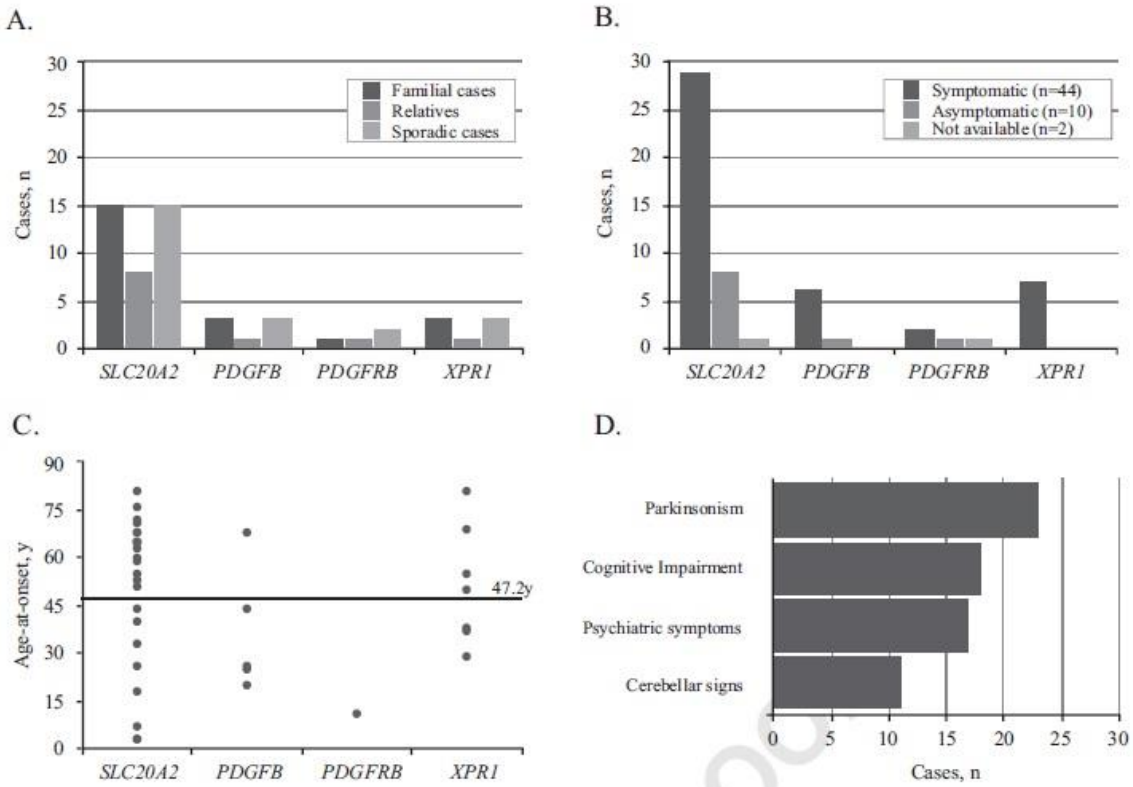

Fig. 1 Clinical presentation of 56 variant carriers. **a** Number of familial (including relatives) and sporadic cases, and **b** number of symptomatic and asymptomatic individuals per ~~variant carrier~~, **c** Distribution of age-at-onset (years) per gene carrier (horizontal line represents the average age of onset across all 37 cases with known age-at-onset). **d** Frequency of main symptoms among the 44 symptomatic variant carriers

Clinical presentation

Herein, we reported a total of 56 PFBC patients (32F; 24M), including the 45 probands that were found to carry VUS or (likely) pathogenic variants, and 11 relatives that had brain calcifications and the same variant as the proband (Fig. 1a). Detailed clinical and radiological data were available in 54/56 patients (Tables 1–4), and at the time of genetic testing, 44 (81.5%) of these were symptomatic (Fig. 1b). Mean age at clinical onset was 47.2 years (Fig. 1c) (median = 52 y, range: 3–81 y, age at onset was unknown for eight cases, including one with onset in childhood) and mean age at last examination was 57.4 years in symptomatic patients and 47.5 in asymptomatic patients. Parkinsonism (alone or combined with other clinical manifestations) was the most frequent finding, present in 24/44 (54.5%) of symptomatic patients, mostly with an akinetic–rigid presentation (Fig. 1d). Cognitive impairment was documented in 19/44 (43.2%) symptomatic cases, as were psychiatric disturbances (depression, psychosis, anxiety), while 13/44 (29.5%) patients had cerebellar signs. In addition, migraine was reported by 10/54 patients (18.5%); in five of these patients neurological examination was unremarkable and therefore they were considered asymptomatic.

Discussion

We screened the four known PFBC-causative genes in a series of 177 PFBC patients and identified 41 distinct variants, in a total of 45 unrelated probands. Taking into account only likely pathogenic and pathogenic variants, for which evidence is sufficient to propose genetic counseling, 34 out of the 177 (19.2%) unrelated probands carried such variants. However, the overall variant detection rate can increase up to 25.4% (45/177), if future studies find new evidence to reclassify the VUS we found as causal. As expected, *SLC20A2* showed the highest contribution with variants identified in 16.9% (30/177) of the probands, followed by *XPR1* and *PDGFB*, each with 3.4% (6/177), and then *PDGFRB* with 1.7% (3/177). These rates are consistent with those reported in other French series that, similar to ours, had patients with and without known family history [33], in contrast to previous reports that showed high

mutation rates in patients with a positive family history [34]. Even though we screened novel unrelated probands, we detected new but also previously reported PFBC variants, sometimes in patients originating from the same country as the original carrier. It should be noted that, based on available family information, none of the patients in our series seem to be related to any of the PFBC carriers already published in the literature.

SLC20A2 was the first PFBC-causative gene to be identified, linking cerebral inorganic phosphate metabolism to PFBC's pathophysiology [3]. Evidence that *SLC20A2* haploinsufficiency causes PFBC is strong as both PTV and total/partial deletions have been identified [3, 26, 29]. This hypothesis has been confirmed in mouse models [5, 35, 36], and by in vitro assessment of some of the missense variants [3]. In our series, including patients with positive family history and apparently sporadic cases, we confirmed *SLC20A2* as the major causative gene, accounting for at least 13.0% of the cases (adding up to 16.9% when including VUS).

XPR1 was the most recent *PFBC* gene to be identified [22], and in our series, variants within ~~these~~ gene are as frequent as *PDGFB* variants. Pathogenicity of *XPR1* variants reported to date has been ascertained based on: strong segregation [22], recurrence among unrelated patients, and/or functional data showing a defect in inorganic phosphate transport [22, 23]. Interestingly, all known pathogenic variants are located in the SPX domain of XPR1, the function of which remains uncertain. We identified three novel missense variants, all predicted damaging, but located outside the SPX domain. Functional analyses are needed to further clarify their role.

The identification of protein-truncating *PDGFB* variants following the identification of missense *PDGFRB* variants, provided the first evidence that decreased PDGFB–PDGFRβ signaling was causative of PFBC. Loss of function and missense variants, as well as a partial *PDGFB* deletion have been identified to date [1, 9, 12, 37], supporting haploinsufficiency as causal mechanism. Here, we report four novel variants, including one PTV, one stop loss and two missense variants, of which one could be classified as likely pathogenic.

Since the original paper identifying *PDGFRB* as a *PFBC* causal gene, only four established pathogenic *PDGFRB* variants have been reported in the literature. These showed strong segregation evidence [6] and/or functional evidence of a loss of protein function [8, 19, 20]. Another missense variant, p.(Glu1071Val), originally considered as VUS has since been reclassified as likely benign based on functional studies [7, 19, 20]. More recently, 2 novel variants were identified in Chinese PFBC cases: a c.3G>A variant leading to a loss of the start codon, and a missense p.(Asp737Asn) variant [38]. Although the latter variant was considered a VUS, the start loss variant could be classified as pathogenic if considered truncating, however its functional effect remains unclear as an alternative in-frame ATG codon could theoretically be used. Herein, we report 3 additional missense variants, though only one of them could be classified as pathogenic based on segregation and functional data.

The PFBC phenotypic spectrum is wide and diverse, with intra and interfamilial heterogeneity. Although some of the variants found in this study are recurrent, their low frequency precluded any genotype-phenotype correlations, and therefore we focused on all carriers. We found that 81.5% of those with clinical information available were considered symptomatic, with severity ranging from minor signs on clinical examination to severe disability. In previous reports, including ~~another~~ French PFBC series and a meta-analysis study, the proportion of symptomatic patients was indeed lower, 58 and 64%, respectively [1, 39]. Here, the relatively high proportion of symptomatic carriers is likely due to an inclusion bias, as symptomatic probands are more likely to be offered genetic screening than asymptomatic individuals and few relatives could be included in the present report (11/56 versus 35/57 in [1]). Age of onset was comparable to previous screens, with a wide range from 3 to 81 years. Consistent with previously published series, the most frequent symptoms in our series were parkinsonism (54.5% of symptomatic individuals), cognitive impairment, and psychiatric signs (43.2% each). Interestingly, 18.5% of the 54 patients with available clinical data reported migraine without atypical features, which is in the same range as the general population [40], suggesting that migraine in patients with brain calcifications may be coincidental. This ratio is consistent with those reported in an independent series and a literature review study [1, 39], while there are also reports that showed lack of segregation between brain calcification and migraine [41].

In summary, by screening the known *PFBC* genes in four cohorts from America and Europe, including sporadic and familial cases, we identified variants interpreted as VUS, likely pathogenic, or pathogenic in 25.4% of the 177 probands. While variants from the latter two classes can be used for genetic counseling, segregation and/or functional studies of the VUS are necessary to help clarify their role in PFBC, and therefore no presymptomatic testing can be recommended given the current level of evidence. The novel variants reported here will help with interpretation of future genetic screens of unrelated PFBC patients and provide a list of candidates for functional studies. Finally, further prospective follow-up studies in patients carrying pathogenic variants in *PFBC*-related genes are needed to widen our knowledge about disease course, genetic and/or environmental factors which could influence disease penetrance and progression.

Acknowledgements We thank all the patients for participating in this study and the physicians who referred patients for the study. The coinvestigators of the French PFBC study group are listed in supplementary information.

~~**Members of French PFBC study group** Lylyan Pimentel, Daniel H Geschwind, Olivier Vanakker, Douglas Galasko, Brent L Fogel, A Micheil Innes, Alison Ross, William B Dobyns, Diana Alcantara, Mark O'Driscoll, Didier Hannequin, Dominique Campion, João R Oliveira, Barbara Garavaglia, Giovanni Coppola, Gaël Nicolas.~~

Funding This study was cosupported by CNR-MAJ, Inserm, European Union and Région Normandie. Europe gets involved in Normandie with European Regional Development Fund (ERDF) (French group). This study received support from FACEPE, CAPES, and CNPq (310150/2016-7,480255/2013-0, 440770/2016-5; BR group). We acknowledge the support of the NINDS Informatics Center for Neurogenetics and Neurogenomics (P30 NS062691), NIH grants R01 NS40752 to DHG, R01NS082094 to BLF, and R01 HL130996 to WBD, the Bev Carrick Memorial Fund to GC (US group), and Cancer Research UK Programme Award C24110/A15394 to MOD. Funding sources had no specific roles.

Compliance with ethical standards

Conflict of interest The authors declare that they have no conflict of interest.

References

1. Nicolas G,Charbonnier C,de Lemos RR, et al. Brain calcification process and phenotypes according to age and sex: lessons from SLC20A2, PDGFB, and PDGFRB mutation carriers. Am J Med Genet B Neuropsychiatr Genet.2015;168:586–94.
2. Ramos EM, Oliveira J, Sobrido MJ, Coppola G. Primary familial brain calcification. In: Adam MP, Ardinger HH, Pagon RA et al, editors. GeneReviews. Seattle, WA: University of Washington; 1993–2018.
3. Wang C, Li Y, Shi L, et al. Mutations in SLC20A2 link familial idiopathic basal ganglia calcification with phosphate homeostasis. Nat Genet. 2012;44:254–6.
4. Lemos RR, Ramos EM, Legati A, et al. Update and mutational analysis of SLC20A2: a major cause of primary familial brain calcification. Human Mutat. 2015;36:489–95.
5. Jensen N, Autzen JK, Pedersen L. Slc20a2 is critical for maintaining a physiologic inorganic phosphate level in cerebrospinal fluid. Neurogenetics. 2016;17:125–30.
6. Nicolas G, Pottier C, Maltete D, et al. Mutation of the *PDGFRB* gene as a cause of idiopathic basal ganglia calcification. Neurology. 2013;80:181–7.
7. Nicolas G, Pottier C, Charbonnier C, et al. Phenotypic spectrum of probable and genetically-confirmed idiopathic basal ganglia calcification. Brain. 2013;136:3395–407.
8. Sanchez-Contreras M, Baker MC, Finch NA, et al. Genetic screening and functional characterization of PDGFRB mutations associated with basal ganglia calcification of unknown etiology. Human Mutat. 2014;35:964–71.
9. Keller A, Westenberger A, Sobrido MJ, et al. Mutations in the gene encoding PDGF-B cause brain calcifications in humans and mice. Nat Genet. 2013;45:1077–82.
10. Keogh MJ, Pyle A, Daud D, et al. Clinical heterogeneity of primary familial brain calcification due to a novel mutation in PDGFB. Neurology. 2015;84:1818–20.
11. Nicolas G, Jacquin A, Thauvin-Robinet C, et al. A de novo nonsense PDGFB mutation causing idiopathic basal ganglia calcification with laryngeal dystonia. Eur J Human Genet. 2014;22:1236–8.
12. Nicolas G, Rovelet-Lecrux A, Pottier C, et al. PDGFB partial deletion: a new, rare mechanism causing brain calcification with leukoencephalopathy. J Mol Neurosci. 2014;53:171–5.
13. Fredriksson L, Li H, Eriksson U. The PDGF family: four gene products form five dimeric isoforms. Cytokine Growth Factor Rev. 2004;15:197–204.
14. Appiah-Kubi K, Lan T, Wang Y, et al. Platelet-derived growth factor receptors (PDGFRs) fusion genes involvement in hematological malignancies. Crit Rev Oncol/Hematol. 2017;109:20–34.
15. Cheung YH, Gayden T, Campeau PM, et al. A recurrent PDGFRB mutation causes familial infantile myofibromatosis. Am J Hum Genet. 2013;92:996–1000.
16. Johnston JJ, Sanchez-Contreras MY, Keppler-Noreuil KM, et al. A point mutation in PDGFRB causes autosomal-dominant penttinen syndrome. Am J Hum Genet. 2015;97:465–74.
17. Martignetti JA, Tian L, Li D, et al. Mutations in PDGFRB cause autosomal-dominant infantile myofibromatosis. Am J Hum Genet. 2013;92:1001–7.
18. Takenouchi T, Yamaguchi Y, Tanikawa A, Kosaki R, Okano H, Kosaki K. Novel overgrowth syndrome phenotype due to recurrent de novo PDGFRB mutation. J Pediatr. 2015;166:483–6.
19. Vanlandewijck M, Lebouvier T, Andaloussi Mae M, et al. Functional characterization of germline mutations in PDGFB and PDGFRB in primary familial brain calcification. PLoS ONE. 2015;10:e0143407.
20. Arts FA, Velghe AI, Stevens M, Renauld JC, Essaghir A, Demoulin JB. Idiopathic basal ganglia calcification-associated PDGFRB mutations impair the receptor signalling. J Cell Mol Med. 2015;19:239–48.
21. Giachelli CM, Jono S, Shioi A, Nishizawa Y, Mori K, Morii H. Vascular calcification and inorganic phosphate. Am J Kidney Dis. 2001;38:S34–37.
22. Legati A, Giovannini D, Nicolas G, et al. Mutations in XPR1 cause primary familial brain calcification associated with altered phosphate export. Nat Genet. 2015;47:579–81.
23. Anheim M, Lopez-Sanchez U, Giovannini D, et al. XPR1 mutations are a rare cause of primary familial brain calcification. J Neurol. 2016;263:1559–64.
24. Richards S, Aziz N, Bale S, et al. Standards and guidelines for the interpretation of sequence variants: a joint consensus recommendation of the American College of Medical Genetics and Genomics and the Association for Molecular Pathology. Genet Med. 2015;17:405–24.
25. Lek M, Karczewski KJ, Minikel EV, et al. Analysis of protein-coding genetic variation in 60,706 humans. Nature. 2016;536:285–91.
26. David S, Ferreira J, Quenez O, et al. Identification of partial SLC20A2 deletions in primary brain calcification using whole-exome sequencing. Eur J Human Genet. 2016;24:1630–4.
27. Klambauer G, Schwarzbauer K, Mayr A, et al. cn.MOPS: Mixture of Poissons for discovering copy number variations in next-generation sequencing data with a low false discovery rate. Nucleic Acids Res. 2012;40:e69.
28. Carecchio M, Varrasi C, Barzaghi C, et al. Phenotypic heterogeneity of movement disorders due to intracranial calcifications with or without SLC20A2 mutations. Mov Disord. 2014;29:S47.
29. Baker M, Strongosky AJ, Sanchez-Contreras MY, et al. SLC20A2 and THAP1 deletion in familial basal ganglia calcification with dystonia. Neurogenetics. 2014;15:23–30.
30. Mi TM, Mao W, Cai YN et al. Primary familial brain calcifications linked with a novel SLC20A2 gene mutation in a Chinese family. J Neurogenet. 2017;31:149–52.

31. Taglia I, Mignarri A, Olgiati S, et al. Primary familial brain calcification: genetic analysis and clinical spectrum. Mov Disord. 2014;29:1691–5.
32. Yamada M, Tanaka M, Takagi M, et al. Evaluation of SLC20A2 mutations that cause idiopathic basal ganglia calcification in Japan. Neurology. 2014;82:705–12.
33. Nicolas G, Richard AC, Pottier C, et al. Overall mutational spectrum of SLC20A2, PDGFB and PDGFRB in idiopathic basal ganglia calcification. Neurogenetics. 2014;15:215–6.
34. Hsu SC, Sears RL, Lemos RR, et al. Mutations in SLC20A2 are a major cause of familial idiopathic basal ganglia calcification. Neurogenetics. 2013;14:11–22.
35. Jensen N, Schroder HD, Hejbol EK, Fuchtbauer EM, de Oliveira JR, Pedersen L. Loss of function of Slc20a2 associated with familial idiopathic Basal Ganglia calcification in humans causes brain calcifications in mice. J Mol Neurosci. 2013;51:994–9.
36. Wallingford MC, Chia JJ, Leaf EM, et al. SLC20A2 deficiency in mice leads to elevated phosphate levels in cerbrospinal fluid and glymphatic pathway-associated arteriolar calcification, and recapitulates human idiopathic basal ganglia calcification. Brain Pathol. 2017;27:64–76.
37. Yao XP, Wang C, Su HZ et al. Mutation screening of PDGFB gene in Chinese population with primary familial brain calcification. Gene. 2016.
38. Wang C, Yao XP, Chen HT, et al. Novel mutations of PDGFRB cause primary familial brain calcification in Chinese families. J Human Genet. 2017;62:697–701.
39. Tadic V, Westenberger A, Domingo A, Alvarez-Fischer D, Klein C, Kasten M. Primary familial brain calcification with known gene mutations: a systematic review and challenges of phenotypic characterization. JAMA Neurol. 2015;72:460–7.
40. Lipton RB, Bigal ME. Migraine: Epidemiology, impact, and risk factors for progression. Headache. 2005;45(Suppl 1):S3–S13.
41. Ferreira JB, Pimentel L, Keasey MP, et al. First report of a de novo mutation at SLC20A2 in a patient with brain calcification. J Mol Neurosci. 2014;54:748–51.

Affiliations

Eliana Marisa Ramos[1] · Miryam Carecchio[2,3,4] · Roberta Lemos[5] · Joana Ferreira[5] · Andrea Legati[1] · Renee Louise Sears[1] · Sandy Chan Hsu[1] · Celeste Panteghini[2] · Luca Magistrelli[6] · Ettore Salsano[7] · Silvia Esposito[3] · Franco Taroni[8] · Anne-Claire Richard[9] · Christine Tranchant[10,11] · Mathieu Anheim[10,11] · Xavier Ayrignac[12] · Cyril Goizet[13,14] · Marie Vidailhet[15] · David Maltete[16] · David Wallon[17] · Thierry Frebourg[9] · Lylyan Pimentel[5] · Daniel H. Geschwind[1] · Olivier Vanakker[18] · Douglas Galasko[19] · Brent L. Fogel[20] · A Micheil Innes[21] · Alison Ross[22] · William B. Dobyns[23] · Diana Alcantara[24] · Mark O'Driscoll[24] · Didier Hannequin[25] · Dominique Campion[9,26] · João R. Oliveira[5] · Barbara Garavaglia[2] · Giovanni Coppola[1] · Gaël Nicolas[9]The French PFBC study group

[1] Department of Psychiatry, David Geffen School of Medicine, University of California Los Angeles, Los Angeles, CA, USA

[2] Molecular Neurogenetics Unit, Movement Disorders Section, IRCCS Foundation Carlo Besta Neurological Institute, Via L. Temolo n. 4, Milan 20116, Italy

[3] Department of Pediatric Neurology, IRCCS Foundation Carlo Besta Neurological Institute, Via Celoria 11, Milan 20131, Italy

[4] PhD Programme in Translational and Molecular Medicine, Milan Bicocca University, Monza, Italy

[5] Keizo Asami Laboratory, Universidade Federal de Pernambuco, Recife, Brazil

[6] Department of Neurology, University of Eastern Piedmont, C.so Mazzini 18, Novara 28100, Italy

[7] Department of Clinical Neurosciences, IRCCS Foundation Carlo Besta Neurological Institute, Via Celoria 11, Milan 20131, Italy

[8] IRCCS Foundation Carlo Besta Neurological Institute, Via Amadeo 42, Milan 20133, Italy

[9] Department of Genetics and CNR-MAJ, Normandy Center for Genomic and Personalized Medicine, Normandie Univ, UNIROUEN, Inserm U1245, Rouen University Hospital, Rouen F 76000, France

[10] Service de Neurologie, Hôpitaux Universitaires de Strasbourg, Hôpital de Hautepierre; Fédération de Médecine Translationnelle de Strasbourg (FMTS), Université de Strasbourg, Strasbourg, France

[11] Institut de Génétique et de Biologie Moléculaire et Cellulaire (IGBMC), INSERM-U964/CNRS-UMR7104/Université de Strasbourg, Strasbourg, Illkirch, France

[12] Department of Neurology, Montpellier University Hospital, Montpellier, France

[13] CHU Bordeaux, Service de Génétique Médicale, Bordeaux 33000, France

[14] INSERM U1211 Univ Bordeaux, Laboratoire Maladies Rares, Génétique et Métab, Bordeaux 33000, France

[15] Département de neurologie, Hôpital Pitié-Salpêtrière, Assistance Publique—Hôpitaux de Paris, Paris, UPMC Univ Paris 06, Inserm U1127, CNRS UMR 7225, ICM, Sorbonne Universites, Paris F-75013, France

[16] Department of Neurology, Normandie Univ, UNIROUEN, Inserm U1073, Rouen University Hospital, Rouen F 76000, France

[17] Department of Neurology and CNR-MAJ, Normandy Center for Genomic and Personalized Medicine, Normandie Univ, UNIROUEN, Inserm U1245 and Rouen University Hospital, Rouen F 76000, France

[18] Center for Medical Genetics, Ghent University Hospital, De Pintelaan 185, Ghent B-9000, Belgium

[19] Veterans Affairs Medical Center, San Diego and University of California, San Diego, USA

[20] Departments of Neurology and Human Genetics, David Geffen

School of Medicine, University of California Los Angeles, Los Angeles, CA, USA

[21] Department of Medical Genetics and Alberta Children's Hospital Research Institute, Cumming School of Medicine, University of Calgary, Calgary, Canada

[22] Department of Clinical Genetics, Ashgrove House, Foresterhill, Aberdeen, UK

[23] Departments of Pediatrics and Neurology, University of Washington; and Center for Integrative Brain Research, Seattle Children's Research Institute, Seattle, WA, USA

[24] Genome Damage & Stability Centre, University of Sussex, Brighton, UK

[25] Department of Neurology, Department of Genetics and CNR-MAJ, Normandy Center for Genomic and Personalized Medicine, Normandie Univ, UNIROUEN, Inserm U1245 and Rouen University Hospital, Rouen F 76000, France

[26] Department of Research Rouvray Psychiatric Hospital, Sotteville-lès-Rouen, Rouen, France

Supplementary Methods

Inclusions. The French PFBC series included a total of 90 unrelated probands that were referred from multiple French centers to the Inserm U1245 research Unit in Rouen from January 2015 to February 2017. One of these patients, carrying an *XPR1* variant, has already been reported in detail elsewhere.[1] Patients referred to this center before January 2015 were already reported and not included in this study.[2-4]

The Italian series included 49 unrelated probands referred to the Molecular Neurogenetics Unit of C. Besta Neurological Institute in Milan from April 2014 to April 2017. Of these, one patient carrying an *SLC20A2* variant, has previously been reported in detail elsewhere.[5]

The US group, included a total of 16 primary brain calcification unrelated probands referred to UCLA from April 2014 up until January 2017. Patients referred to this center before April 2014 were already reported and not included in this study.[3, 6-8]

A total of 22 patients from multiple Brazil centers, referred to the Keizo Asami Laboratory – LIKA / Federal University of Pernambuco – UFPE in Recife from April 2014 to January 2017, were included in this study as part of the Brazilian series. Patients referred to this center before April 2014 were previously reported and not included in this study.[4, 9]

Genetic screening of the Italian patients using a NGS panel. Target regions included the exons of each gene ±20 bp intronic flanking sequence. Samples were sequenced with a Miseq sequencer (Illumina) with 50x average depth. Raw reads were aligned to the human genome (GRCh37 assembly), variants were called and annotated using Variant-Studio (Illumina) and then filtered, focusing on rare (MAF <1% in 1000 Genome Project, Exome Aggregation Consortium - ExAC, and Exome Sequencing Project databases) and potentially damaging variants (Polyphen2, SIFT and MutationTaster). Variants were confirmed by Sanger sequencing in probands and available relatives.

In the Italian series, where other genes responsible for diseases characterized by cerebral calcification were also screened, only one patient received an alternative genetic diagnosis (Cockayne syndrome type B, MIM #133540), carrying compound heterozygous *ERCC6* pathogenic variants (NM_000124.3: c.2143G>T, p.(Gly715Ter) and c.229C>T, p.(Arg77Ter)).

Functional assessment of the PDGFRB p.Asp844Gly variant. MYC-DDK(FLAG)-tagged-*PDGFRB* (NM_002609) ORF (Clone # RC206377) encoding human platelet-derived growth factor receptor beta polypeptide (PDGFRβ) was obtained from Origene, and patient variants

engineered using QuikChange® Site-Directed Mutagenesis Kit (cat# *200518)* from Agilent Technologies (Stratagene), using the following primer pairs:

p.D844G	5'-GTCAAGATCTGTGGCTTTGGCCTGGC-3'
	5'-GCCAGGCCAAAGCCACAGATCTTGAC-3'
p.W566R	5'-GTTACGAGATCCGACGGAAGGTGATTGAG-3'
	5'-CTCAATCACCTTCCGTCGGATCTCGTAAC-3'

HEK293 cells, grown in DMEM with 10% foetal calf serum, L-GLN and Pen-Strep, were transfected using calcium phosphate method. 48hrs post-transfection, cells were extracted using IP buffer (50mM Tris.HCl pH7.5, 150mM NaCl, 2mM EDTA, 2mM EGTA, 50mM NaF, 25mM β-glycerolphosphate, 0.1mM Na-orthovanadate, 0.2% Triton-X100, 0.3% IGEPAL, protease inhibitor cocktail (Roche)). 300µg of extract used for immunoprecipitation via anti-FLAG® M2 Affinity Gel (A2220) from Sigma-Aldrich. The antibodies used subsequently for western blotting included phospho-Tyrosine mouse monoclonal p-Tyr-100 (cat# 9411) from Cell Signaling Technologies and monoclonal mouse anti-FLAG® M2 antibody (F3165) from Sigma-Aldrich.

Supplementary Figure 1

Following ectopic over-expression of FLAG-tagged PDGFRβ constructs and immunoprecipitation (IP) using FLAG affinity beads, increasing amounts of IP'd extract was western blotted using anti-phosphotyrosine (pY) antibody to detect PDGFRβ trans-autophosphorylation. Blotting using anti-FLAG antibody confirmed IP. Auto-phosphorylation of the D844G variant was undetectable under these conditions, compared to that of wild-type (WT). W566R, a known hyper-active infantile myofibromatosis variant was included as a control.[10]

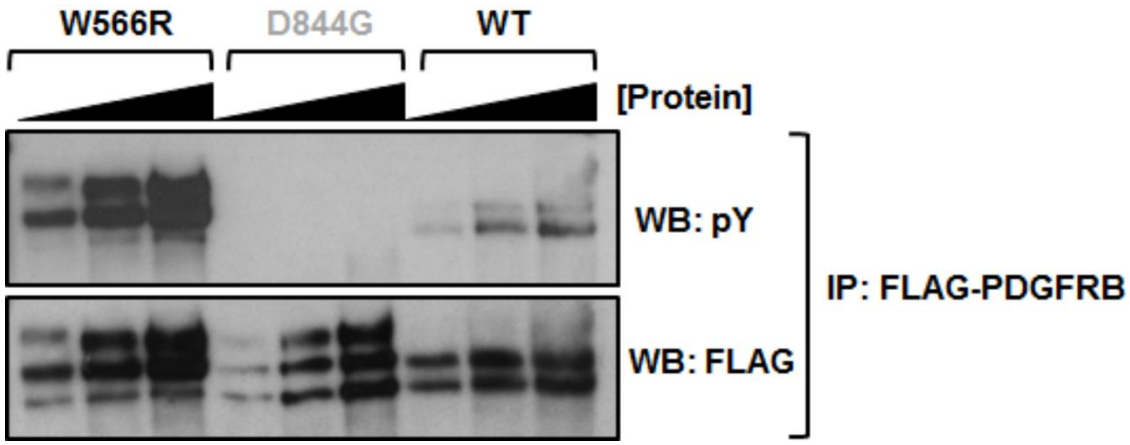

Supplementary Table 1. Genetic screening in the 4 series

Case series	Total probands screened	Likely pathogenic (class 4) and pathogenic (class 5) variants, n unrelated proband carriers [genes]	Detection rate (class 4+5)	Variants of unknown significance (class3), n unrelated probands carriers [genes]	Detection rate (class 3)	Overall detection rate	N affected relatives included	Total affected individuals
France	90	19 [*SLC20A2*: n=12*, *PDGFB*: n=4 *XPR1*: n=3**]	21.1%	6 [*SLC20A2*: n=4, *PDGFB*: n=1 *XPR1*: n=1]	6.7%	25/90 (27.8%)	4	29
Italy	49	7 *[SLC20A2*: n=5***, *XPR1**: n=2]	14.3%	5 [*SLC20A2*: n=3, *PDGFRB*: n=2]	10.2%	12/49 (24.5%)	2	14
US	16	7 *[SLC20A2*: n=5, *PDGFB*: n=1 *PDGFRB*: n=1]	43.8%	0	0	7/16 (43.8%)	4	11
Brazil	22	1 [*SLC20A2*]	4.5%	0	0	1/22 (4.5%)	1	2
Total	177	34	19.2%	11	6.2%	45/177 (25.4%)	11	56

*2 unrelated probands carried the same variant

**including one previously reported patient[1]

***including one previously reported patient[5]

REFERENCES

1. Anheim M, Lopez-Sanchez U, Giovannini D, et al. XPR1 mutations are a rare cause of primary familial brain calcification. Journal of neurology 2016;263:1559-1564.

2. David S, Ferreira J, Quenez O, et al. Identification of partial SLC20A2 deletions in primary brain calcification using whole-exome sequencing. European journal of human genetics : EJHG 2016;24:1630-1634.

3. Legati A, Giovannini D, Nicolas G, et al. Mutations in XPR1 cause primary familial brain calcification associated with altered phosphate export. Nat Genet 2015;47:579-581.

4. Nicolas G, Charbonnier C, de Lemos RR, et al. Brain calcification process and phenotypes according to age and sex: Lessons from SLC20A2, PDGFB, and PDGFRB mutation carriers. American journal of medical genetics Part B, Neuropsychiatric genetics : the official publication of the International Society of Psychiatric Genetics 2015;168:586-594.

5. Carecchio M, Varrasi C, Barzaghi C, et al. Phenotypic heterogeneity of movement disorders due to intracranial calcifications with or without SLC20A2 mutations. Movement Disorders 2014;29:S47 (abstract 125).

6. Hsu SC, Sears RL, Lemos RR, et al. Mutations in SLC20A2 are a major cause of familial idiopathic basal ganglia calcification. Neurogenetics 2013;14:11-22.

7. Keller A, Westenberger A, Sobrido MJ, et al. Mutations in the gene encoding PDGF-B cause brain calcifications in humans and mice. Nat Genet 2013;45:1077-1082.

8. Rosby O, Legati A, Coppola G. Primary familial brain calcification in a Norwegian family, caused by a novel SLC20A2 gene mutation. Journal of neurology 2016;263:594-596.

9. Lemos RR, Ramos EM, Legati A, et al. Update and Mutational Analysis of SLC20A2: A Major Cause of Primary Familial Brain Calcification. Human mutation 2015;36:489-495.

10. Arts FA, Sciot R, Brichard B, et al. PDGFRB gain-of-function mutations in sporadic infantile myofibromatosis. Human molecular genetics 2017;26:1801-1810.

APÊNDICE B – Artigo publicado no periódico *Journal of Molecular Neuroscience*

L.F. Pimentel, R.R. Lemos, J.R. Oliveira (2017). Phosphate Transporters Expression in Patients with Primary Familial Brain Calcifications. *Journal of Molecular Neuroscience*. 62:276–280. DOI: 10.1007/s12031-017-0934-9

Fator de impacto 2018: 2,504

Classificação Qualis na área Ciências Biológicas I (2016): B1

Previous studies have shown that *SLC20A2* gene has a lower expression in PFBC patients with nonsense mutations. Zhang et al. (2013) had found a 30% reduction in a blood sample of a patient compared with a healthy control, in the presence of a heterozygous nonsense variation in *SLC20A2*, exon 4, resulting in a non-functional protein (Zhang et al. 2013). More recently, Ferreira et al. (2014) reported the first de novo nonsense mutation in *SLC20A2* on exon 8, in a Brazilian PFBC patient, together with a gene expression analysis that showed a 10% decrease in *SLC20A2* mRNA expression (Ferreira et al. 2014).

In order to explore different ways to correlate genetic findings with other parameters such as gene expression level, here, we analyzed mRNA expression of three phosphate transporters, *SLC20A1*, *SLC20A2*, and *XPR1* in blood sample of patients with confirmed PFBC.

Methods

Samples and Subjects

We studied 24 samples of which 3 non-related individuals were affected by PFBC and previously reported to have *SLC20A2* mutations (Fig. 1a, (a–c)) (Wang et al. 2012; Lemos et al. 2013; Ferreira et al. 2014). The remaining 21 samples are family members who were divided into four classes: patients with positive brain CT scan and confirmed clinical manifestations were classified as *affected* (Nicolas et al. 2013); asymptomatic individuals with negative brain CT scan results were classified as *unaffected*. Asymptomatic subjects whose brain CT scan was not available were classified as having *unknown status*; asymptomatic individuals with affected offspring and negative brain CT scan results or unavailable CT scan were classified as *obligate carriers*, in accordance to the autosomal dominant inheritance of the PFBC. All affected individuals were screened for mutations in *SLC20A2*, *PDGFβ*, *PDGFRβ*, and *XPR1* using Sanger sequencing (Fig. 1a, (d–h); Fig. 1b). Because we did not have access to the RNA sample of one patient, we analyzed gene expression of *SLC20A1*, *SLC20A2*, and *XPR1* in nine patients and 14 controls. Samples were processed using PAXgene Blood RNA kit (Qiagen, #762164, Switzerland).

Molecular and Statistical Analysis

All molecular experiments were carried out as described in Ferreira et al. 2014. Genetic screening was performed in the five new probands in order to investigate a PFBC causative mutation. qPCR analysis was performed in a ViiA7™ Real-Time PCR System (Applied Biosystems, USA) with TaqMan probes (Applied Biosystems, USA) and normalized with *GAPDH* (*SLC20A1* Hs00965587_m1; *SLC20A2* Hs00198840_m1; *XPR1* Hs00173707_m1; *GAPDH* Hs02758991_g1).

Differences between the groups were analyzed using either one-way ANOVA or Mann Whitney test and the data values are shown as mean and standard deviation (+/− SD). Statistical analysis was performed using the GraphPad Prism 5 program (GraphPad Software, Inc., San Diego CA); the null hypothesis was rejected at the 0.05 level.

Results

Sanger sequencing did not identified genetic variations in the patients tested for the main genes linked to PFBC, *SLC20A2*, *PDGFβ*, *PDGFRβ*, and *XPR1*. Therefore, the patients were divided in two groups for expression analysis: mutated (with mutation in *SLC20A2* gene; two female and one male; mean age 39 ± 5.2 years) and unmutated (without mutation in the genes related to PFBC; three female and three male; mean age 54.2 ± 15 years). Control group was composed of 14 individuals (four classified as unaffected and ten as having unknown status; mean age 48.5 ± 15.6 years; all Caucasian), of which four have undergone radiological exam with negative results (three female, 40, 62, and 71 years old; one male, 35 years old).

Real-time qPCR analysis showed a significant reduction in *SLC20A2* mRNA expression (~40%) in the patients carrying a mutation compared with control group ($p < 0.01$), whereas statistical assessment has shown no significant differences between control group and unmutated patients in *SLC20A2* expression (Fig. 2). Either regarding to *SLC20A1* and *XPR1* expression, no difference was detected in mutated or unmtated individuals relative to control group ($p > 0.05$).

Discussion

SLC20A2 (PiT2) and its homologous, *SLC20A1* (PiT1), are transmembrane proteins involved with phosphate homeostasis in mammalian cells transporting Pi through the cell membrane from the extracellular media to the cytosol (Bøttger and Pedersen 2011). Loss of function variants in *SLC20A2* gene has been associated with most of the PFBC cases and knockout model has confirmed that the reduced PiT2 expression causes imbalance of Pi levels and vascular brain calcification, including in basal ganglia and thalamus (Hsu et al. 2013; Jensen et al. 2013, 2016).

These results suggest that the reduction of *SLC20A2* expression alone can trigger a pattern of brain calcification similar to that found in PFBC patients. Because PiT2 protein is highly and widely expressed, it would be a challenge to detect small quantitative differences in *SLC20A2* expression. However, here, we showed that *SLC20A2* pathogenic variants are responsible for decreasing its expression in blood samples

of PFBC patients (~40%), whereas no significant change was detected within the affected individuals without mutation.

This data supports previous evidences according to which *SLC20A2* variants result in haplo-insufficiency and causes reduction of its expression (Wang et al. 2012; Ferreira et al. 2014b). However, the decreasing of *SLC20A2* is subtle and it might be explained by the compensation by the wild-type allele unleashed by allelic loss. Additionally, Wang and co-workers demonstrated that *SLC20A2* mutations resulted in significant damaged ^{32}Pi uptake in *Xenopus* oocytes (Wang et al. 2012).

Xenotropic and polytropic retrovirus receptor 1 (*XPR1*) gene encodes a cell-surface membrane protein that mediates phosphate export through the membrane of mammalian cells (Giovannini et al. 2013). Recently, *XPR1* missense variants were identified in PFBC patients. Functional analysis has shown that pathogenic mutations in *XPR1* leads to decreased cell membrane localization and phosphate efflux impairment in both HEK cells and PBMC of patients harboring the mutations (Legati et al. 2015; Anheim et al. 2016).

Because *SLC20A1*, *SLC20A2*, and *XPR1* are involved with phosphate transport, even that in opposite directions, it is common to hypothesize that they can coregalute each other such that a dysfunction in one of these genes would affect the others. Also, studies suggest that impairment of *XPR1* function could trigger increased intracellular phosphate concentration and thus downregulate PiT2 expression, affecting Pi transport (Jensen et al. 2016). Herein, we showed that different mutations in *SLC20A2* gene dropped its mRNA expression in blood of PFBC patients, but did not affect *SLC20A1* and *XPR1* expressions. Our results are consistent with previous data that found that *XPR1* mutations specifically decreased phosphate efflux, as an effect of *XPR1* impairment, but no effect on PiT1 and PiT2 either on phosphate uptake was observed (Legati et al. 2015; Anheim et al. 2016).

Finally, our study adds more evidences that suggest that phosphate import and export are independent functions and that pathogenic variations are capable of modifying gene expression in a level that can be detected in blood samples. However, a larger cohort would be needed in order to confirm if expression levels or mutation analysis could correlate with clinical severity but this analysis reinforce previous evidence that blood samples should be considered as a future source to screen biomarkers linked to PFBC.

Acknowledgments We wish to thank Joana Ferreira and Matheus Oliveira for their valuable collaboration; Conselho Nacional de Desenvolvimento Científico e Tecnológico (CNPq) (457556/2013-7; 307909/2012-3; 400540/2013-4; 480225/2013-0; 310150/2016-7; 480255/2013-0); Pró-Reitoria para Assuntos de Pesquisa e Pós-Graduação - Universidade Federal de Pernambuco (UFPE) - INOVA-Saúde; L.F.P. and R.R.L. holds a fellowship grant from Fundação de Amparo à Ciência e Tecnologia do Estado de Pernambuco (FACEPE); Coordenação de Aperfeiçoamento de Pessoal de Nível Superior (CAPES).

Compliance with Ethical Standards

Conflict of Interest The authors declare that they have no conflict of interest.

References

Anheim M, López-Sánchez U, Giovannini D, Richard A, Touhami J, N'Guyen L, Rudolf G, Thibault-Stoll A, Frebourg T, Hannequin D, Campion D, Battini J-L, Sitbon M, Nicolas G (2016) XPR1 mutations are a rare cause of primary familial brain calcification. J Neurol 263:1559–1564

Bøttger P, Pedersen L (2011) Mapping of the minimal inorganic phosphate transporting unit of human PiT2 suggests a structure universal to PiT-related proteins from all kingdoms of life. BMC Biochem 12:21

Ferreira JB, Pimentel L, Keasey MP, Lemos RR, Santos LM, Oliveira MF et al (2014) First report of a de novo mutation at SLC20A2 in a patient with brain calcification. J Mol Neurosci 54(4):748–751

Giovannini D, Touhami J, Charnet P, Sitbon M, Battini J (2013) Inorganic phosphate export by the retrovirus receptor XPR1 in metazoans. Cell rep 3:1866–1873

Hsu SC, Sears RL, Lemos RR et al (2013) Mutations in SLC20A2 are a major cause of familial idiopathic basal ganglia calcification. Neurogenetics 14:11–22

Jensen N, Schrøder HD, Hejbøl EK, Füchtbauer E-M, de Oliveira JRM, Pedersen L (2013) Loss of function of SLC20A2 associated with familial idiopathic basal ganglia calcification in humans causes brain calcifications in mice. J Mol Neurosci 51:994–999

Jensen N, Autzen JK, Pedersen L (2016) SLC20A2 is critical for maintaining a physiologic inorganic phosphate level in cerebrospinal fluid. Neurogenetics 17:125–130

Keasey MP, Lemos RR, Hagg T, Oliveira JRM (2016) Vitamin-D receptor agonist calcitriol reduces calcification in vitro through selective upregulation of SLC20A2 but not SLC20A1 or XPR1. Sci rep 6:25802

Keller A, Westenberger A, Sobrido MJ et al (2013) Mutations in the gene encoding PDGF-B cause brain calcifications in humans and mice. Nat Genet 45:1077–1082

Legati A, Giovannini D, Nicolas G et al (2015) Mutations in XPR1 cause primary familial brain calcification associated with altered phosphate export. Nat Genet 47:579–581

Lemos RR, Oliveira MF, Oliveira JRM (2013) Reporting a new mutation at the SLC20A2 gene in familial idiopathic basal ganglia calcification. Eur J Neurol 20:e43–e44

Lemos RR, Ramos EM, Legati A, Nicolas G, Jenkinson EM, Livingston JH, Crow YJ, Campion D, Coppola G, Oliveira JRM (2015) Update and mutational analysis of SLC20A2: a major cause of primary familial brain calcification. Hum Mutat 36:489–495

Nicolas G, Pottier C, Charbonnier C et al (2013) Phenotypic spectrum of probable and genetically-confirmed idiopathic basal ganglia calcification. Brain a J Neurol 136:3395–3407

Villa-Bellosta R, Ravera S, Sorribas V, Stange G, Levi M, Murer H, Biber J, Forster IC (2009) The Na+−Pi cotransporter PiT-2 (SLC20A2) is expressed in the apical membrane of rat renal proximal tubules and regulated by dietary Pi. Am J Physiol Renal Physiol 296:F691–F699

Wallingford MC, Gammill HS, Giachelli CM (2015) SLC20A2 deficiency results in fetal growth restriction and placental calcification associated with thickened basement membranes and novel CD13 and lamininα1 expressing cells. Reprod Biol 16:13–26

Wang C, Li Y, Shi L, Ren J et al (2012) Mutations in SLC20A2 link familial idiopathic basal ganglia calcification with phosphate homeostasis. Nat Genet 44:254–256

Zhang Y, Guo X, Wu A (2013) Association between a novel mutation in SLC20A2 and familial idiopathic basal ganglia calcification. PLoS One 8:e57060

ANEXO A – Artigo publicado no periódico *Journal of Cell Science*

Keasey MP, Jia C, Pimentel LF, et al. (2017). Blood vitronectin is a major activator of LIF and pro-inflammatory IL-6 in the brain through integrin-FAK and uPAR signaling. *Journal of Cell Science*

Fator de Impacto 2015: 4,706

Classificação Qualis na área Ciências Biológicas I (2016): A2

© 2018. Published by The Company of Biologists Ltd | Journal of Cell Science (2018) 131, jcs202580. doi:10.1242/jcs.202580

RESEARCH ARTICLE

Blood vitronectin is a major activator of LIF and IL-6 in the brain through integrin–FAK and uPAR signaling

Matthew P. Keasey[1], Cuihong Jia[1], Lylyan F. Pimentel[1,2], Richard R. Sante[1], Chiharu Lovins[1] and Theo Hagg[1,*]

ABSTRACT

We defined how blood-derived vitronectin (VTN) rapidly and potently activates leukemia inhibitory factor (LIF) and pro-inflammatory interleukin 6 (IL-6) *in vitro* and after vascular injury in the brain. Treatment with VTN (but not fibrinogen, fibronectin, laminin-111 or collagen-I) substantially increased LIF and IL-6 within 4 h in C6-astroglioma cells, while $VTN^{-/-}$ mouse plasma was less effective than that from wild-type mice. LIF and IL-6 were induced by intracerebral injection of recombinant human (rh)VTN in mice, but induction seen upon intracerebral hemorrhage was less in $VTN^{-/-}$ mice than in wild-type littermates. *In vitro*, VTN effects were inhibited by RGD, αvβ3 and αvβ5 integrin-blocking peptides and antibodies. VTN activated focal adhesion kinase (FAK; also known as PTK2), whereas pharmacological- or siRNA-mediated inhibition of FAK, but not PYK2, reduced the expression of LIF and IL-6 in C6 and endothelial cells and after traumatic cell injury. Dominant-negative FAK (Y397F) reduced the amount of injury-induced LIF and IL-6. Pharmacological inhibition or knockdown of uPAR (also known as PLAUR), which binds VTN, also reduced cytokine expression, possibly through a common target of uPAR and integrins. We propose that VTN leakage into tissues promotes inflammation. Integrin–FAK signaling is therefore a novel IL-6 and LIF regulation mechanism relevant to the inflammation and stem cell fields.

KEY WORDS: FAK, IL-6, Integrin, LIF, Vitronectin, uPAR

INTRODUCTION

Vitronectin (VTN) is mainly produced in the liver by hepatocytes and endothelial cells (Seiffert et al., 1991, 1995) and is found at high concentrations in blood serum (Hayman et al., 1983). $VTN^{-/-}$ mice display no overt phenotype (Zheng et al., 1995) but exhibit delayed angiogenesis and poor wound healing (Jang et al., 2000), and defective vascular repair, causing persistent leakiness after injury (Li et al., 2012). Thus, leaked VTN may induce tissue repair responses. VTN has been detected in tissues in inflammatory rheumatoid arthritis (Tomasini-Johansson et al., 1998) and lung, liver and kidney fibrosis (Jang et al., 2000). Both VTN and fibronectin (another enriched plasma protein) leak into the brain after stroke (del Zoppo et al., 2012) and can activate microglia *in vitro* (Milner and Campbell, 2003; Welser-Alves et al., 2011).

[1]Department of Biomedical Sciences, Quillen College of Medicine, East Tennessee State University, Johnson City, TN 37614, USA. [2]Keizo Asami Laboratory (LIKA), Universidade Federal de Pernambuco, Recife, PE, Brasil.

*Author for correspondence (haggt1@etsu.edu)

M.P.K., 0000-0002-1236-3840; C.J., 0000-0002-9693-0012; L.F.P., 0000-0002-1467-7624; R.R.S., 0000-0002-9517-0752

Received 10 February 2017; Accepted 6 December 2017

Microglia and astrocytes express the VTN receptors αvβ3 and αvβ5 integrin (Herrera-Molina et al., 2012; Kang et al., 2008; Milner, 2009; Welser-Alves et al., 2011). Microglia and astrocytes, as well as endothelial cells, are major producers of pro-inflammatory cytokines, such as IL-6 and TNFα, *in vitro* and after traumatic or ischemic injury to the brain (Banner et al., 1997; Erta et al., 2012; Lau and Yu, 2001) or upon self-induction by IL-6 (Van Wagoner and Benveniste, 1999). IL-6 is a major regulator of a variety of inflammatory disorders and a target for therapies (Hunter and Jones, 2015). Its levels are almost non-existent in the normal brain but increase rapidly and greatly after acute injuries, such as stroke (Kang et al., 2013; Suzuki et al., 2009; Van Wagoner and Benveniste, 1999). The initial trigger(s) for IL-6 induction in the brain remains largely unresolved (Suzuki et al., 2009), but might include leakage of blood proteins upon blood–brain barrier disruption, which occurs rapidly after stroke (Krueger et al., 2015).

LIF is a GP130 (also known as IL6ST) receptor-activating cytokine, and as such related to the IL-6 family of cytokines (Zigmond, 2012). LIF is well known for playing a role during development and for promoting stem cell self-renewal *in vitro* and *in vivo* (Bauer and Patterson, 2006; Cartwright et al., 2005). LIF is also expressed by astrocytes (Banner et al., 1997), microglia (Nakanishi et al., 2007) and endothelial cells (Mi et al., 2001). It can also be pro-inflammatory (Kerr and Patterson, 2004; Pan et al., 2008; Suzuki et al., 2009), facilitating neutrophil activation (Borish et al., 1986) and macrophage infiltration, as demonstrated by conditioned medium experiments from $LIF^{-/-}$ and $IL\text{-}6^{-/-}$ Schwann cell preparations from denervated mouse sciatic nerves (Tofaris et al., 2002). LIF is expressed at very low levels throughout the body, but increases following brain injury (Banner et al., 1997) and stroke (Kang et al., 2013). Its expression in injured peripheral nerves is decreased again after repair (Dowsing et al., 2001), perhaps coincident with re-establishment of vascular integrity. The mechanisms regulating LIF expression are not well understood, but may include stimulation by IL-1β, possibly through mRNA stabilization (Carlson et al., 1996).

VTN has an RGD motif (Suzuki et al., 1985) with which it binds to the VTN receptors αvβ3 and αvβ5 integrin (Plow et al., 2000). It also interacts with several other proteins (Leavesley et al., 2013). Besides its cell adhesive properties, VTN activates integrin intracellular signaling molecules (Giancotti and Ruoslahti, 1999), including FAK (also known as PTK2), one of the major integrin transducers. Phosphorylation of Y397 is critical to FAK activation (Liu et al., 2003) and induces a number of signaling cascades (Keasey et al., 2013). Phosphorylation of FAK at Y397 is critical for TNFα-stimulated expression of IL-6 (Schlaepfer et al., 2007), suggesting that it might be a signaling node for cytokine regulation. VTN is unique among extracellular matrix (ECM) molecules because it also binds to urokinase-type plasminogen activator (uPA)

Journal of Cell Science

Journal of Cell Science (2018) 131, jcs202580. doi:10.1242/jcs.202580

receptor (uPAR; also known as PLAUR) (Madsen et al., 2007), a membrane-bound glycoprotein that serves as the receptor for uPA.

Here, we determined whether blood-derived proteins such as VTN regulate LIF and IL-6 expression through integrin–FAK and/or uPAR signaling, by using cultured astroglioma and endothelial cell, and adult mouse models.

RESULTS

VTN uniquely increases LIF and IL-6 expression *in vitro*

We had previously shown that some ECM molecules, including VTN, inhibit CNTF through integrin signaling (Keasey et al., 2013). To determine whether the related cytokines LIF and IL-6 are regulated by such blood proteins we first used serum, which has very high levels of ECM proteins such as VTN, fibronectin (FN1) and fibrinogen (Hayman et al., 1985). We cultured C6 astroglioma cells for 24 h in 10% fetal bovine serum (FBS), then changed the medium to low 1% (v/v) or regular 10% serum medium for an additional 24 h. In 1% serum, LIF and IL-6 mRNA levels were only ~33 and 45% (Fig. 1A,B), respectively, of that found when cells were in 10% serum. CNTF was upregulated in 1% serum (Fig. 1C), consistent with our previous study (Keasey et al., 2013), and suggesting that the decreases in LIF and IL-6 were not a general cellular response to serum withdrawal. We followed up this broad approach by testing specific ECM proteins. C6 cells were seeded onto plastic culture plates and maintained for 24 h and serum-deprived for a further 24 h. VTN, fibronectin, fibrinogen, laminin-111 (the isoform comprising α1, β1 and γ1 chains) or collagen-I were then added directly to the culture medium. Remarkably, after 4 h, only VTN produced a significant ~8-fold increase in LIF (Fig. 1D) and ~4-fold increase in IL-6 mRNA expression (Fig. 1E). VTN treatment for 24 h showed no discernable differences relative to vehicle controls (data not shown, n=2), suggesting that LIF and IL-6 are rapidly induced but then return to baseline levels. This could be due to VTN endocytosis and subsequent degradation (Memmo and McKeown-Longo, 1998). VTN effects were dose dependent (Fig. 1F,G) and resulted in increased LIF and IL-6 protein release from cells as confirmed with a dot blot assay of conditioned medium (Fig. 1H,I). In addition, C6 cells were grown in a medium containing 1% (v/v) plasma from $VTN^{-/-}$ or $VTN^{+/+}$ littermate mice, but without fetal bovine serum. After 4 h, LIF and IL-6 mRNA increases with $VTN^{-/-}$ plasma were only ~30% and 50%, respectively, of that seen with $VTN^{+/+}$ plasma (Fig. 1J,K). This suggests that native mouse VTN can increase LIF and IL-6 expression, and that an additional plasma molecule(s) also has such effects.

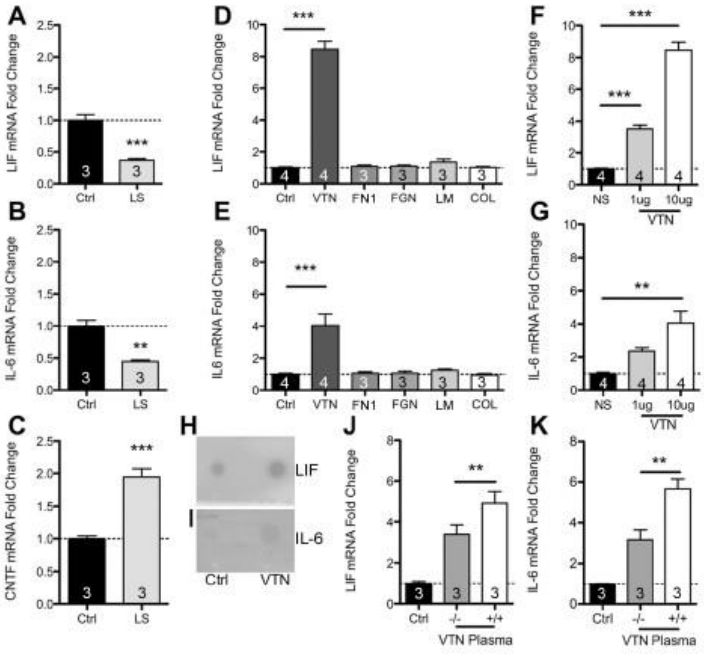

Fig. 1. Among ECM proteins, VTN uniquely activates LIF and IL-6 expression in C6 astroglioma cells. Serum contains a variety and various abundances of integrin-binding ECM proteins. We plated C6 cells for 24 h in 10% serum, then replaced the medium with a low serum formulation (1% v/v; LS) for 24 h, which reduced LIF (A) and IL-6 (B) mRNA expression, as measured by RT-qPCR, relative to that seen in control 10% serum (Ctrl). (C) In the same experiment as in A and B, CNTF mRNA was increased, likely due to inhibitory activity of serum ECMs, such as VTN, on CNTF expression which is negatively regulated by integrin–FAK signaling. In further experiments, we seeded C6 cells and maintained them for 24 h before serum was removed for a further 24 h. Then, VTN was 'spiked' into the medium (10 µg/ml concentration), where it rapidly (within 4 h) and robustly induced LIF (D) and IL-6 (E) mRNA relative to what was seen upon addition of PBS control (vehicle, no ECM substrate). Fibronectin (FN1), fibrinogen (FGN), laminin-111 (LM) or collagen-I (COL) addition had no effect. VTN increased LIF (F) and IL-6 (G) in a dose-dependent fashion. NS, no serum; concentrations of VTN are µg/ml. VTN treatment for 4 h caused increased release of LIF (H) and IL-6 (I) protein in conditioned medium, as shown by a dot blot assay (representative of three independent experiments). Plasma from $VTN^{-/-}$ mice induced LIF (J) and IL-6 (K) gene expression by less than plasma from $VTN^{+/+}$ littermates when added for 4 h to C6 cells that had been serum-deprived for 24 h. Data are means±s.e.m. of three or four independent experiments (as denoted in columns). $^{**}P$<0.01, $^{***}P$<0.001.

Journal of Cell Science (2018) 131, jcs202580. doi:10.1242/jcs.202580

Recombinant VTN and VTN from blood leaked into the brain upregulate brain LIF and IL-6 in adult mice

Recombinant human (rh)VTN was injected into the striatum of the brains of young adult mice. In $VTN^{+/+}$ (wild-type) mice, striatal LIF (2.8-fold) and IL-6 (2.5-fold) mRNA levels were increased 24 h later, relative to that seen after PBS control injections (Fig. 2A,C). In $VTN^{-/-}$ littermates (used to avoid the confounding effects of endogenous VTN), LIF (~5-fold) and IL-6 (~11-fold) were upregulated to higher levels than in the $VTN^{+/+}$ mice (Fig. 2A,C). This may represent an adaptive response to VTN deficiency. Heat inactivated (denatured) rhVTN injected into the striatum had no effect on either LIF or IL-6 mRNA expression (Fig. 2A,C), suggesting that the response to VTN is not due to an immune response against human protein. LIF (~4-fold) and IL-6 (~10-fold) protein expression was also induced in the striatum by VTN, relative to PBS injections, as measured by an ELISA in the contralateral side of these mice (Fig. 2B,D).

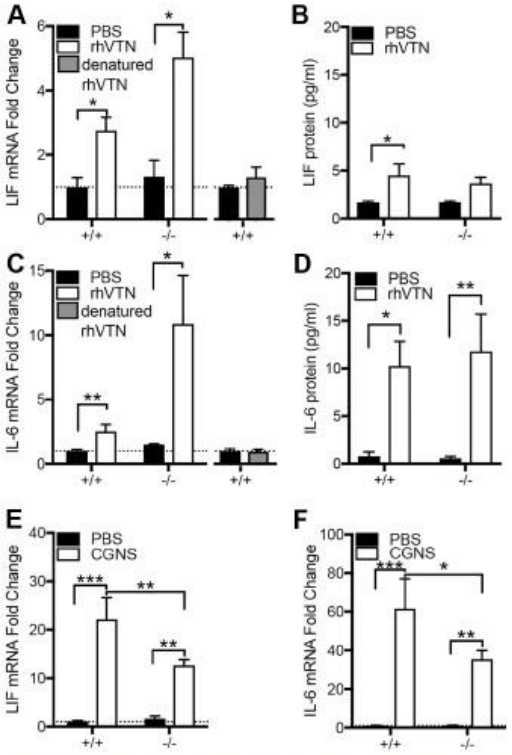

Fig. 2. VTN regulates LIF and IL-6 expression in mouse brain. Injection of 1 µg rhVTN into the striatum of adult $VTN^{+/+}$ or $VTN^{-/-}$ littermate mice leads to increased LIF mRNA (A), with no induction observed with heat denatured rhVTN (B). (C) rhVTN also induced IL-6 mRNA expression at 24 h relative to that seen upon PBS injections ($VTN^{+/+}$ mice: PBS n=7, VTN n=7; $VTN^{-/-}$ mice: PBS, n=5, VTN, n=5) with no difference seen when using heat denatured rhVTN (D). Total LIF (E) and IL-6 (F) protein were induced by rhVTN injection into the striatum of the same mice as measured by ELISA. Hemorrhagic leakage induced through collagenase injection into the striatum caused a greater increase in LIF (G) and IL-6 (H) mRNA in $VTN^{+/+}$ than in $VTN^{-/-}$ littermate mice after 24 h (n=6–7/group). Data are means±s.e.m. *P<0.05, **P<0.01, ***P<0.001.

To test the effects of leaked endogenous VTN from the blood, we induced a hemorrhage by injecting collagenase into the striatum of adult VTN mice. After 24 h, LIF expression was increased ~22-fold relative to PBS control injections in $VTN^{+/+}$ mice but only by half as much in $VTN^{-/-}$ littermates (Fig. 2E). IL-6 expression was increased ~62-fold in $VTN^{+/+}$ mice but by a lower amount (~35-fold) in $VTN^{-/-}$ littermates (Fig. 2F). This confirms that endogenous VTN leakage into the brain contributed to increases in LIF and IL6, and that the rhVTN data are not an artefact of or an immune response to human protein.

VTN induces LIF and IL-6 expression through integrins and uPAR

To test whether VTN acts through integrins, C6 cells were co-incubated with a broad-spectrum inhibitor (RGDS) of RGD-dependent integrin ligands and a more potent integrin (P11) non-RGD-dependent blocking peptide (HSDVHK), thought to be αvβ3 specific (Choi et al., 2010, but see Fig. 6B,C). RGDS attenuated VTN-induced LIF and IL-6 mRNA expression at 4 h relative to control RAD peptide (Arg-Ala-Asp-D-Phe-Val) peptide (Fig. 3A,B), and to the same extent as P11. No cell detachment was observed after 4 h of treatment with P11 or RGDS. Expression of LIF and IL-6 was still high relative to that seen without VTN, suggesting that non-integrin mechanisms contributed to the VTN-mediated effects. VTN is known to bind to uPAR as well as affecting uPA binding to trigger ligand-independent integrin signaling via FAK (Madsen et al., 2007). The uPAR inhibitor BC-11, which functions through blocking the uPA N-terminal binding to uPAR (Longo et al., 2015; Magnussen et al., 2014) attenuated VTN-induced LIF and IL-6 induction in C6 cells, but had no effect by itself (Fig. 3C,D). Co-incubation of both P11 and BC-11 did not further decrease the VTN-mediated LIF and IL-6 induction (Fig. 3C,D), suggesting that both inhibitors function by inhibiting a common downstream pathway. Knockdown of uPAR in C6 cells significantly attenuated the VTN-mediated expression of LIF and IL-6 (Fig. 3E,F), while uPAR knockdown was confirmed by reverse transcription real-time quantitative PCR (RT-qPCR) (Fig. 3G).

VTN- or injury-mediated LIF and IL-6 expression is blocked by FAK inhibition *in vitro*

FAK is a major transducer of integrin signaling (Mitra et al., 2005). C6 cells were seeded onto plates pre-coated with VTN or plastic only (controls). VTN activated FAK (as judged by measuring Y397 phosphorylation, denoted pFAK-Y397) but not the closely related PYK2 (also known as PTK2B) at Y402, in C6 cells 4 h after seeding (Fig. 4A). The FAK inhibitor PF573228 added to the culture medium immediately after seeding completely blocked VTN-induced FAK phosphorylation (Fig. 4B), and also completely abolished the induction of LIF and IL-6 (Fig. 4C,D). Plating C6 cells onto culture plates pre-coated with rhVTN led to a similar induction of LIF and IL-6 to that seen when proteins were added directly to medium (Figs 1D,E and 4C,D). In separate experiments, other FAK inhibitors PF562271 and PND-1186, but surprisingly not Y11, also decreased pFAK-Y397 (Fig. S1A) and dose-dependently reduced baseline (without VTN) LIF and IL-6 expression after 4 h (Fig. S1B,C). We also found that FAK inhibition suppresses VTN-induced LIF and IL-6 expression when VTN was added directly to medium (Fig. 4E,F). Together, this shows that FAK signaling is a major regulator of VTN-mediated LIF and IL6 expression. Integrin blockade by P11, β3- or β5-blocking antibodies did not attenuate this induction (data not shown), suggesting that other mechanisms play a role.

Journal of Cell Science (2018) 131, jcs202580. doi:10.1242/jcs.202580

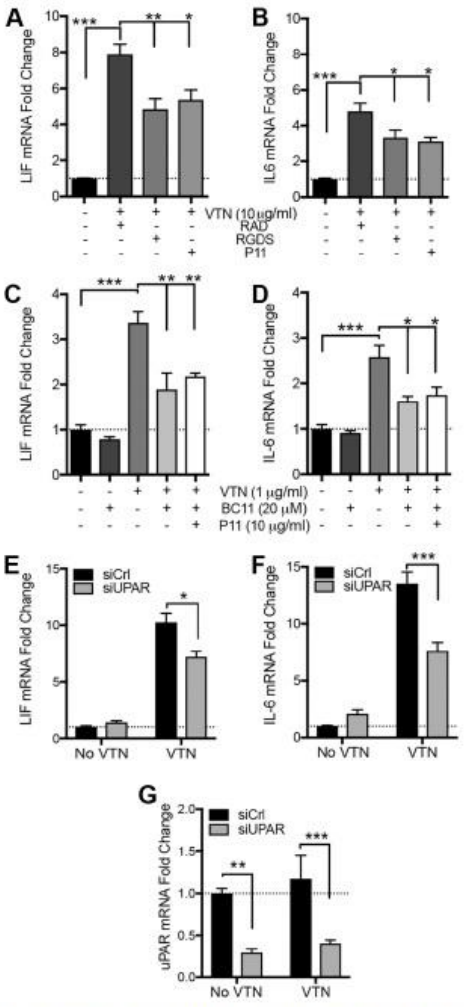

Fig. 3. Integrins mediate VTN-induced LIF and IL-6 in C6 cells. C6 cells were seeded onto plastic for 24 h in serum-containing medium, then serum starved for 24 h before addition of VTN to the medium for 4 h. Co-treatment with RGD or αvβ3 (P11) integrin-blocking peptides reduced the effects of VTN on LIF (A) and IL-6 (B) mRNA expression. RAD is a non-RGD control peptide. LIF and IL-6 expression were not completely abolished in these experiments, suggesting that there is an additional VTN-activated mechanism. Indeed, BC-11, a uPA–uPAR inhibitor, decreased VTN-induced LIF (C) and IL-6 (D) mRNA expression, but did not have any effect alone, after 4 h. Data are means±s.e.m. of four independent experiments. Since 1 µg/ml VTN was effective in inducing LIF and IL-6, we only chose this dosage for these experiments. Co-incubation of both P11 and BC-11 could not further decrease the VTN-mediated LIF and IL-6 induction. Finally, knockdown of uPAR by means of siRNA (siUPAR) reduced by LIF (E) and IL-6 (F) induction by VTN (10 µg/ml). uPAR knockdown was confirmed by RT-qPCR (G, n=3). *P<0.05, **P<0.01, ***P<0.001.

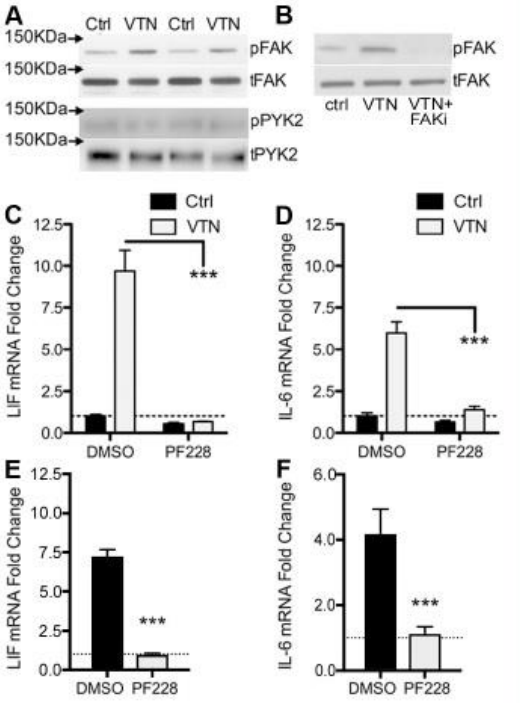

Fig. 4. FAK inhibition abolishes VTN mediated LIF and Il-6 induction. C6 cells were seeded onto VTN-coated tissue culture plates (50 µg/ml) or non-treated control (Ctrl) plates and maintained for 4 h. (A) In these conditions, VTN stimulates phosphorylation of Y397-FAK (pFAK) but not of PYK2 at the corresponding Y402 residue (pPYK2), as shown in western blots. Loading controls are total FAK (tFAK) and PYK2 (tPYK2). Two representative lanes per group from three independent experiments are shown (n=3). (B) FAK antagonist PF573228 (10 µM, FAKi) completely blocked the VTN-stimulated pY397-FAK formation when added immediately after cells were seeded (n=3). In addition, the FAK inhibitor PF573228 (PF228) completely abolished VTN-induced LIF (C) and IL-6 (D) gene expression as measured by RT-qPCR. Control (Ctrl) vehicle is 0.1% DMSO (mean±s.e.m.; n=4 independent experiments). In further experiments, C6 cells were cultured in serum-free medium for 24 h before VTN was added directly to medium with or without FAK inhibition (PF228), (E) LIF and IL-6 (F) induction by VTN was also completely abolished by FAK inhibition in these conditions (mean±s.e.m.; n=3).

Both LIF and IL-6 are activated after injury to the brain (Banner et al., 1997; Lau and Yu, 2001), and we therefore sought to define the role of FAK in their injury-induced upregulation *in vitro*. C6 cells were seeded onto tissue culture plates (no coating) and maintained for 48 h before monolayers were removed and mechanically dissociated (swipe injury). Cells were allowed to re-adhere for 4 h in 10% (v/v) serum-containing medium, before RNA isolation. The injury caused ∼50% cell loss by 2 and 6 h as measured by MTT and Trypan Blue counts (Fig. S2A,B). LIF and IL-6 mRNA expression were increased ∼4- and 8-fold, respectively, in surviving cells relative to uninjured controls (Fig. 5A,B). Incubation of the validated FAK inhibitors PF573228, PND-1186 or PF562271 (Fig. S1) during the 4 h recovery abolished the injury-induced upregulation of LIF and IL-6 mRNA expression (Fig. 5A, B). The FAK inhibitor Y11, which had no effect on pY397-FAK (Fig. S1A) or LIF and IL-6 mRNA expression (Fig. S1B,C) in uninjured C6 cells, did not alter injury-induced LIF expression (Fig. 5A). Surprisingly, Y11 increased IL-6 expression above that caused by injury, suggesting that it was biologically active but had

Journal of Cell Science (2018) 131, jcs202580. doi:10.1242/jcs.202580

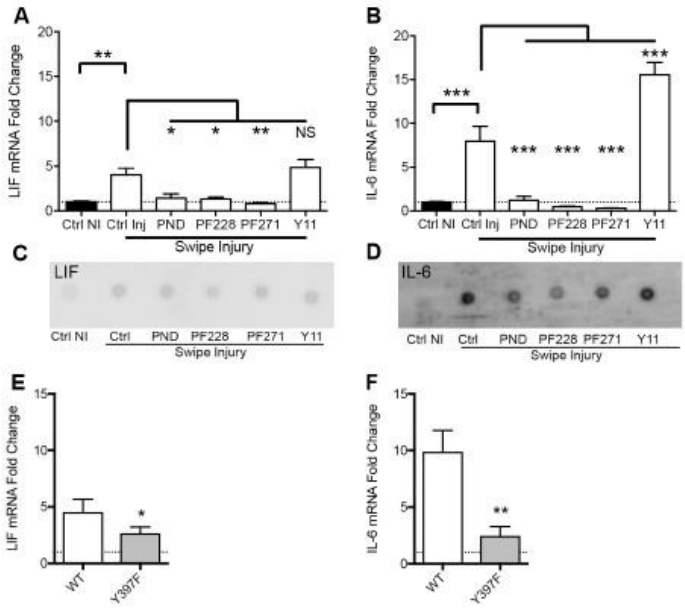

Fig. 5. FAK mediates injury-induced LIF and IL-6 induction in C6 cells. C6 cells were seeded and maintained for 48 h in serum-containing medium without added VTN. Cells were then injured in an *in vitro* trauma model (swipe injury) with or without FAK inhibitors added at the time of injury. LIF (A) and IL-6 (B) mRNA expression were strongly induced (Ctrl Inj) at 4 h after injury compared to no injury controls (Ctrl NI), but were abolished by treatment with FAK antagonists, PND-1186 (PND), PF573228 (PF228), PF562271 (PF271), but not Y11. Surprisingly, Y11 further increased IL-6 expression after injury. Data are means ±s.e.m. of three independent experiments and expressed as a fold change relative to uninjured controls, first normalized to GAPDH to account for differences in cell numbers. *P<0.05; **P<0.01; ***P<0.001; NS, not significant. In the same conditions as described for A and B, LIF (C) and IL-6 (D) protein expression and release was increased after injury, and attenuated by all inhibitors, except Y11, as shown by dot blots of conditioned medium (representative of three independent experiments). In addition, we found that C6 cells overexpressing wild-type (WT) FAK expressed significantly more LIF (E) and IL-6 (F) than cells overexpressing dominant negative Y397F mutant FAK following injury (mean±s.e.m.; n=3).

off-target effects (Fig. 5B). LIF and IL-6 proteins released into culture medium were induced by injury and were suppressed by FAK inhibition, as shown by dot blot assays (Fig. 5C,D). The larger increases seen in dot blots relative to mRNA induction could be explained by an accumulative effect of stable protein in the medium, while LIF and IL-6 mRNA are being actively turned over. LIF and IL-6 mRNA half-life is typically 30–45 min (Derigs and Boswell, 1993; Iwasaki et al., 2011). Also, it is possible that the uninjured controls retain much more of the IL-6 within the cytoplasm. The effects of the FAK inhibitors was not due to cell loss as they did not appear to affect cell viability after injury (data not shown). We also confirmed the importance of FAK Y397 phosphorylation, which is key to FAK activation (Sieg et al., 2000), as transfection of mutated functionally dead FAK Y397F plasmids into C6 cells significantly reduced LIF (Fig. 5E) and IL-6 (Fig. 5F) mRNA levels at 4 h following cell injury.

FAK also regulates LIF and IL-6 expression in endothelial cells

To test whether FAK had a similar role in other cell types, we chose human (hCMEC) and mouse (bEnd5) brain endothelial cell lines. They were chosen due to their importance, together with microglia and astrocytes, in the acute response of the neurovascular unit to insults (Hawkins, 2005). Furthermore, IL-6 is highly expressed by endothelial cells (Gertz et al., 2012) as well as in our cultures, making it easier to test reductions in baseline expression levels after FAK inhibition than in C6 cells. We first tested endothelial cell responsiveness to ECM proteins. After passaging, cells were re-suspended in serum-free medium and maintained in suspension for 1 h, before being seeded onto culture plates coated with vehicle (PBS), VTN, laminin-111 or fibronectin. Western blot analysis showed that there was a marked increase in pFAK-Y397 in cells maintained on VTN over control (vehicle), laminin-111 or fibronectin (Fig. 6A, n=3). Intriguingly, phosphorylation of STAT3 Y705, which positively regulates IL-6 production (Peruzzi et al., 2012), was also increased (Fig. 6A) in VTN-treated cells. To confirm the role of integrins in VTN-induced LIF and IL-6, we used function-blocking integrin antibodies on CMEC cells plated onto VTN. P11 peptide and anti-β5 antibody reduced the effects of VTN on LIF expression (P<0.05, n=4–6) with the anti-β3 antibody block not being significant (P=0.08, Fig. 6B). VTN-induced IL-6 expression was blocked by P11, and antibodies against β3 and β5 (P<0.05, n=4–6, Fig. 6C). In addition, we tested the specificity of P11 by co-incubation with the β3- and β5-blocking antibodies. No further effect was found on LIF and IL-6, suggesting that P11 acts through β3 and β5 integrins.

Some FAK antagonists reportedly also inhibit PYK2 (Slack-Davis et al., 2007). Therefore, we performed siRNA knockdown of FAK and PYK2 in CMEC cells over 6 days, with specificity confirmed by qPCR (Fig. S3A,B) and western blotting (Fig. S3C). ILK, another integrin signaling mediator, was not altered (Fig. S3C). Baseline LIF and IL-6 expression were decreased to ∼70% in FAK-knockdown CMECs relative to non-targeting siRNA controls (Fig. 6D,E). Cells were maintained in 5% serum as it can induce these cytokines (Fig. 1A,B). Knockdown of PYK2 had no effect (Fig. 6D,E), revealing the specificity of FAK signaling in LIF and IL-6 regulation. CNTF mRNA expression was increased upon treatment with siRNA against FAK (siFAK) but not against PYK2 (siPYK2) (Fig. 6F), consistent with our previous findings that FAK inhibition induces CNTF (Keasey et al., 2013).

We also tested for FAK specificity in the bEnd5 mouse endothelial cells. Targeted knockdown of FAK with siRNA was confirmed by decreased total FAK protein (Fig. S3D), with no effect on ILK expression (Fig. S3E). siFAK reduced LIF and IL-6 mRNA expression to ∼60% of controls (Fig. 6G,H) but increased CNTF by ∼30% (Fig. 6I). Pharmacological FAK inhibition in bEnd5 cells cultured in 10% serum with PF573228 for 4 h suppressed LIF and IL-6 expression to ∼25% and ∼50% that of controls, respectively

Journal of Cell Science (2018) 131, jcs202580. doi:10.1242/jcs.202580

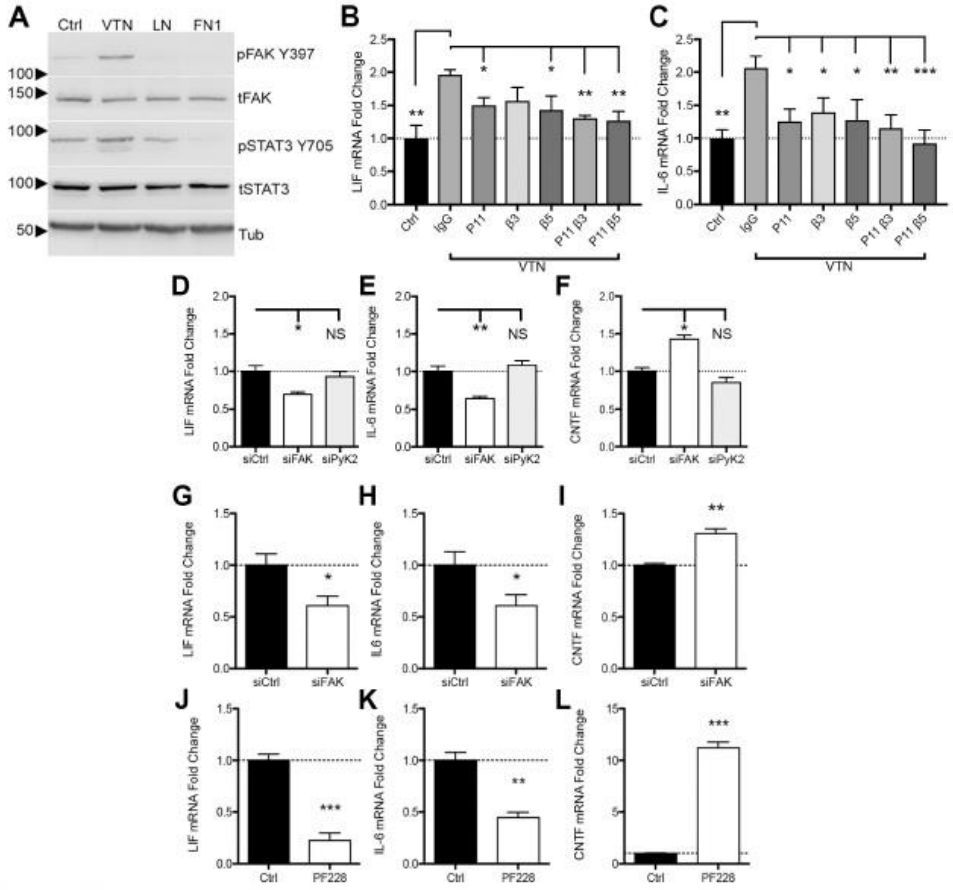

Fig. 6. FAK, but not PYK2, regulates LIF and IL-6 expression in human and mouse brain endothelial cells. Human CMEC cells were passaged and resuspended in serum-free medium and maintained in suspension for 1 h. Cells were then plated onto plastic (PBS; Ctrl), or VTN-, laminin- (LN) or fibronectin (FN1)-treated plates for 1 h. (A) VTN caused a much greater increase in pFAK Y397 and STAT3 Y705 over laminin and fibronectin. CMEC cells were pre-incubated with integrin β3- or β5-blocking antibodies before plating onto VTN. At 4 h after plating, induction of LIF (B) and IL-6 (C) by VTN were reduced when CMEC cells were pre-incubated with P11, β3- or β5-blocking antibodies (mean±s.e.m.; n=4–6, ANOVA with Fisher LSD test). To determine the role and specifity of FAK in regulating baseline LIF and IL-6 mRNA expression, we performed knockdown of FAK (siFAK) or PYK2 (siPYK2) using siRNAs in human CMEC cells over 6 days. siFAK reduced LIF (A) and IL-6 (B), while increasing CNTF (C) gene expression relative to non-targeting control siRNA. siPYK2 had no effect. In bEnd5 cells, siFAK also diminished both LIF (D) and IL-6 (E) expression while increasing CNTF (F) (mean±s.e.m.; n=3). Pharmacological FAK inhibition for 4 h with PF573228 (PF228) also suppressed LIF (G) and IL-6 (H) while upregulating CNTF (I) mRNA expression relative to vehicle-treated controls (Ctrl), as measured by RT-qPCR (n=4). Data are means±s.e.m. from n=4 independent experiments each. *P<0.05, **P<0.01, ***P<0.001; NS, not significant.

(Fig. 6J,K). CNTF mRNA was dramatically induced by PF573228 in the same cells (Fig. 6L). The changes in LIF and IL-6 after the 6-day siRNA treatment were smaller than that seen with the 4 h treatment with the pharmacological inhibitor, perhaps due to adaptive responses independent of FAK signaling.

FAK antagonists suppress LIF and IL-6 specifically through inhibition of FAK

To further confirm the specificity of the FAK antagonists, siFAK pre-treated CMEC cells were incubated with PF573228 or PND-1186. PF573228 has been used successfully *in vitro* and *in vivo* (Keasey et al., 2013) PND-1186 suppressed LIF expression at lower concentrations (Fig. S1B) and were selected for these experiments. Quantitative capillary western blots confirmed that total FAK protein (Fig. 7A–C) and pFAK-Y397 (Fig. 7D–F) were reduced by siFAK (DMSO vehicle) but, as expected, were not further reduced by PF573228 or PND-1186. The reduction in LIF and IL-6 mRNA expression caused by PF573228 and PND-1186 was not significantly different when inhibitors are combined with a non-targeting siRNA control or siFAK, (Fig. 7G,H), suggesting that these inhibitors acted specifically through FAK and did not have off-target effects.

DISCUSSION

Our data has identified a VTN–integrin–FAK signaling pathway that rapidly and robustly induces expression of LIF and IL-6 *in vitro* and in adult mice after a cerebrovascular injury (Fig. 8A,B). This is

Journal of Cell Science (2018) 131, jcs202580. doi:10.1242/jcs.202580

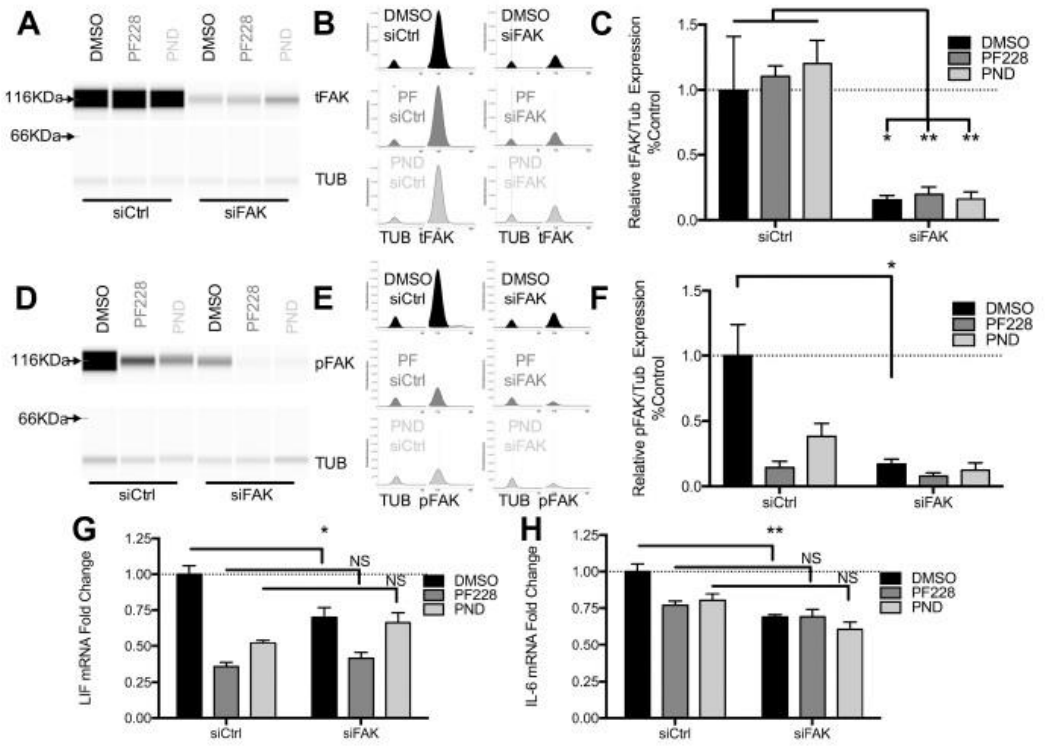

Fig. 7. Pharmacological FAK inhibitors are specific in suppressing LIF and IL-6 in CMEC cells. To confirm the specificity of PF573228 (PF228) and PND-1186 (PND), FAK was first knocked down in CMECs with siRNA for 5 days followed by 4 h inhibitor treatments. Total FAK (tFAK) and pFAK protein knockdown was quantified by capillary western blots (A). For illustration purposes, synthetic bands were produced from chemiluminescence spectrograms (B). TUB, α-tubulin. (C) Quantification showing that siFAK decreases total FAK normalized to α-tubulin, which is not affected by the inhibitors PF228 or PND. (D–F) Similarly, siFAK decreased pY397-FAK levels, with the PF228 and PND decreasing pFAK only under control siRNA conditions (siCtrl). Critically, LIF (G) and IL-6 (H) gene expression (RT-qPCR) were not significantly different when the inhibitors were incubated with siCtrl or siFAK, and provided no additive suppression in the presence of siFAK, showing that their effects were entirely mediated through FAK. Data are means±s.e.m. of four independent experiments and presented relative to DMSO- and control (siCtrl)-treated cells. *P<0.05; **P<0.01; NS, not significant.

consistent with the finding that FAK can mediate TNFα-induced IL-6 expression in cancer cells and myoblasts (Schlaepfer et al., 2007). Prior to this study, gp130–JAK–STAT3, p38 MAPK and nuclear factor (NF)-κB signaling was well known to regulate IL-6, which can also regulate its own expression (Kang et al., 2013). The finding that ligand–integrin binding induces LIF and IL-6 expression in concert with suppression of CNTF is novel. Others have reported that α2 laminins induce IL-6 (Delimont et al., 2014) but did not study involvement of integrins. Regulation of LIF through integrins or FAK was previously unknown. In the absence of LIF, laminin-111 and -511 (laminin-511 is composed of α5, β1 and γ1 chains) promote stem cell renewal *in vitro* through α6β1 integrin (Cattavarayane et al., 2015). This might involve induction of LIF, since it is widely used to maintain self-renewal. However, here, LIF was not affected by laminin-111.

Our results suggest that FAK is unique in regulating LIF and IL-6 compared to other ECM–integrin signaling transducers such as the highly related PYK2 (Mitra et al., 2005), which can also be activated by αvβ3 integrin (Butler and Blystone, 2005). The potential specificity of FAK would make it a good therapeutic target, for example, to downregulate LIF and/or IL-6. In fact, we have previously shown that systemic FAK inhibitor treatment promotes adult neurogenesis in mice (Keasey et al., 2013). Here, FAK inhibitors could completely attenuate injury-induced LIF and IL-6 in C6 glioma cells. FAK inhibitors also reduced baseline LIF and IL-6 in endothelial cells, suggesting that FAK is a major signal transducer for LIF and IL-6 signaling. Integrin blockade did not reduce cytokine induction, possibly due to the mechanical trauma and stretching of cells, which is known to activate pFAK Y397 (Delimont et al., 2014; Tornatore et al., 2011). Together, our data suggest that FAK inhibition would be beneficial in inflammatory diseases where IL-6 plays a major role, such as rheumatoid arthritis, diabetes, cancer and neurodegenerative diseases (Mauer et al., 2015; Rothaug et al., 2016). FAK inhibitors have been and are in clinical Phase I and II trials for solid tumors (www.clinicaltrials.gov) and seem to be well tolerated after systemic administration.

The rapid and potent effects of VTN in cultured C6 cells were mediated by αvβ3 and/or αvβ5 integrins, and by downstream FAK, as shown by pharmacological inhibitors and siRNA knockdown. Integrin αvβ3 is expressed by aorta endothelial cells where it mediates increased FAK phosphorylation and downstream ERK and JNK activation upon shear stress (Li et al., 1997). This is

Journal of Cell Science (2018) 131, jcs202580. doi:10.1242/jcs.202580

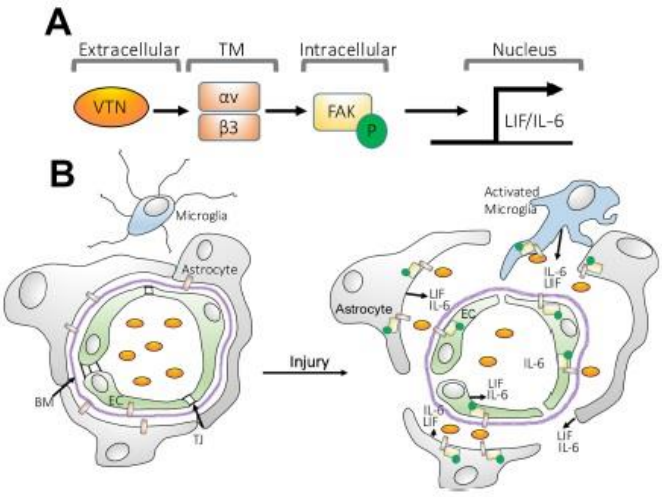

Fig. 8. Blood VTN leaks into the brain after stroke. (A) Schematic showing an overview of the signaling pathway by which VTN induces LIF and IL-6 gene expression, by binding to αvβ3 integrin and specifically activating downstream FAK. (B) Proposed model of VTN leakage after blood–brain barrier (BBB) breakdown. Under normal conditions, the intact BBB, characterized by tight junctions (TJ) between endothelial cells (EC), keeps VTN in blood from entering the central nervous system (CNS) tissue. BM, basement membrane. Under pathological conditions that cause BBB breakdown, such as stroke and hemorrhage, leakage of VTN in the brain parenchyma induces LIF and IL-6 expression by astrocytes (gray cells), microglia (blue cells) and endothelial cells (green cells).

consistent with our findings showing that FAK signaling induces LIF and IL-6 in two types of brain endothelial cells. Others have shown that treatment with another αvβ3-blocking peptide reduces FAK phosphorylation and infarct volume after ischemic cerebral stroke in rats (Shimamura et al., 2006). It is possible that this was in part due to a reduction in LIF and IL-6, as suggested by our findings that P11 peptide, a reported antagonist of αvβ3 (Bang et al., 2011), and antibodies against β3 suppress LIF and IL-6 expression. Our data suggest that P11 acts both on β3 or β5 integrins because no additive effect of the antibodies was seen in reducing LIF or IL-6. The αvβ5 integrin likely also plays a role, as antibodies to the β5 subunit, which exists only in αvβ5 integrin, were similarly effective to β3 inhibition in blocking VTN-induced LIF and IL-6 expression. IL-6 is well known to promote inflammation after spinal cord injury (Lacroix et al., 2002). LIF mediates neutrophil activation and macrophage recruitment in culture (Borish et al., 1986; Tofaris et al., 2002), and microglia and macrophage activation in the injured spinal cord (Kerr and Patterson, 2004). If substantiated in animal models, such specificity may provide opportunities for more selective therapies in regulating detrimental inflammation.

In vitro, VTN was unique among the other ECM molecules, fibronectin, fibrinogen, laminin and collagen, in its ability to activate LIF and IL-6. This is consistent with VTN, but not fibronectin or laminin, promoting the formation of pFAK-Y397 in CMEC cells. This was surprising because fibrinogen and fibronectin also bind to αvβ3 integrin via RGD domains (Charo et al., 1990). Also, both VTN and fibronectin activate microglia (Milner et al., 2007) and support endothelial cell survival via α5β1 and αvβ3 integrins (Wang and Milner, 2006). Fibronectin enhances IL-1-mediated induction of IL-6 *in vitro* (Ostberg et al., 1995), but its effect on IL-6 alone has not been tested. Differential activation through the same integrins has been found, for example, fibronectin or osteopontin, but not VTN, activate FAK in osteoblast cells (Liu et al., 1997). Also, chronic exposure to VTN leads to greater upregulation of pro-MMP9 than fibronectin (Milner et al., 2007). Our integrin-blocking experiments suggested that there is an additional non-integrin mechanism mediating the effects of VTN, perhaps not shared by fibronectin or fibrinogen. VTN can be cleaved to produce a peptide that binds to the uPAR (Wei et al., 1994), which can boost VTN-mediated cell motility via interaction with αvβ3 (Degryse et al., 2005). In addition, uPAR has been implicated in FAK activation together with α5β1 integrin (Aguirre Ghiso, 2002). Indeed, here we found that pharmacological and siRNA uPAR inhibition reduced VTN-mediated LIF and IL-6 expression *in vitro*. However, it remains to be determined whether the unique effects of VTN compared to the other ECM molecules is due to its ability to bind uPAR. Inhibition of both αvβ3 integrin and uPAR did not attenuate VTN-induced LIF and IL-6 more than either alone, suggesting a common mechanism may exist in their signaling pathways. FAK inhibition alone completely blocked VTN-mediated LIF and IL-6 induction, suggesting that both mechanisms are dependent on FAK signaling. Others have shown that uPAR leads to integrin and FAK activation (Aguirre Ghiso, 2002). The possibility of uPAR mediating LIF and IL-6 expression through FAK is a new idea. The mechanism that uPAR uses to achieve this is likely associated with integrins, given that P11 did not further suppress VTN-mediated LIF and IL-6 induction in the presence of BC-11. The interaction between uPAR and integrins would be an intriguing area for further study. It remains to be determined how unique VTN is compared to other ECM molecules in its potential to regulate inflammatory signalling through integrin receptors *in vivo*. There probably are additional ECM proteins that regulate cytokine expression, including α2 laminin, which induces IL-6 in kidney cells (Delimont et al., 2014), while α1 laminin does not, consistent with our finding that laminin-111 was without effects. It also remains to be determined how VTN, fibronectin and laminin-111 can downregulate CNTF in C6 astroglioma cells (Keasey et al., 2013), while only VTN induces LIF and IL-6, possibly providing opportunities to develop pharmacological approaches for differential cytokine regulation.

Collectively, our data suggest that VTN leaks into the brain after trauma and induces LIF and IL-6 expression. It is perhaps not surprising that major blood proteins should trigger inflammation and possibly also subsequent repair. Consistent with our results is the finding that lipopolysaccharide (LPS) injections into lungs of mice lead to upregulation of VTN, which induces IL-1β, MIP-2 (also known as CXCL2) and IL-6 expression, as shown in VTN$^{-/-}$ mice (Tsuruta et al., 2007). Our data suggest that other leaked blood proteins could also play a pro-inflammatory role because

Journal of Cell Science (2018) 131, jcs202580. doi:10.1242/jcs.202580

hemorrhage in VTN$^{-/-}$ mice and plasma from VTN$^{-/-}$ mice *in vitro* induces about half as much LIF and IL-6 as was the case for the wild-type mice or plasma, respectively. This suggests that VTN is important but not the exclusive molecule that regulates LIF and IL-6 cytokine expression, and that other blood-derived molecules involved in this process remain to be identified. VTN and fibronectin leak into the brain after stroke (del Zoppo et al., 2012) or demyelinating injuries (Milner et al., 2007), where they have detrimental effects, and can activate microglia (Milner and Campbell, 2003). Here, fibronectin did not induce LIF or IL-6 *in vitro*, raising the possibility that leaked blood fibronectin regulates inflammation through different signaling mechanisms from VTN. VTN probably also contributes to induction of repair processes because VTN$^{-/-}$ mice have delayed and poor wound healing and angiogenesis (Jang et al., 2000), as well as persistent blood leakiness after injury (Li et al., 2012). Such defects are also seen in IL-6$^{-/-}$ mice (Gertz et al., 2012; Lin, 2003), probably because IL-6 is important for angiogenesis (Gertz et al., 2012).

Astrocytes, microglia, infiltrating macrophages and endothelial cells probably respond directly to VTN leakage to produce LIF and IL-6. All of these cells express αvβ3 integrin (Herrera-Molina et al., 2012; Milner, 2009; Wang and Milner, 2006), and can produce LIF and IL-6 after injury (Ishibashi et al., 2006; Van Wagoner and Benveniste, 1999). The astrocytes and microglia are in a prime location around microvessels to act as first-responders upon blood–brain barrier disruption (Fig. 8B). The luminal side of endothelial cells is always exposed to VTN but αvβ3 integrin–FAK clusters may be predominantly in an abluminal localization in endothelial cells (Li et al., 1997). LIF is a chemoattractant to macrophages (Tofaris et al., 2002) and their recruitment to ischemic injuries is reduced in VTN$^{-/-}$ mice (Li et al., 2012). This suggests that VTN-induced LIF attracts macrophages into injured tissue where they can respond to VTN to produce IL-6 (Antonov et al., 2011).

Compared to IL-6, much less is known about LIF gene regulation. LIF mRNA is increased by cAMP and MEK signaling in Schwann cells, astrocytes and non-neuronal lineages (Banner and Patterson, 1994; Nagamoto-Combs et al., 1999), as well as by TGFβ1 through PKCβ (Matsuoka et al., 1997). MEK signaling appears to be downstream of FAK in astrocytes (Schlaepfer et al., 2007), while PKCβ plays a role in regulating focal adhesion turnover in keratinocytes (Vandenberghe et al., 2013). Fibronectin promotes stem cell differentiation through increased FAK activation and focal adhesion formation (Hayashi et al., 2007). However, the role of FAK in regulating LIF expression had not been previously reported. This new insight may provide additional tools to influence biological processes where LIF plays an important role, including stem cell behavior (Bauer and Patterson, 2006), inflammatory processes (Kerr and Patterson, 2004; Sugiura et al., 2000) or trophoblast implantation (Vogiagis and Salamonsen, 1999).

FAK inhibition induced CNTF *in vitro*, as we reported previously (Keasey et al., 2013), while reducing LIF and IL-6 expression. This opposing effect seems consistent with the findings that endogenous CNTF is anti-inflammatory (Linker et al., 2002), and that LIF and CNTF have opposite effects on neural stem cell self-renewal and neurogenesis (Bauer and Patterson, 2006; Yang et al., 2008). It is conceivable that FAK signaling differentially regulates these cytokines to avoid contrasting gp130 signaling and biological outcomes. The involvement of cAMP in LIF expression in cultured astrocytes (Murphy et al., 1995) may explain why LIF and CNTF are differentially regulated, where cAMP downregulates CNTF (Yang et al., 2008), and may be downstream of integrin–FAK signaling.

In conclusion, we propose that leaked VTN plays a major and specific role in acutely and robustly activating cerebral and, possibly, other inflammatory processes. This provides new insight into potential pathophysiological mechanisms caused by the loss of vascular integrity that occurs in a variety of disorders. Furthermore, integrin–FAK signaling is a novel therapeutic target for regulating the inflammatory response following injury or disease, with pharmacological FAK inhibition representing a potent tool for attenuating inflammatory cytokine induction. We suggest that plasma VTN might act as a flagging molecule, directly triggering cytokine expression in injured tissues to recruit inflammatory cells (Fig. 8).

MATERIALS AND METHODS

Cell culture

We used rat astroglioma C6 cells (Cat #CCL-107, ATCC), mouse bEnd5 endothelial cells (a gift from Dr Engelhardt, University of Bern, Switzerland) and human CMEC/D3 endothelial cells (Cat# CLU512, Cellutions Biosystems). Cells were tested for contamination by fluorescent staining with DAPI. C6 cells were maintained in high serum (HS) medium [Dulbecco's modified Eagle's medium (DMEM) supplemented with 10% fetal bovine serum, 2 mM L-glutamine and 1% penicillin-streptomycin] or low serum (LS) medium (advanced DMEM supplemented with 1% fetal bovine serum, 2 mM L-glutamine and 1% penicillin-streptomycin) where noted. BEnd5 cells were maintained in DMEM supplemented with 10% fetal bovine serum (FBS), 4 mM L-glutamine, 1% penicillin-streptomycin, 1 mM sodium pyruvate and 1× non-essential amino acids. CMEC cells were grown in fetal bovine serum (5%), penicillin-streptomycin (5%), hydrocortisone (1.4 µM, Sigma, Cat# H0135), ascorbic acid (5 µg/ml), chemically defined lipid concentrate (1%, Invitrogen Cat# 11905031), HEPES (10 mM), basic fibroblast growth factor (1 ng/ml, Sigma, Cat# F0291) in endothelial basal media-2 (Lonza, Cat# 00190860). Cells were maintained in a humidified CO_2 (5%) incubator at 37°C. C6 cells were plated at 160,000 per ml, and bEnd5 and CMEC cells at 100,000 per ml. All cells were maintained for 24 h after plating before commencing experiments.

Cell cultures with ECM proteins and integrin blockade

C6 cells were serum-deprived for 24 h. Recombinant human VTN (1 or 10 µg/ml, Cat# SRP3186), fibronectin (10 µg/ml, Cat# F3667), fibrinogen (50 µg/ml, #F3879), collagen-I (10 µg/ml, Cat# C5533), or laminin-111 (EHS murine sarcoma basement membrane, 10 µg/ml, Cat# L2020), all from Sigma, were re-suspended in sterile water and added directly to the medium. Alternatively, cells treated with VTN (10 µg/ml) were co-incubated with RGDS (10 µg/ml, Cat# 3498, Tocris), αvβ3 peptide antagonist (P11, HSDVHK, 10 µg/ml, Cat# 4744, Tocris; Choi et al., 2010) or control RAD peptides (Arg-Ala-Asp-D-Phe-Val, 10 µg/ml, Cat# BML-AM1010-0001, ENZO). P11 has been reported to function through binding to the metal ion-dependent adhesion site (MIDAS) and adjacent to MIDAS (ADMIDAS) (Bang et al., 2011; Choi et al., 2010), reducing ligand binding and αv and β3 subunit interaction (Xiong, 2002). P11 has been demonstrated to act with high potency on the αvβ3 integrin receptor with an IC_{50} of 1.74 pg/ml (Lee et al., 2004). Its specificity for αvβ3 has been demonstrated over α5β1 and α3β1 (Choi et al., 2010). After 4 h, total RNA or protein was isolated for RT-qPCR or western blotting, respectively. CMEC cells were passaged and resuspended in regular culture medium without serum (0% FBS) and maintained for 1 h in suspension (at 500,000/ml) using non-tissue culture-treated plates. Cells were then transferred to tissue culture plates pre-coated with vehicle (PBS), VTN, laminin or fibronectin (50 µg/ml, Keasey et al., 2013). Cells were lysed after 1 h and protein collected for analyses. Integrin-blocking antibodies used were against β3 (Biolegend, Cat# 304414, 10 µg/ml) and β5 (Ebioscience, Cat# 14-0497-82, 10 µg/ml) and added to the suspended CMEC cells. The cell suspension was then transferred to VTN-coated plates for 4 h before RNA isolation. C6 cells were seeded directly onto precoated plates without the 1 h suspension used for the CMEC cells and maintained with or without PF573228 (FAKi) added at the same time as seeding for 4 h.

Journal of Cell Science (2018) 131, jcs202580. doi:10.1242/jcs.202580

In vitro drug treatments

Cells were incubated with pharmacological antagonists of FAK for 4 h before RNA or protein isolation. FAK antagonists were PF573228 (Cat# 3239, Tocris), PF562271 (Cat# S2890, Selleck), PND-1186 (Cat# S7653, Selleck) and Y11 (Cat# 4498, Tocris), used at concentrations between 0.1 µM to 10 µM as noted. BC-11 was used at 20 µM (Cat# 4372, Tocris). It has been shown that the N-terminal fragments of uPA preadsorbed with BC-11 limit the growth-suppressing activity of BC-11 (Longo et al., 2015). In addition, incubating high molecular mass uPA with plasminogen reduces plasmin formation, as determined by plasminogen zymography (Magnussen et al., 2014). This suggests that BC-11 functions through blockade of the enzymatic activity of uPA which may occur in addition to blockade of the binding uPA N-terminal fragments to uPAR. More recently, BC-11 was shown to reduce uPAR cleavage by uPA in a similar fashion to that seen for the serine protease inhibitor aprotinin (Magnussen et al., 2017). Drugs were dissolved in up to 0.1% DMSO of final volume in culture medium (vehicle).

Transfections

siRNAs against human FAK (PTK2, Cat# L-003164) or PYK2 (PTK2B, Cat# L-003165) or a non-targeting negative control (Cat# D-001810-10), all from Dharmacon, were transfected into CMEC cells 24 h after plating (200,000 cells/well) on six-well plates at 50 nM siRNA and 0.5% Lipofectamine-2000 (Cat#11668-019, Invitrogen). A second transfection was performed at 48 h due to FAK's long protein half-life (Ochel et al., 1999). Cells were maintained for a further 5 days before analysis or treatment with FAK antagonists. Transfection efficiency was ∼60–80% as visualized by performing fluorescent microscopy after co-transfection with siGLO RNA (Cat# D-001630-02, Dharmacon). Knockdown of uPAR in rat C6 glioma cells was performed with siRNA (Cat# L-1000500, Dharmacon, 50 nM). Transfection was performed with Lipofectamine-3000 [(0.25%) Cat# L3000015, Invitrogen] according to the manufacturer's instructions. Experiments were performed at ∼36 h post transfection.

FAK-Y397F mutant transfections

Wild-type pGFP-FAK (Addgene plasmid #50515) and pGFP-FAK Y397F (Addgene plasmid #50516) were obtained from Addgene and were both deposited by Kenneth Yamada (Gu et al., 1999). Transfections using Lipofectamine 3000 were performed according to the manufacturer's protocol, at a final concentration of 0.25% with 1 µg of plasmid DNA in a single well of a six-well plate. Western blotting with anti-phospho-Y397 antibody was used to confirm plasmids were expressed the wild-type and Y397F protein.

In vitro swipe injury model

C6 cells were plated at 320,000 cells/ml in 6-well plates with 10% fetal bovine serum medium, and grown to confluency for 48 h. No exogenous ECM protein was used in this assay. In the same growth medium, cells were removed by scraping the bottom of the well with an inverted sterile p1000 pipette tip and then triturated 10× with a p1000 pipette to mechanically dissociate them. Afterward, the cells were allowed to re-adhere in the same wells, and maintained for 2–6 h to assess cell viability or 4 h for RNA isolation. Cell survival was assessed by use of MTT (50 µg/ml, Cat# M6494, Invitrogen) added to culture medium for 2 h, before cells were washed with ice-cold PBS. Resulting formazan was dissolved with 500 µl acidified isopropanol, which was transferred to 96-well plates for spectrophotometric analysis at 570 nm. Trypan Blue (0.2%, Cat#15250061, Invitrogen) was added to cells dissociated with trypsin, and mixed 1:1 with culture medium to inactivate trypsin. Counts were performed using a hemocytometer.

Western blotting

Total protein was isolated from cell lysates using 1 ml of RIPA buffer supplemented with protease and phosphatase inhibitors as described (Keasey et al., 2013). Proteins were separated by SDS-PAGE and after transfer, PVDF membranes were incubated with antibodies for pY397-FAK (1:1000, Cat#3283, RRID AB_2173659), tFAK (1:1000, Cat#3285, RRID AB_2269034), pY402-PYK2 (1:1000, Cat#3291, RRID AB_2300530), PYK2 (1:1000, Cat# 3480, RRID AB_2174093), α-tubulin (1:2000; Cat#2125, RRID AB_2619646), STAT3 Y705 (1:1000, Cat#9145, RRID AB_2491009) and STAT3 (1:1000, Cat# 12640, RRID AB_2629499) all from Cell Signaling Technology, pS246-ILK (1:1000, Cat# AB1076, RRID AB_11211802, Millipore), tILK (1:1000, Cat# 04-1149, RRID AB_1977290, Millipore), followed by appropriate secondary antibodies (anti-mouse-IgG, Cat# 7076; anti-rabbit-IgG, Cat# 7074, Cell Signaling), as described previously (Keasey et al., 2013). Enhanced chemiluminescence (ECL; Cat# 34080, ThermoFisher) was used to visualize the antibody staining through use of a Li-Cor chemiluminescence imager (Li-Cor model Odyssey-FC 2800) or standard X-ray film.

Quantitative capillary ProteinSimple western blotting

Analysis of protein expression was performed according to the ProteinSimple protocol guide with reagents from the kit (Cat# PS-MK01, ProteinSimple) except where noted. Briefly, cell lysates were diluted to 0.2 µg/µl with 0.1× sample buffer supplemented with 1× fluorescent molecular mass markers and 40 mM DTT for a 5 µl reaction (1 µg protein/reaction). Samples were heated at 95°C for 5 min before loading into 24 single designated wells of a pre-filled plate along with blocking reagent, primary antibodies (1:50, 1:50 or 1:500 in antibody diluent, pFAK, FAK, α-tubulin, with pFAK and Tubulin or FAK and Tubulin mixed together for detection within the same capillary), horseradish peroxidase (HRP)-conjugated anti-rabbit-IgG secondary antibody, luminol-peroxide mix, to generate chemiluminescence, and washing buffer. Plates were loaded into the automated ProteinSimple 'Wes' for electrophoresis and imaged for fluorescence in real-time by means of a CCD camera for immunodetection in the capillary system at default settings (electrophoresis, 375 volts, 25 min; blocking, 5 min; primary antibody, 30 min; secondary antibody, 30 min). Data was analyzed by using Compass software (ProteinSimple) with data displayed as peak intensity or synthetic bands. Quantification was performed by normalizing areas under protein peaks to α-tubulin loading control.

Conditioned medium and dot blots

Conditioned cell culture medium (1.5 ml from one well of a six-well plate/condition) was collected from C6 cells, centrifuged at 5000 rpm for 10 min to remove cell debris and the supernatant frozen overnight at −80°C before lyophilization. The dehydrated proteins were resuspended in 500 µl ddH_2O, and concentrated in protein concentration columns (Cat# UFC500324, Millipore) according to manufacturer's protocol. After centrifugation, the retained 50 µl volume was re-diluted ten-fold in fresh ddH_2O to dilute salts from culture medium and then re-centrifuged. Western blotting revealed no visible bands for either LIF or IL-6. We therefore chose to run dot blots. 1 µl of the retained protein was pipetted onto a nitrocellulose membrane (Thermo Fisher, Cat# 88024) and allowed to dry at room temperature. Membranes were blocked in 5% BSA in TBS:Tween 20 (0.1%, v/v) for 1 h before overnight incubation with rabbit anti-IL-6 (1:1000, Cat# AF506, RRID AB_355398, R&D Systems), rabbit anti-LIF (1:200, Cat# SC-20087, RRID AB_2136098, Santa Cruz Biotechnology) antibodies in 5% BSA TBS:Tween. Membranes were washed 3×5 min with TBS:T then incubated with HRP-conjugated anti-rabbit-IgG or anti-mouse-IgG antibodies. Signal was visualized by ECL according to standard methods and visualized with a Li-Cor chemiluminescence imager.

RT-qPCR

Total RNA was collected from cells according to the manufacturer's protocol (Cat# 74106, Qiagen RNAeasy) and RT-qPCR was performed as described previously (Keasey et al., 2013). Briefly, 500 ng of RNA was reverse-transcribed and used at a final concentration of 20% in RT-qPCR reactions using TaqMan probes for rat C6 cells, GAPDH (Rn9999916_s1), LIF (Rn00573491_g1), IL-6 (Rn01410330_m1), CNTF (Rn00755092_m1), for human CMEC cells, GAPDH (Hs02758991_g1), LIF (Hs01055668_m1), IL-6 (Hs00174360_m1), CNTF (Hs00173456_m1), for mouse bEnd5 cells intracerebral injection brains, GAPDH (4352932E), LIF (Mm00434762_g1), IL-6 (Mm00446190_m1), CNTF (Mm00446373_m1), TNFα (Mm00443258_m1), CD45 (Mm01293575_m1) and CD68 (Mm03047340_m1). All reactions were performed in triplicate and normalized to the levels of GAPDH. Data were analyzed according to the ΔΔCt method.

Journal of Cell Science (2018) 131, jcs202580. doi:10.1242/jcs.202580

Animals

Vitronectin-null ($VTN^{-/-}$; JAX Stock 004371) were purchased from Jackson Laboratory (Bar Harbor, ME) and had been on a C57BL/6 background for 12 generations. Heterozygous mice were bred to produce $VTN^{+/+}$ (wild type) and $VTN^{-/-}$ littermates for experiments. They were bred behind a barrier in our AALAC-accredited vivarium. Tail snips were collected and genotyping was performed with the protocol provided by The Jackson Laboratory. Males were used for the collagenase intracerebral injection hemorrhage experiments at 8–12 weeks of age. All mice were housed with food and water available *ad libitum*, and maintained on a 12 h light–12 h dark on/off cycle. All procedures were approved by the East Tennessee State University IACUC, in compliance with the NIH Guide on Care and Use of Animals.

Plasma isolation from mice

Whole blood (125 µl) collected retro-orbitally or vena cava blood (500 µl) from adult $VTN^{+/+}$ and $VTN^{-/-}$ littermate mice was placed in EDTA-coated mini-capillary collection tubes (Cat# 07 6011, Ram Scientific) and centrifuged at 4000 *g* for 20 min at 4°C to separate plasma. Plasma from three mice was pooled and aliquots were stored at −80°C and used at the indicated concentrations *in vitro* and *in vivo*.

Stereotaxic intrastriatal injections in mice

Intrastriatal injections were performed as described previously (Kang et al., 2012). Briefly, mice were anesthetized with Avertin (2,2,2-tribromoethanol, 400 mg/kg body weight, Sigma-Aldrich) and placed in a Kopf stereotaxic apparatus. A 1 mm burr hole was drilled at coordinates 1 mm rostral and 1.5 mm lateral from Bregma. The needle of a 10 µl Hamilton syringe was clamped in an electrode holder and lowered 3.5 mm ventral to the dura to the center of the striatum. After 2 min, 1 µl PBS or 1 µl PBS plus active or denatured (60°C for 30 min) recombinant human VTN (1 µg/µl, Cat# SRP3186, Sigma-Aldrich) was injected over 3 min, followed by a 2 min pause to reduce backflow. After the needle was withdrawn, the skin was sutured and mice were kept on the heating pad until they fully recovered. The striatum was collected 24 h later from 2 mm brain slices and snap frozen in liquid nitrogen, and stored at −80°C for later analysis. To induce intracerebral hemorrhage (Mracsko et al., 2014), 0.5 µl collagenase (0.03 units, Cat# C2399, Sigma) or 0.5 µl control PBS was injected into the striatum. At 24 h, these mice were transcardially perfused with ice-cold PBS and the striatum tissue collected.

LIF and IL-6 ELISA from adult mouse brain

Protein levels were measured in extracts from the striatum of the hemorrhage mice and those injected with rhVTN by ELISA, using kits for mouse IL-6 (Cat # MLF00, R&D Systems) and LIF (Cat # MLF00, R&D Systems) and performed according to manufacturer's protocol.

Statistical analyses

Statistical analyses were performed in GraphPad Prism (version 5a or 7). A one-way ANOVA with Dunnett post hoc tests or a two-way ANOVA with multiple comparisons was used when comparing genotypes or siRNA treatments combined with pharmacological inhibitors. If only two groups were compared, a Student's *t*-test was used. Statistical analysis for Fig. 2A,C was performed with a non-parametric Kruskal–Wallis test, as the data were not normally distributed. ELISA data in Fig. 2B,D was analyzed by two-way ANOVA, which showed no difference in genotype or genotype treatment interaction but showed a treatment effect. We therefore performed a Fisher's least squares difference (LSD) test, which treats both groups as individual experiments and for the effect of treatment within each genotype. A value of $P<0.05$ was considered to be statistically significant.

Acknowledgements

We express our gratitude to Hannah Malone for animal care, and Rhesa Dykes and Michelle Duffourc of the Microbiology Core Facility for guidance in the WES technology. Dr Engelhardt of the Theodor Kocher institute graciously provided the bEnd5 cells.

Competing interests

The authors declare no competing or financial interests.

Author contributions

Conceptualization: M.P.K., T.H.; Methodology: M.P.K., C.J., L.F.P., T.H.; Validation: M.P.K., T.H.; Formal analysis: M.P.K., C.J., T.H.; Investigation: M.P.K., C.J., L.F.P., R.R.S., C.L.; Resources: T.H.; Data curation: M.P.K., T.H.; Writing - original draft: M.P.K., T.H.; Writing - review & editing: M.P.K., T.H.; Visualization: M.P.K., C.J., T.H.; Supervision: M.P.K., T.H.; Project administration: M.P.K., T.H.; Funding acquisition: T.H.

Funding

Funding was provided by National Institutes of Health (NIH) (R01 grant AG29493, and in part by C06RR0306551) and the Quillen College of Medicine at East Tennessee State University. L.F.P. was supported by grants from Conselho Nacional de Desenvolvimento Científico e Tecnológico (454077/2014-9), Fundação do Amparo a Ciência e Tecnologia (AMD-0291-2.00/14) and Coordenadoria de Aperfeiçoamento de Pessoal de Nível Superior (88881.133822/2016-01). Deposited in PMC for release after 12 months.

Supplementary information

Supplementary information available online at
http://jcs.biologists.org/lookup/doi/10.1242/jcs.202580.supplemental

References

Aguirre Ghiso, J. A. (2002). Inhibition of FAK signaling activated by urokinase receptor induces dormancy in human carcinoma cells in vivo. *Oncogene* **21**, 2513-2524.

Antonov, A. S., Antonova, G. N., Munn, D. H., Mivechi, N., Lucas, R., Catravas, J. D. and Verin, A. D. (2011). αVβ3 integrin regulates macrophage inflammatory responses via PI3 kinase/Akt-dependent NF-κB activation. *J. Cell. Physiol.* **226**, 469-476.

Bang, J.-Y., Kim, E.-Y., Kang, D.-K., Chang, S.-I., Han, M. H., Baek, K.-H. and Kang, I.-C. (2011). Pharmacoproteomic analysis of a novel cell-permeable peptide inhibitor of tumor-induced angiogenesis. *Mol. Cell Proteomics* **10**, M110.005264.

Banner, L. R. and Patterson, P. H. (1994). Major changes in the expression of the mRNAs for cholinergic differentiation factor/leukemia inhibitory factor and its receptor after injury to adult peripheral nerves and ganglia. *Proc. Natl. Acad. Sci. USA* **91**, 7109-7113.

Banner, L. R., Moayeri, N. N. and Patterson, P. H. (1997). Leukemia inhibitory factor is expressed in astrocytes following cortical brain injury. *Exp. Neurol.* **147**, 1-9.

Bauer, S. and Patterson, P. H. (2006). Leukemia inhibitory factor promotes neural stem cell self-renewal in the adult brain. *J. Neurosci.* **26**, 12089-12099.

Borish, L., O'Reilly, D., Klempner, M. S. and Rocklin, R. E. (1986). Leukocyte Inhibitory Factor (Lif) Potentiates Neutrophil Responses to Formyl-Methionyl-Leucyl-Phenylalanine. *J. Immunol.* **137**, 1897-1903.

Butler, B. and Blystone, S. D. (2005). Tyrosine phosphorylation of beta3 integrin provides a binding site for Pyk2. *J. Biol. Chem.* **280**, 14556-14562.

Carlson, C. D., Bai, Y., Jonakait, G. M. and Hart, R. P. (1996). Interleukin-1 beta increases leukemia inhibitory factor mRNA levels through transient stimulation of transcription rate. *Glia* **18**, 141-151.

Cartwright, P., McLean, C., Sheppard, A., Rivett, D., Jones, K. and Dalton, S. (2005). LIF/STAT3 controls ES cell self-renewal and pluripotency by a Myc-dependent mechanism. *Development* **132**, 885-896.

Cattavarayane, S., Palovuori, R., Tanjore Ramanathan, J. and Manninen, A. (2015). α6β1- and αV-integrins are required for long-term self-renewal of murine embryonic stem cells in the absence of LIF. *BMC Cell Biol.* **16**, 3.

Charo, I. F., Nannizzi, L., Smith, J. W. and Cheresh, D. A. (1990). The vitronectin receptor alpha v beta 3 binds fibronectin and acts in concert with alpha 5 beta 1 in promoting cellular attachment and spreading on fibronectin. *J. Cell Biol.* **111**, 2795-2800.

Choi, Y., Kim, E., Lee, Y., Han, M. H. and Kang, I.-C. (2010). Site-specific inhibition of integrin alpha v beta 3-vitronectin association by a ser-asp-val sequence through an Arg-Gly-Asp-binding site of the integrin. *Proteomics* **10**, 72-80.

Degryse, B., Resnati, M., Czekay, R.-P., Loskutoff, D. J. and Blasi, F. (2005). Domain 2 of the urokinase receptor contains an integrin-interacting epitope with intrinsic signaling activity: generation of a new integrin inhibitor. *J. Biol. Chem.* **280**, 24792-24803.

del Zoppo, G. J., Frankowski, H., Gu, Y.-H., Osada, T., Kanazawa, M., Milner, R., Wang, X., Hosomi, N., Mabuchi, T. and Koziol, J. A. (2012). Microglial cell activation is a source of metalloproteinase generation during hemorrhagic transformation. *J. Cereb. Blood Flow Metab.* **32**, 919-932.

Delimont, D., Dufek, B. M., Meehan, D. T., Zallocchi, M., Gratton, M. A., Phillips, G. and Cosgrove, D. (2014). Laminin α2-mediated focal adhesion kinase activation triggers Alport glomerular pathogenesis. *PLoS ONE* **9**, e99083.

Derigs, H. G. and Boswell, H. S. (1993). LIF mRNA expression is transcriptionally regulated in murine bone marrow stromal cells. *Leukemia* **7**, 630-634.

Dowsing, B. J., Romeo, R. and Morrison, W. A. (2001). Expression of leukemia inhibitory factor in human nerve following injury. *J. Neurotrauma* **18**, 1279-1287.

Erta, M. A., Quintana, A. and Hidalgo, J. (2012). Interleukin-6, a major cytokine in the central nervous system. *Int. J. Biol. Sci.* **8**, 1254-1266.
Gertz, K., Kronenberg, G., Kälin, R. E., Baldinger, T., Werner, C., Balkaya, M., Eom, G. D., Hellmann-Regen, J., Kröber, J., Miller, K. R. et al. (2012). Essential role of interleukin-6 in post-stroke angiogenesis. *Brain* **135**, 1964-1980.
Giancotti, F. G. and Ruoslahti, E. (1999). Integrin signaling. *Science* **285**, 1028-1032.
Gu, J., Tamura, M., Pankov, R., Danen, E. H. J., Takino, T., Matsumoto, K. and Yamada, K. M. (1999). Shc and FAK differentially regulate cell motility and directionality modulated by PTEN. *J. Cell Biol.* **146**, 389-403.
Hawkins, B.T. (2005). The blood-brain barrier/neurovascular unit in health and disease. *Pharmacol. Rev.* **57**, 173-185.
Hayashi, Y., Furue, M. K., Okamoto, T., Ohnuma, K., Myoishi, Y., Fukuhara, Y., Abe, T., Sato, J. D., Hata, R.-I. and Asashima, M. (2007). Integrins regulate mouse embryonic stem cell self-renewal. *Stem Cells* **25**, 3005-3015.
Hayman, E. G., Pierschbacher, M. D., Ohgren, Y. and Ruoslahti, E. (1983). Serum spreading factor (vitronectin) is present at the cell surface and in tissues. *Proc. Natl. Acad. Sci. USA* **80**, 4003-4007.
Hayman, E. G., Pierschbacher, M. D., Suzuki, S. and Ruoslahti, E. (1985). Vitronectin–a major cell attachment-promoting protein in fetal bovine serum. *Exp. Cell Res.* **160**, 245-258.
Herrera-Molina, R., Frischknecht, R., Maldonado, H., Seidenbecher, C. I., Gundelfinger, E. D., Hetz, C., Aylwin, M. L., Schneider, P., Quest, A. F. G. and Leyton, L. (2012). Astrocytic αVβ3 integrin inhibits neurite outgrowth and promotes retraction of neuronal processes by clustering Thy-1. *PLoS ONE* **7**, e34295.
Hunter, C. A. and Jones, S. A. (2015). IL-6 as a keystone cytokine in health and disease. *Nat. Immunol.* **16**, 448-457.
Ishibashi, T., Dakin, K. A., Stevens, B., Lee, P. R., Kozlov, S. V., Stewart, C. L. and Fields, R. D. (2006). Astrocytes promote myelination in response to electrical impulses. *Neuron* **49**, 823-832.
Iwasaki, H., Takeuchi, O., Teraguchi, S., Matsushita, K., Uehata, T., Kuniyoshi, K., Satoh, T., Saitoh, T., Matsushita, M., Standley, D. M. et al. (2011). The IκB kinase complex regulates the stability of cytokine-encoding mRNA induced by TLR–IL-1R by controlling degradation of regnase-1. *Nat. Immunol.* **12**, 1167-1175.
Jang, Y.-C., Tsou, R., Gibran, N. S. and Isik, F. F. (2000). Vitronectin deficiency is associated with increased wound fibrinolysis and decreased microvascular angiogenesis in mice. *Surgery* **127**, 696-704.
Kang, W.-S., Choi, J.-S., Shin, Y.-J., Kim, H.-Y., Cha, J.-H., Lee, J.-Y., Chun, M.-H. and Lee, M.-Y. (2008). Differential regulation of osteopontin receptors, CD44 and the alpha(v) and beta(3) integrin subunits, in the rat hippocampus following transient forebrain ischemia. *Brain Res.* **1228**, 208-216.
Kang, S. S., Keasey, M. P., Cai, J. and Hagg, T. (2012). Loss of neuron-astroglial interaction rapidly induces protective CNTF expression after stroke in mice. *J. Neurosci.* **32**, 9277-9287.
Kang, S. S., Keasey, M. P. and Hagg, T. (2013). P2X7 Receptor Inhibition Increases CNTF in the Subventricular Zone, But Not Neurogenesis or Neuroprotection After Stroke in Adult Mice. *Transl. Stroke Res.* **4**, 533-545.
Keasey, M. P., Kang, S. S., Lovins, C. and Hagg, T. (2013). Inhibition of a novel specific neuroglial integrin signaling pathway increases STAT3-mediated CNTF expression. *Cell Commun. Signal.* **11**, 35.
Kerr, B. J. and Patterson, P. H. (2004). Potent pro-inflammatory actions of leukemia inhibitory factor in the spinal cord of the adult mouse. *Exp. Neurol.* **188**, 391-407.
Krueger, M., Bechmann, I., Immig, K., Reichenbach, A., Härtig, W. and Michalski, D. (2015). Blood-brain barrier breakdown involves four distinct stages of vascular damage in various models of experimental focal cerebral ischemia. *J. Cereb. Blood Flow Metab.* **35**, 292-303.
Lacroix, S., Chang, L., Rose-John, S. and Tuszynski, M. H. (2002). Delivery of hyper-interleukin-6 to the injured spinal cord increases neutrophil and macrophage infiltration and inhibits axonal growth. *J. Comp. Neurol.* **454**, 213-228.
Lau, L. T. and Yu, A. C.-H. (2001). Astrocytes produce and release interleukin-1, interleukin-6, tumor necrosis factor alpha and interferon-gamma following traumatic and metabolic injury. *J. Neurotrauma* **18**, 351-359.
Leavesley, D. I., Kashyap, A. S., Croll, T., Sivaramakrishnan, M., Shokoohmand, A., Hollier, B. G. and Upton, Z. (2013). Vitronectin—Master controller or micromanager? *IUBMB Life* **65**, 807-818.
Lee, Y., Kang, D.-K., Chang, S.-I., Han, M. H. and Kang, I.-C. (2004). High-throughput screening of novel peptide inhibitors of an integrin receptor from the hexapeptide library by using a protein microarray chip. *J. Biomol. Screen.* **9**, 687-694.
Li, S., Kim, M., Hu, Y. L., Jalali, S., Schlaepfer, D. D., Hunter, T., Chien, S. and Shyy, J. Y. (1997). Fluid shear stress activation of focal adhesion kinase. Linking to mitogen-activated protein kinases. *J. Biol. Chem.* **272**, 30455-30462.
Li, R., Ren, M., Chen, N., Luo, M., Zhang, Z. and Wu, J. (2012). Vitronectin increases vascular permeability by promoting VE-cadherin internalization at cell junctions. *PLoS ONE* **7**, e37195.
Lin, Z.-Q. (2003). Essential involvement of IL-6 in the skin wound-healing process as evidenced by delayed wound healing in IL-6-deficient mice. *J. Leukoc. Biol.* **73**, 713-721.
Linker, R. A., Mäurer, M., Gaupp, S., Martini, R., Holtmann, B., Giess, R., Rieckmann, P., Lassmann, H., Toyka, K. V., Sendtner, M. et al. (2002). CNTF is a major protective factor in demyelinating CNS disease: a neurotrophic cytokine as modulator in neuroinflammation. *Nat. Med.* **8**, 620-624.
Liu, E., Côté, J.-F. and Vuori, K. (2003). Negative regulation of FAK signaling by SOCS proteins. *EMBO J.* **22**, 5036-5046.
Liu, Y.-K., Uemura, T., Nemoto, A., Yabe, T., Fujii, N., Ushida, T. and Tateishi, T. (1997). Osteopontin involvement in integrin-mediated cell signaling and regulation of expression of alkaline phosphatase during early differentiation of UMR cells. *FEBS Lett.* **420**, 112-116.
Longo, A., Librizzi, M., Chuckowree, I. S., Baltus, C. B., Spencer, J. and Luparello, C. (2015). Cytotoxicity of the Urokinase-Plasminogen Activator Inhibitor Carbamimidothioic Acid (4-Boronophenyl) Methyl Ester Hydrobromide (BC-11) on Triple-Negative MDA-MB231 Breast Cancer Cells. *Molecules* **20**, 9879-9889.
Madsen, C. D., Ferraris, G. M. S., Andolfo, A., Cunningham, O. and Sidenius, N. (2007). uPAR-induced cell adhesion and migration: vitronectin provides the key. *J. Cell Biol.* **177**, 927-939.
Magnussen, S., Hadler-Olsen, E., Latysheva, N., Pirila, E., Steigen, S. E., Hanes, R., Salo, T., Winberg, J.-O., Uhlin-Hansen, L. and Svineng, G. (2014). Tumour microenvironments induce expression of urokinase plasminogen activator receptor (uPAR) and concomitant activation of gelatinolytic enzymes. *PLoS ONE* **9**, e105929.
Magnussen, S. N., Hadler-Olsen, E., Costea, D. E., Berg, E., Jacobsen, C. C., Mortensen, B., Salo, T., Martinez-Zubiaurre, I., Winberg, J.-O., Uhlin-Hansen, L. et al. (2017). Cleavage of the urokinase receptor (uPAR) on oral cancer cells: regulation by transforming growth factor - β1 (TGF-β1) and potential effects on migration and invasion. *BMC Cancer* **17**, 350.
Matsuoka, I., Nakane, A. and Kurihara, K. (1997). Induction of LIF-mRNA by TGF-beta 1 in Schwann cells. *Brain Res.* **776**, 170-180.
Mauer, J., Denson, J. L. and Brüning, J. C. (2015). Versatile functions for IL-6 in metabolism and cancer. *Trends Immunol.* **36**, 92-101.
Memmo, L. M. and McKeown-Longo, P. (1998). The alphavbeta5 integrin functions as an endocytic receptor for vitronectin. *J. Cell Sci.* **111**, 425-433.
Mi, H., Haeberle, H. and Barres, B. A. (2001). Induction of astrocyte differentiation by endothelial cells. *J. Neurosci.* **21**, 1538-1547.
Milner, R. (2009). Microglial expression of alphavbeta3 and alphavbeta5 integrins is regulated by cytokines and the extracellular matrix: beta5 integrin null microglia show no defects in adhesion or MMP-9 expression on vitronectin. *Glia* **57**, 714-723.
Milner, R. and Campbell, I. L. (2003). The extracellular matrix and cytokines regulate microglial integrin expression and activation. *J. Immunol.* **170**, 3850-3858.
Milner, R., Crocker, S. J., Hung, S., Wang, X., Frausto, R. F. and del Zoppo, G. J. (2007). Fibronectin- and vitronectin-induced microglial activation and matrix metalloproteinase-9 expression is mediated by integrins alpha5beta1 and alphavbeta5. *J. Immunol.* **178**, 8158-8167.
Mitra, S. K., Hanson, D. A. and Schlaepfer, D. D. (2005). Focal adhesion kinase: in command and control of cell motility. *Nat. Rev. Mol. Cell Biol.* **6**, 56-68.
Mracsko, E., Javidi, E., Na, S.-Y., Kahn, A., Liesz, A. and Veltkamp, R. (2014). Leukocyte invasion of the brain after experimental intracerebral hemorrhage in mice. *Stroke* **45**, 2107-2114.
Murphy, G. M., Song, Y., Ong, E., Lee, Y. L., Schmidt, K. G., Bocchini, V. and Eng, L. F. (1995). Leukemia inhibitory factor mRNA is expressed in cortical astrocyte cultures but not in an immortalized microglial cell line. *Neurosci. Lett.* **184**, 48-51.
Nagamoto-Combs, K., Vaccariello, S. A. and Zigmond, R. E. (1999). The levels of leukemia inhibitory factor mRNA in a Schwann cell line are regulated by multiple second messenger pathways. *J. Neurochem.* **72**, 1871-1881.
Nakanishi, M., Niidome, T., Matsuda, S., Akaike, A., Kihara, T. and Sugimoto, H. (2007). Microglia-derived interleukin-6 and leukaemia inhibitory factor promote astrocytic differentiation of neural stem/progenitor cells. *Eur. J. Neurosci.* **25**, 649-658.
Ochel, H.-J., Schulte, T. W., Nguyen, P., Trepel, J. and Neckers, L. (1999). The benzoquinone ansamycin geldanamycin stimulates proteolytic degradation of focal adhesion kinase. *Mol. Genet. Metab.* **66**, 24-30.
Ostberg, C. O., Zhu, P., Wight, T. N. and Qwarnstrom, E. E. (1995). Fibronectin attachment is permissive for IL-1 mediated gene regulation. *FEBS Lett.* **367**, 93-97.
Pan, W., Yu, C., Hsuchou, H., Zhang, Y. and Kastin, A. J. (2008). Neuroinflammation facilitates LIF entry into brain: role of TNF. *Am. J. Physiol. Cell. Physiol.* **294**, C1436-C1442.
Peruzzi, B., Cappariello, A., Del Fattore, A., Rucci, N., De Benedetti, F. and Teti, A. (2012). c-Src and IL-6 inhibit osteoblast differentiation and integrate IGFBP5 signalling. *Nat. Comms.* **3**, 630.
Plow, E. F., Haas, T. K., Zhang, L., Loftus, J. and Smith, J. W. (2000). Ligand binding to integrins. *J. Biochem.* **275**, 21785-21788.
Rothaug, M., Becker-Pauly, C. and Rose-John, S. (2016). The role of interleukin-6 signaling in nervous tissue. *Biochim. Biophys. Acta* **1863**, 1218-1227.

Schlaepfer, D. D., Hou, S., Lim, S.-T., Tomar, A., Yu, H., Lim, Y., Hanson, D. A., Uryu, S. A., Molina, J. and Mitra, S. K. (2007). Tumor necrosis factor-alpha stimulates focal adhesion kinase activity required for mitogen-activated kinase-associated interleukin 6 expression. *J. Biol. Chem.* **282**, 17450-17459.

Seiffert, D., Keeton, M., Eguchi, Y., Sawdey, M. and Loskutoff, D. J. (1991). Detection of vitronectin mRNA in tissues and cells of the mouse. *Proc. Natl. Acad. Sci. USA* **88**, 9402-9406.

Seiffert, D., Iruela-Arispe, M. L., Sage, E. H. and Loskutoff, D. J. (1995). Distribution of vitronectin mRNA during murine development. *Dev. Dyn.* **203**, 71-79.

Shimamura, N., Matchett, G., Yatsushige, H., Calvert, J. W., Ohkuma, H. and Zhang, J. (2006). Inhibition of integrin alphavbeta3 ameliorates focal cerebral ischemic damage in the rat middle cerebral artery occlusion model. *Stroke* **37**, 1902-1909.

Sieg, D. J., Hauck, C. R., Ilić, D., Klingbeil, C. K., Schaefer, E., Damsky, C. H. and Schlaepfer, D. D. (2000). FAK integrates growth-factor and integrin signals to promote cell migration. *Nat. Cell Biol.* **2**, 249-256.

Slack-Davis, J. K., Martin, K. H., Tilghman, R. W., Iwanicki, M., Ung, E. J., Autry, C., Luzzio, M. J., Cooper, B., Kath, J. C., Roberts, W. G. et al. (2007). Cellular characterization of a novel focal adhesion kinase inhibitor. *J. Biol. Chem.* **282**, 14845-14852.

Sugiura, S., Lahav, R., Han, J., Kou, S.-Y., Banner, L. R., de Pablo, F. and Patterson, P. H. (2000). Leukaemia inhibitory factor is required for normal inflammatory responses to injury in the peripheral and central nervous systems in vivo and is chemotactic for macrophages in vitro. *Eur. J. Neurosci.* **12**, 457-466.

Suzuki, S., Oldberg, A., Hayman, E. G., Pierschbacher, M. D. and Ruoslahti, E. (1985). Complete amino acid sequence of human vitronectin deduced from cDNA. Similarity of cell attachment sites in vitronectin and fibronectin. *EMBO J.* **4**, 2519-2524.

Suzuki, S., Tanaka, K. and Suzuki, N. (2009). Ambivalent aspects of interleukin-6 in cerebral ischemia: inflammatory versus neurotrophic aspects. *J. Cereb. Blood Flow Metab.* **29**, 464-479.

Tofaris, G. K., Patterson, P. H., Jessen, K. R. and Mirsky, R. (2002). Denervated Schwann cells attract macrophages by secretion of leukemia inhibitory factor (LIF) and monocyte chemoattractant protein-1 in a process regulated by interleukin-6 and LIF. *J. Neurosci.* **22**, 6696-6703.

Tomasini-Johansson, B. R., Milbrink, J. and Pejler, G. (1998). Vitronectin expression in rheumatoid arthritic synovia–inhibition of plasmin generation by vitronectin produced in vitro. *Br. J. Rheumatol.* **37**, 620-629.

Tornatore, T. F., Dalla Costa, A. P., Clemente, C. F. M. Z., Judice, C., Rocco, S. A., Calegari, V. C., Cardoso, L., Cardoso, A. C., Goncalves, A. J. and Franchini, K. G. (2011). A role for focal adhesion kinase in cardiac mitochondrial biogenesis induced by mechanical stress. *Am. J. Physiol. Heart Circ. Physiol.* **300**, H902-H912.

Tsuruta, Y., Park, Y.-J., Siegal, G. P., Liu, G. and Abraham, E. (2007). Involvement of vitronectin in lipopolysaccaride-induced acute lung injury. *J. Immunol.* **179**, 7079-7086.

Van Wagoner, N. J. and Benveniste, E. N. (1999). Interleukin-6 expression and regulation in astrocytes. *J. Neuroimmunol.* **100**, 124-139.

Vandenberghe, M., Raphaël, M., Lehen'kyi, V., Gordienko, D., Hastie, R., Oddos, T., Rao, A., Hogan, P. G., Skryma, R. and Prevarskaya, N. (2013). ORAI1 calcium channel orchestrates skin homeostasis. *Proc. Natl. Acad. Sci. USA* **110**, E4839-E4848.

Vogiagis, D. and Salamonsen, L. A. (1999). Review: The role of leukaemia inhibitory factor in the establishment of pregnancy. *J. Endocrinol.* **160**, 181-190.

Wang, J. and Milner, R. (2006). Fibronectin promotes brain capillary endothelial cell survival and proliferation through alpha5beta1 and alphavbeta3 integrins via MAP kinase signalling. *J. Neurochem.* **96**, 148-159.

Wei, Y., Waltz, D. A., Rao, N., Drummond, R. J., Rosenberg, S. and Chapman, H. A. (1994). Identification of the urokinase receptor as an adhesion receptor for vitronectin. *J. Biol. Chem.* **269**, 32380-32388.

Welser-Alves, J. V., Boroujerdi, A., Tigges, U. and Milner, R. (2011). Microglia use multiple mechanisms to mediate interactions with vitronectin; non-essential roles for the highly-expressed αvβ3 and αvβ5 integrins. *J. Neuroinflammation* **8**, 157.

Xiong, J.-P. (2002). Crystal Structure of the Extracellular Segment of Integrin alpha Vbeta 3 in Complex with an Arg-Gly-Asp Ligand. *Science* **296**, 151-155.

Yang, P., Arnold, S. A., Habas, A., Hetman, M. and Hagg, T. (2008). Ciliary neurotrophic factor mediates dopamine D2 receptor-induced CNS neurogenesis in adult mice. *J. Neurosci.* **28**, 2231-2241.

Zheng, X., Saunders, T. L., Camper, S. A., Samuelson, L. C. and Ginsburg, D. (1995). Vitronectin is not essential for normal mammalian development and fertility. *Proc. Natl. Acad. Sci. USA* **92**, 12426-12430.

Zigmond, R. E. (2012). gp130 cytokines are positive signals triggering changes in gene expression and axon outgrowth in peripheral neurons following injury. *Front. Mol. Neurosci.* **4**, 62.

ANEXO B – Análise funcional da variação do gene *RYR3* no transporte de cálcio *in vitro* (Programa de Doutorado Sanduíche no Exterior - CAPES)

Em meados do final de 2016, eis que surgira a oportunidade para um segundo intercâmbio acadêmico no laboratório do Dr. Theoddor Hagg, Chefe do Departamento de Ciências Biomédicas da Universidade do Leste o Tennessee (ETSU – EUA). Durante os meses de abril a outubro de 2017, envolvi-me em diversos projetos simultaneamente, mas com enfoque na finalização do artigo iniciado em 2015 (Anexo A).

Após a triagem dos resultados do exoma, alguns genes foram eliminados restando apenas o *RYR3* como o mais promissor, ainda que fosse necessária a reavaliação clínica dos pacientes para dar maior robustez ao achado. Procuramos obter mais informações clínicas e de neuroimagem de alguns membros da família brasileira, porém, por questões éticas, decidimos dar continuidade aos trabalhos com os dados coletados até então, sem causar transtornos para os pacientes e seus familiares.

Devido ao contexto em que me inseria, trabalhando de perto com técnicas de mutagênese e biologia celular em um laboratório com vasta experiência no tema, julgamos oportuno avaliar o impacto funcional da variação missense encontrada no gene *RYR3* (c.2486G>A:p.Arg829His) no transporte de fosfato em modelo *in vitro*. Por meio da inserção da mutação (*knock-in*) com o sistema de edição gênica CRISPR-Cas9 em células da linhagem de osteosarcoma, SaOS-2, planejei a realização experimentos funcionais que revelassem os efeitos da variação na função transportadora da proteína Ryr3 (morfologia, crescimento e migração celular, expressão gênica, influxo de cálcio, etc).

Com o uso de ferramentas *in silico*, cinco RNA-guias foram desenhados, testados, em seguida sintetizados e clonados no plasmídeo de expressão pSpCas9(BB)-2A-Puro (PX459) V2.0 (www.addgene.org). Selecionamos dois RNA-guias para clonagem no plasmídeo, seguida de transformação em células competentes de *E. coli* (DH5α) e sequenciamento do DNA a fim de averiguar a correta inserção das fitas de RNA no constructo, fato que foi posteriormente confirmado. Em seguida, foi realizada a transfecção do DNA extraído das bactérias DH5α, nas células SaOS-2 com posterior sequenciamento, a fim de verificar a eficiência da clivagem dos RNA-guias. Infelizmente, o sequenciamento não conseguiu cobrir a região onde as fitas de RNA deveriam estar

inseridas, não sendo capaz, então, de responder à questão acerca da eficiência dos guias. Tentei avaliar, então, os níveis de mRNA do *RYR3* nas SAOS-2 e em amostras de cérebro e do músculo esquelético de camundongo (controles positivos), por meio de RT-qPCR, como uma forma indireta de testar a eficiência do constructo. Os ensaios realizados com sondas Taqman não detectaram expressão do gene nas amostras usadas, sugerindo uma possível ineficiência dos primers. Diante das dificuldades e ao tempo limitado, após os experimentos serem reavaliados, modificados e repetidos inúmeras vezes, o projeto precisou ser interrompido e prioridade foi dada aos trabalhos referentes ao trabalho proposto inicialmente.

ANEXO C – Participação em trabalho apresentado no congresso da Sociedade de Neurociências

← Search Results

Print Page

Share Page

Add To Itinerary

Session 304 - Neuroinflammation in Neurodegenerative Diseases

304.25 / Y14 - Blood vitronectin robustly induces LIF and pro-inflammatory IL-6 expression *In vitro* and in the mouse brain through integrin-FAK signaling

November 13, 2017, 8:00 AM - 12:00 PM | Halls A-C

Presenter at Poster
Mon, Nov. 13, 2017, 8:00 AM - 9:00 AM

Session Type
Poster

Grant Support
NIH R01 grant AG29493

Grant Support
Quillen College of Medicine at ETSU

Authors
***M. P. KEASEY**[1], C. JIA[2], L. PIMENTEL[2], R. SANTE[2], C. LOVINS[2], T. HAGG[3];
[1]East Tennessee State Univ., Johnson City, TN; [2]Dept. of Biomed. Sci., East Tennessee State Univ., Mountain Home, TN; [3]Dept. of Biomed. Sci., East Tennessee State Univ., Johnson City, TN

Disclosures
M.P. Keasey: None. **C. Jia:** None. **L. Pimentel:** None. **R. Sante:** None. **C. Lovins:** None. **T. Hagg:** None.

Abstract
We have identified a novel function for vitronectin (VTN), an abundant blood protein, as a rapid and potent inducer of leukemia inhibitory factor (LIF) and pro-inflammatory interleukin-6 (IL-6) both in vivo and in vitro. In contrast to VTN, laminin-111, fibrinogen, fibronectin or collagen-1 had no effect on either cytokine after 4 hours in cultured C6 astroglioma cells. Also in vitro, plasma from VTN -/- mice was a less effective inducer of LIF and IL-6 relative to wild type plasma. In adult mice, intra-striatal injection of VTN but not heat-denatured VTN significantly increased LIF and IL-6. Conversely, VTN -/- mice had reduced LIF and IL-6 in response to intracerebral haemorrhage relative to wild type mice. In vitro, VTN induction of LIF and IL-6 were suppressed by RGD-integrin blocking peptides, including one specific for αvβ3 integrin. Pharmacological blockade of the urokinase plasminogen activator receptor (uPAR), which can bind VTN, also reduced LIF and IL-6 induction by VTN. Further, pharmacological blockade of focal adhesion kinase (FAK) activation and siRNA against FAK, but not the related PYK2, suppressed both LIF and IL-6 in endothelial cells. Overexpression of mutated FAK (Y397F) in cultured cells reduced mechanical injury-mediated LIF and IL-6 induction. We propose that VTN leakage from the blood is an important mediator of cytokine and inflammatory signalling. Integrin-FAK activation may represent a novel target for the regulation of both LIF and IL-6 with implications for the stem cell and inflammation fields.

Blood vitronectin is a major activator of LIF and IL-6 in the brain through integrin-FAK and uPAR signaling

Poster Y14
Abstract 304.25

Keasey MP, Jia C, Pimentel LF, Sante RS, Lovins C, Hagg T

DEPARTMENT of BIOMEDICAL SCIENCES
Quillen College of Medicine
EAST TENNESSEE STATE UNIVERSITY

Introduction

Vitronectin (VTN) is found in high concentrations in the blood (1). VTN leakage into tissues has been detected in several inflammatory conditions, including rheumatoid arthritis (2) and lung, liver and kidney fibrosis (3) as well as stroke (4). IL-6 is a pro-inflammatory cytokine that triggers Gp130-JAK/STAT signaling. Leukemia inhibitory factor (LIF) can also trigger pro-inflammatory signaling. Little is known of the mechanisms that regulate LIF and the initial trigger for IL-6 induction in the brain.

Here, we determined whether blood-derived proteins such as VTN regulate LIF and IL-6 expression through integrin-FAK and/or uPAR signaling, using cultured astroglioma and endothelial cells, and adult mice.

Abstract 14640 (Jia C) shows that CNTF, LIF and IL-6 are induced by VTN in naïve mice through the integrin-FAK pathway, and differentially through different MAPKs.

1- Hayman, E. G et al., (1983).. *Proc. Natl. Acad. Sci. U.S.A.* 80, 4003–4007.
2- Tomasini-Johansson, B. R et al., (1996). *Br. J. Rheumatol.* 37, 620–629.
3- Jang, Y. C et al., (2000). *Surgery* 127, 696–704.
4- Del Zoppo, G. J et al., (2012). *J Cereb Blood Flow Metab* 32, 919–932.

Methods

RT-qPCR: Isolated RNA reverse transcribed and relative gene expression quantified with TaqMan primers and ΔΔCt
ELISA: IL-6 and LIF ELISA performed using standard method
Western blotting: Tissue processed using Trizol method
Intra Striatal injections: From Bregma RC +1.0, ML -1.5, DV -3.5
In vitro: C6 astroglioma or immortalised human brain microvascular endothelial cells maintained under standard conditions

Intra-striatal injection of rhVTN induces LIF and IL-6 mRNA and protein in adult male mice

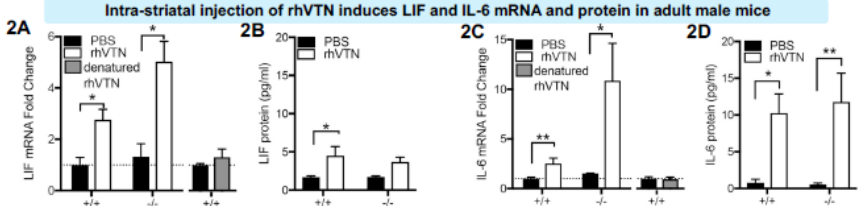

VTN regulates LIF and IL-6 expression in adult mouse brain. A) Injection of 1 µg recombinant human VTN (but not denatured) into the striatum of adult VTN+/+ or VTN-/- littermate mice increased LIF mRNA. **B)** LIF protein (ELISA) was also induced in the striatum. **C)** IL-6 mRNA expression was also induced at 24 hrs relative to PBS injections (VTN+/+ mice: PBS n=7, VTN n=7; VTN-/- mice PBS n=5, VTN n=5). **D)** IL-6 protein (ELISA) was induced by rhVTN in the striatum of the same mice.

Hemorrhagic induces LIF and IL-6 less in VTN KO mice

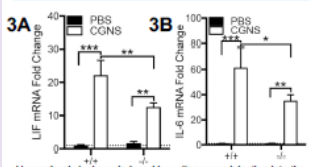

Hemorrhagic leakage induced by collagenase injection into the striatum caused a greater increase in LIF (**A**) and IL-6 (**B**) mRNA in VTN+/+ than in VTN-/- littermate mice 24 hr later (n=6-7/group). Data are means ± SEM. * p<0.05, ** p<0.01, *** p<0.001.

VTN-induced LIF and IL-6 is partially mediated by RGD integrins and uPAR in C6 cells

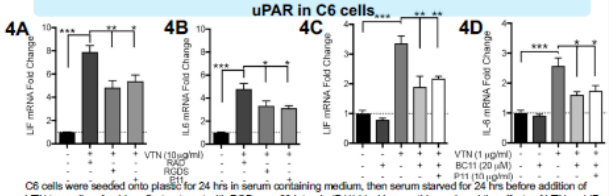

C6 cells were seeded onto plates for 24 hrs in serum containing medium, then serum starved for 24 hrs before addition of VTN to medium for 4 hrs. Co-treatment with RGD or αvβ3 integrin (P11) blocking peptides reduced the effects of VTN on LIF (**A**) and IL-6 (**B**) mRNA expression. LIF and IL-6 expression were not completely abolished, suggesting an additional VTN-activated mechanism(s). Indeed, BC-11, a uPA-uPAR inhibitor decreased VTN-induced LIF (**C**) and IL-6 (**D**) mRNA expression, but did not have any effects by itself, after 4 hr. Data are means ± SEM of 4 independent experiments.

Blood VTN regulates LIF and IL-6 after brain injury - model

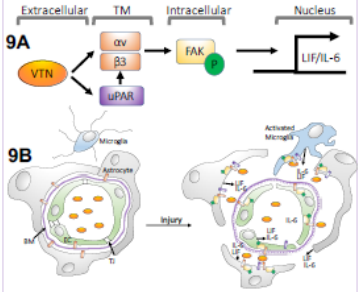

A) Schematic showing VTN-mediated LIF and IL-6 gene expression, binding to αvβ3 integrin and specifically activating downstream FAK.
B) Proposed model of VTN leakage after BBB breakdown. Under normal conditions, the intact BBB characterized by tight junctions (TJ) between endothelial cells (EC) keeps blood VTN from entering the CNS tissue. BM = basement membrane. Under pathological conditions that cause BBB breakdown, such as stroke and hemorrhage, leakage of VTN in the brain parenchyma induces LIF and IL-6 expression by astrocytes (gray cells), microglia (blue cells) and endothelial cells (green cells).

VTN strongly induces LIF and IL-6 mRNA in vitro

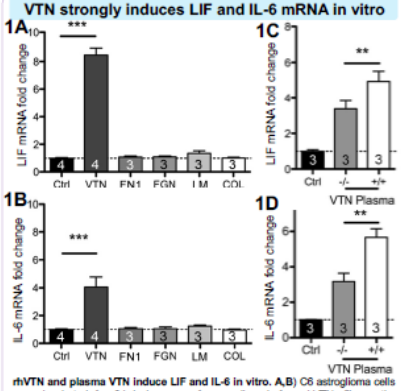

rhVTN and plasma VTN induce LIF and IL-6 in vitro. A,B) C6 astroglioma cells were incubated for 24 h in serum free medium before rhVTN, fibronectin, fibrinogen, laminin or collagen was added to the medium for 4 h. **C,D)** C6 cells were serum starved for 24 h before VTN KO or WT plasma was added to cells for 4 h. One Way ANOVA with Dunnett post hoc.

FAK mediates VTN-induced LIF and IL-6 in C6 cells

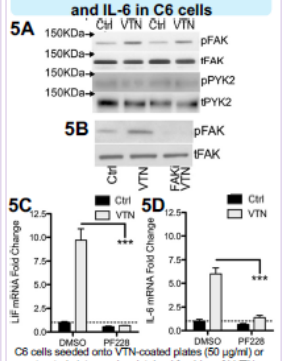

C6 cells seeded onto VTN-coated plates (50 µg/ml) or non-treated plates and maintained for 4 hrs. **A)** VTN stimulates phosphorylation of Y397-FAK (pFAK) but not of PYK2. **B)** FAK inhibitor PF573228 (FAKi) abolishes VTN activated pFAK Y397, as well as the LIF (**C**) and IL-6 mRNA induction (**D**).

FAK inhibitors block VTN effects in C6 cells

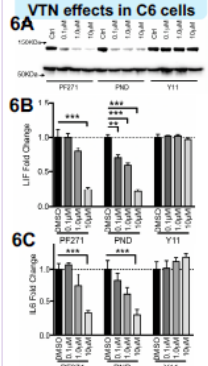

A) FAK inhibitors PF271 and PND, but not Y11, suppress baseline pFAK Y397, and LIF (**B**) and IL-6 (**C**) mRNA in a dose-dependent manner in C6 cells after 4 h (n=4).

VTN activates pFAK Y397 and STAT3 Y705 in human microvascular endothelial CMEC cells

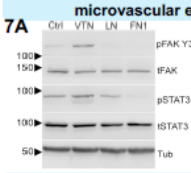

hCMEC cells were passaged and re-suspended in serum-free medium and maintained in suspension for 1 hr. Cells were plated onto plastic (PBS; Ctrl), VTN, laminin (LN) or fibronectin (FN1) treated plates for 1 hr. **A)** VTN showed a greater increase in pFAK Y397 and STAT3 Y705 over laminin and fibronectin (n=4)

VTN induces LIF and IL-6 via FAK, not PYK2, in CMECs

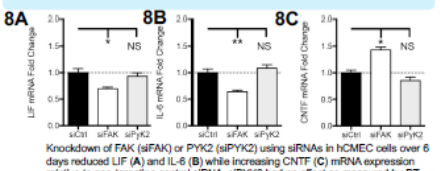

Knockdown of FAK (siFAK) or PYK2 (siPYK2) using siRNAs in hCMEC cells over 6 days reduced LIF (**A**) and IL-6 (**B**) while increasing CNTF (**C**) mRNA expression relative to non-targeting control siRNA. siPYK2 had no effect as measured by RT-qPCR (n=4). Data are means ± SEM from n=4 independent experiments each. * p<0.05, ** p<0.01, *** p<0.001.

Conclusions

(i) VTN regulates LIF and IL-6 expression through integrin-FAK and uPAR signaling

(ii) We propose that leaked plasma VTN might act as a flagging molecule, directly triggering pro-inflammatory cytokine expression in cerebral and other injured tissues

(iii) Integrin-FAK signaling is a novel therapeutic target, with pharmacological FAK inhibition representing a potent tool for attenuating inflammatory cytokine induction

Acknowledgements
We express our gratitude to Hannah Malone for animal care, and Rhesa Dykes and Michelle Duffourc of the Microbiology Core Facility for guidance in the WES technology. Funding was provided by NIH R01 grant AG29493, and in part by C06RR0306551 and the Quillen College of Medicine at ETSU

ANEXO D – Participação em trabalho apresentado no *VIIIth International Symposium on Diagnostics and Therapeutics Xth LIKA Scientific Journey*

CERTIFICATE

SINATER

19 - 21 September 2017

We certify that the work, titled **SEARCHING FOR NEW GENES LINKED TO PRIMARY BRAIN CALCIFICATIONS** authored by **Lemos R.R., Pimentel, L.F., Ferreira, J.B., Borges-Medeiros, R.L., Ferreira, L.D., Santos-Junior, E.F., Cantanhede, I.G., Oliveira, J.R.M.** was presented in the POSTER category during the event "VIII International Symposium on Diagnostics and Therapeutics (SINATER), III International Symposium on Rare Diseases (RDis) and XI LIKA Scientific Journey" (SigProj No. 270372.1384.121666.02052017), promoted by Laboratory of Immunopathology Keizo Asami (LIKA), Federal University of Pernambuco (UFPE), Recife, Brazil, on 19th – 21th September 2017 (20 hours).

José Luiz de Lima Filho
Director of LIKA - UFPE
Coordinator of SINATER, RDis and
LIKA Scientific Journey - Recife, Brazil

James Owen
Professor of University College London
Coordinator of SINATER, RDis and
LIKA Scientific Journey - London, England

Organization:

Universidade Federal de Pernambuco

LIKA Laboratório de Imunopatologia Keizo Asami

UCL University College London

Support:

analítica HEBRON Waters GE Healthcare FLAMAR Biogene CAPES LongLife

ANEXO E – Comentário publicado na sessão *Write Click*© do periódico *Neurology*

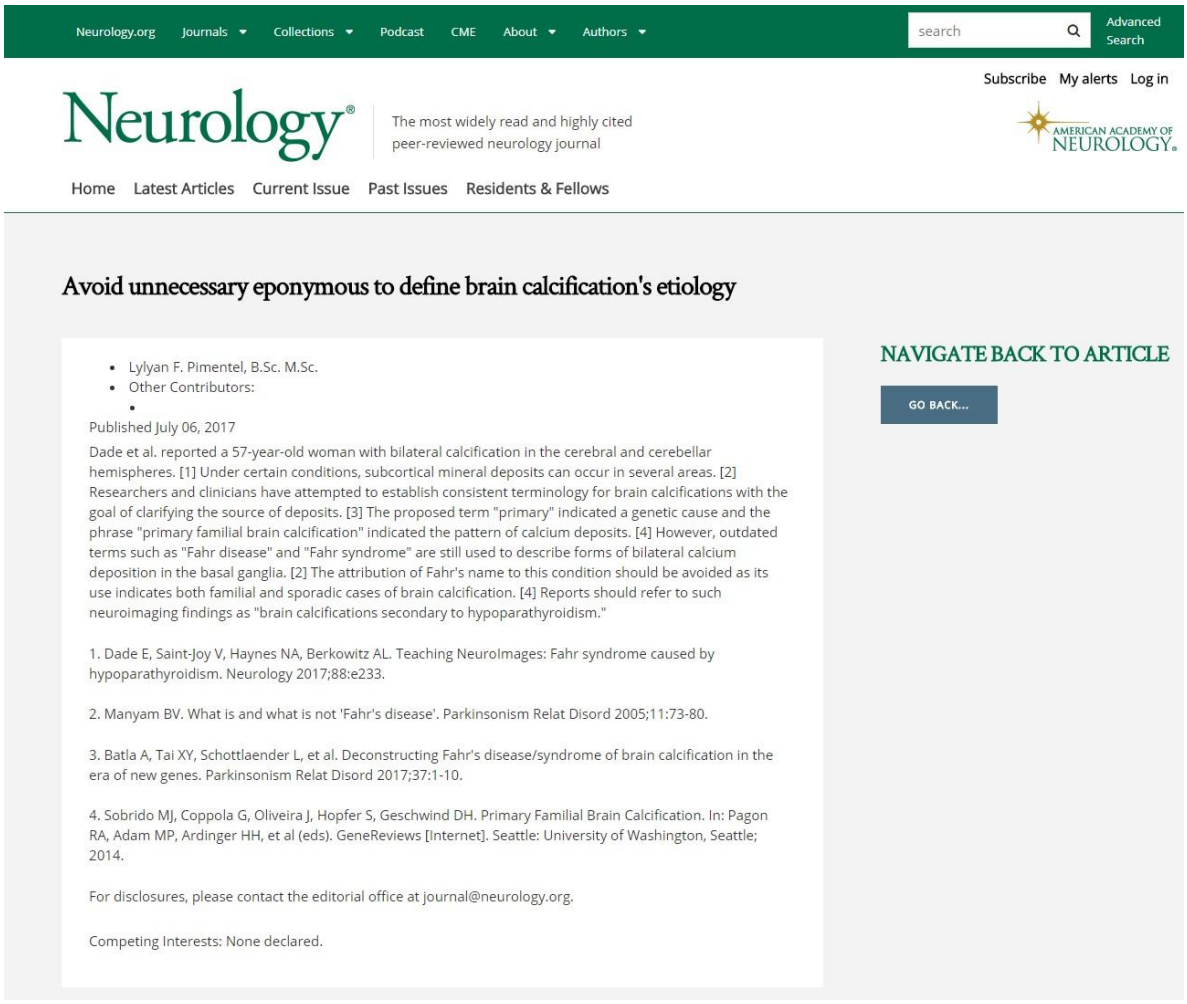

Neurology.org Journals Collections Podcast CME About Authors search Advanced Search

Subscribe My alerts Log in

Neurology®

The most widely read and highly cited peer-reviewed neurology journal

AMERICAN ACADEMY OF NEUROLOGY

Home Latest Articles Current Issue Past Issues Residents & Fellows

Avoid unnecessary eponymous to define brain calcification's etiology

- Lylyan F. Pimentel, B.Sc. M.Sc.
- Other Contributors:
-

Published July 06, 2017

Dade et al. reported a 57-year-old woman with bilateral calcification in the cerebral and cerebellar hemispheres. [1] Under certain conditions, subcortical mineral deposits can occur in several areas. [2] Researchers and clinicians have attempted to establish consistent terminology for brain calcifications with the goal of clarifying the source of deposits. [3] The proposed term "primary" indicated a genetic cause and the phrase "primary familial brain calcification" indicated the pattern of calcium deposits. [4] However, outdated terms such as "Fahr disease" and "Fahr syndrome" are still used to describe forms of bilateral calcium deposition in the basal ganglia. [2] The attribution of Fahr's name to this condition should be avoided as its use indicates both familial and sporadic cases of brain calcification. [4] Reports should refer to such neuroimaging findings as "brain calcifications secondary to hypoparathyroidism."

1. Dade E, Saint-Joy V, Haynes NA, Berkowitz AL. Teaching NeuroImages: Fahr syndrome caused by hypoparathyroidism. Neurology 2017;88:e233.

2. Manyam BV. What is and what is not 'Fahr's disease'. Parkinsonism Relat Disord 2005;11:73-80.

3. Batla A, Tai XY, Schottlaender L, et al. Deconstructing Fahr's disease/syndrome of brain calcification in the era of new genes. Parkinsonism Relat Disord 2017;37:1-10.

4. Sobrido MJ, Coppola G, Oliveira J, Hopfer S, Geschwind DH. Primary Familial Brain Calcification. In: Pagon RA, Adam MP, Ardinger HH, et al (eds). GeneReviews [Internet]. Seattle: University of Washington, Seattle; 2014.

For disclosures, please contact the editorial office at journal@neurology.org.

Competing Interests: None declared.

NAVIGATE BACK TO ARTICLE

GO BACK...

ANEXO F – Trabalho apresentado no *Vth International Symposium on Diagnostics and Therapeutics* (SINATER) and *VIIIth LIKA Scientific Journey*

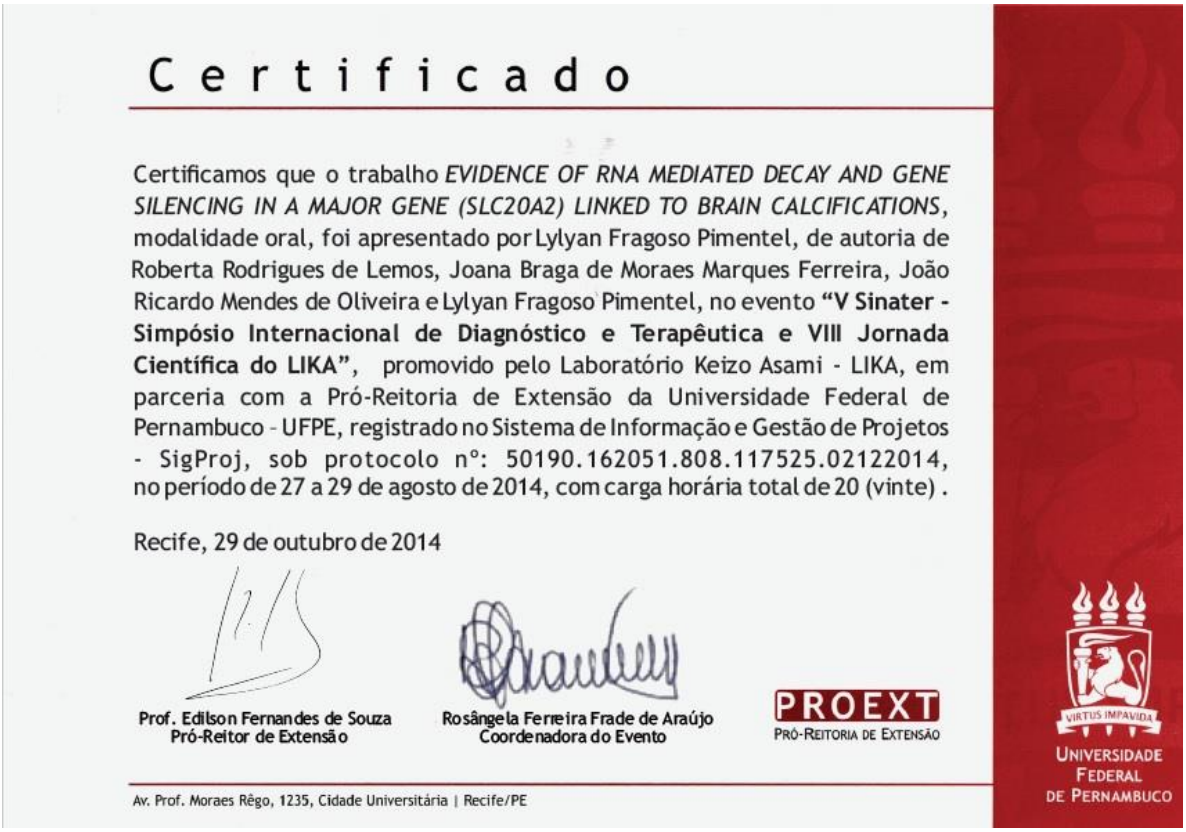

Certificado

Certificamos que o trabalho *EVIDENCE OF RNA MEDIATED DECAY AND GENE SILENCING IN A MAJOR GENE (SLC20A2) LINKED TO BRAIN CALCIFICATIONS*, modalidade oral, foi apresentado por Lylyan Fragoso Pimentel, de autoria de Roberta Rodrigues de Lemos, Joana Braga de Moraes Marques Ferreira, João Ricardo Mendes de Oliveira e Lylyan Fragoso Pimentel, no evento **"V Sinater - Simpósio Internacional de Diagnóstico e Terapêutica e VIII Jornada Científica do LIKA"**, promovido pelo Laboratório Keizo Asami - LIKA, em parceria com a Pró-Reitoria de Extensão da Universidade Federal de Pernambuco - UFPE, registrado no Sistema de Informação e Gestão de Projetos - SigProj, sob protocolo nº: 50190.162051.808.117525.02122014, no período de 27 a 29 de agosto de 2014, com carga horária total de 20 (vinte).

Recife, 29 de outubro de 2014

Prof. Edilson Fernandes de Souza
Pró-Reitor de Extensão

Rosângela Ferreira Frade de Araújo
Coordenadora do Evento

PROEXT
PRÓ-REITORIA DE EXTENSÃO

Av. Prof. Moraes Rêgo, 1235, Cidade Universitária | Recife/PE

VIRTUS IMPAVIDA
UNIVERSIDADE FEDERAL DE PERNAMBUCO